Suivi du patient transplanté rénal traité par tacrolimus par pharmacocinétique de population et machine learning

Alexandre Destere

▶ **To cite this version:**

Alexandre Destere. Suivi du patient transplanté rénal traité par tacrolimus par pharmacocinétique de population et machine learning. Médecine humaine et pathologie. Université de Limoges, 2022. Français. NNT : 2022LIMO0109 . tel-04402665

HAL Id: tel-04402665
https://theses.hal.science/tel-04402665

Submitted on 18 Jan 2024

HAL is a multi-disciplinary open access archive for the deposit and dissemination of scientific research documents, whether they are published or not. The documents may come from teaching and research institutions in France or abroad, or from public or private research centers.

L'archive ouverte pluridisciplinaire **HAL**, est destinée au dépôt et à la diffusion de documents scientifiques de niveau recherche, publiés ou non, émanant des établissements d'enseignement et de recherche français ou étrangers, des laboratoires publics ou privés.

Thèse de doctorat

Université de Limoges

ED 615 - Sciences Biologiques et Santé (SBS)

P&T – Pharmacology and Transplantation – INSERM U1248

Thèse pour obtenir le grade de

Docteur de l'Université de Limoges

Pharmacologie, infectiologie et sciences du médicament

Présentée et soutenue par

Alexandre Destere

Le 5 décembre 2022

Suivi du patient transplanté rénal traité par tacrolimus par pharmacocinétique de population et machine learning

Thèse dirigée par Dr Aurélie Prémaud et le Dr Jean-Baptiste Woillard

JURY :

Président du jury

M. Pierre MARQUET, Professeur universitaire, INSERM U1248 P&T, Université de Limoges

Rapporteurs

M. Zoubir DJERADA, Professeur universitaire, EA 3801HERVI, Université de Reims

M. Laurent BOURGUIGNON, Maitre de conférences universitaire, UMR CNRS 5558 LBBE, Université de Lyon

Examinateurs

Mme. Françoise STANKE-LABESQUE, Professeur universitaire, INSERM U1042 HP2, Université de Grenoble

Mme. Aurélie PREMAUD, Maitre de conférences universitaire, INSERM U1248 P&T, Université de Limoges

M. Jean-Baptiste WOILLARD, Maitre de conférences universitaire, INSERM U1248 P&T, Université de Limoges

Licence CC BY-NC-ND 3.0

Le plus grand péril se trouve au moment de la victoire.
Napoléon Bonaparte

Licence CC BY-NC-ND 3.0

Remerciements

Au Professeur MARQUET, je tenais à vous remercier chaleureusement pour le soutien, la formation et les connaissances que vous m'avez apporté durant toutes ces années au sein de votre laboratoire. Je vous adresse mon respect le plus sincère et une profonde reconnaissance.

Je tiens à présenter mes remerciements les plus sincères au Professeur Zoubir DJERADA et au Docteur Laurent BOURGUIGNON d'avoir accepté de juger mes travaux de thèse de sciences. Vos connaissances approfondies en pharmacologie mais également en pharmacocinétique de population et machine learning permettront assurément d'enrichir ce manuscrit. Je suis profondément reconnaissant de l'intérêt que vous avez porté à mes travaux. Au Professeur Françoise STANKE-LABESQUE, je vous présente mes plus sincères remerciements pour m'honorer de votre présence dans ce jury de thèse.

Au Docteur Aurélie PREMAUD, merci pour ces 3 ans d'encadrement ensemble. Merci de m'avoir recadré, à certains moments, quand les idées partaient dans tous les sens, de m'avoir soutenu lors de certains difficiles. Sois assuré de ma plus profonde reconnaissance.

Au Docteur Jean-Baptiste WOILLARD, je ne trouverai jamais les mots pour te remercier pour tout ce que tu as pu m'apporter durant toutes ces années sous ta direction. Tu m'as donné le goût de la recherche et certainement ta folie aussi. Ce fût un plaisir quotidien de travail avec toi malgré tes idées incessantes et incontrôlées. J'espère pouvoir continuer à travailler avec toi durant de nombreuses années ! Sois assuré de mon plus profond respect !

Au Docteur Caroline MONCHAUD, au Professeur Franck SAINT-MARCOUX et au docteur Souleiman EL BALKHI, je vous remercie d'avoir supporté mes coups d'éclats, de m'avoir canalisé et avoir fait de moi une personne meilleure.

Au laboratoire de Pharmacologie, Toxicologie et Pharmacovigilance du CHU de Limoges, je tenais à vous remercier profondément pour avoir partagé tous ces moments avec moi, les bons comme les mauvais surtout les mauvais !

A mes co-internes, Pauline, Ali, Marc, Joseph, Robin, Céline, merci d'avoir été toujours là pour me soutenir durant toutes ses années même quand les moments étaient difficiles !

A mes amis, grâce à vous, ses années d'études ont été plus douces !

A Arnaud et William, pour tous ces moments passés ensemble, ces dégustations en tout genre et de ces grandes discussions, merci !

A ma famille, merci pour les sacrifices que vous avez réalisés pour que je devienne l'homme que je suis. J'espère vous avoir rendu fiers.

A toi, Aurélie, toi qui m'as toujours soutenu quel que soit mes choix et mes sauts d'humeurs. Merci de partager ma vie depuis tant d'années. A tes côtés, tout devient possible, je t'aime !

Licence CC BY-NC-ND 3.0

Droits d’auteurs

Cette création est mise à disposition selon le Contrat :
« **Attribution-Pas d'Utilisation Commerciale-Pas de modification 3.0 France** »
disponible en ligne : *http://creativecommons.org/licenses/by-nc-nd/3.0/fr/*

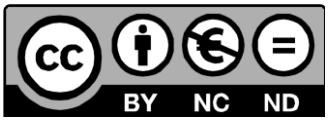

Licence CC BY-NC-ND 3.0

Table des matières

I. Introduction 12
I.1. Le Tacrolimus 13
I.1.1. Origine 13
I.1.2. Pharmacologie du tacrolimus 13
I.1.2.1. Mécanisme d'action 13
I.1.2.2. Pharmacocinétique et source de variabilité 15
I.1.3. Utilisation clinique du tacrolimus en transplantation rénale 18
I.1.4. Relation exposition/effets indésirables du tacrolimus 19
I.1.4.1 Neurotoxicité 19
I.1.4.2. Néphrotoxicité 21
I.1.4.3. Diabète post-transplantation 22
I.1.4.4. Infections 25
I.2. Évaluation de la fonction rénale et son intérêt de le suivi du patient 25
I.2.1. Le débit de filtration glomérulaire 25
I.2.2. Évaluation de la fonction rénale 26
I.2.2.1. Les composés endogènes 26
I.2.2.1.1. La créatinine et les formules d'estimation du débit de filtration glomérulaire 26
I.2.2.1.2. La cystatine C 27
I.2.2.2. Les composés exogènes 28
I.2.2.2.1. Les radio-isotopes 28
I.2.2.2.2. L'iohexol 29
I.2.2. Intérêt du suivi de la fonction rénale 29
I.3. Définition du suivi thérapeutique pharmacologique et exemple du tacrolimus 29
I.4. La Pharmacocinétique de population 30
I.4.1. La pharmacocinétique de population paramétrique 32
I.4.2. La pharmacocinétique de population non paramétrique 33
I.4.3. Définition d'un estimateur Bayésien empirique 34
I.5. Utilisation de la pharmacocinétique de population et des estimateurs Bayésiens dans le suivi du patient 35
I.6. L'intelligence artificielle 37
I.6.1. Les différents types d'apprentissage et algorithmes dans l'intelligence artificielle 37
I.6.2. Utilisation de l'intelligence artificielle en model-informed precision dosing 39
Partie II. Résultats 41
II.1. IMPAKT Study: Clinical Pharmacokinetics and Bayesian Estimators for the Individual Dose Adjustment of a Generic Formulation of Tacrolimus in Adult Kidney Transplant Recipients 41
II.2. A single Bayesian estimator for iohexol clearance estimation in ICU, liver failure and renal transplant patients 55
II.3. A hybrid model associating population pharmacokinetic and machine learning: a case study with iohexol clearance estimation 69
II.4. A hybrid algorithm combining population pharmacokinetic and machine learning for isavuconazole exposure prediction 84
II.5. Longitudinal exposure to tacrolimus and new onset diabetes mellitus in renal transplant patients 108
Partie III. Discussion et Conclusion 141
Références bibliographiques 145

Licence CC BY-NC-ND 3.0

Table des illustrations

Figure 1 : Mécanisme d'action des immunosuppresseurs d'après www.pharmgkb.org 14

Figure 2 : Voie d'absorption et de métabolisme du tacrolimus d'après www.pharmgkb.org... 15

Figure 3 : Représentation graphique du métabolisme et transport du tacrolimus dans les principaux organes d'après Tron et al.[12] 18

Figure 4 : Présentation des différents troubles neurologiques pouvant être induits par le tacrolimus d'après Faravelli et al. [13] 19

Figure 5 : Voie de toxicité du tacrolimus sur les cellules β du pancréas d'après Rodriguez-Rodriguez et al. [25] 23

Figure 6 : Distribution normale d'un paramètre PK de moyenne μ et d'écart-type σ et problème de détection des sous-populations. 33

Figure 7 : Exemple de distribution des paramètres pharmacocinétiques dans un modèle de pharmacocinétique de population non-paramétrique. CL = clairance, KCP = constate d'échange entre le compartiment central vers le compartiment périphérique..... 34

Figure 8 : Exemple de probability of target attainment de l'oxfendazole en fonction de différentes posologies d'après Bach et al. [78] 36

Licence CC BY-NC-ND 3.0

Table des tableaux

Tableau 1 : Différents mécanismes supposés de néphrotoxicité (aiguë et/ou chronique) du tacrolimus 21

Tableau 2 : Stratégies thérapeutique du tacrolimus dans les indications de la transplantation rénal et hépatique en fonction de l'âge, du risque immunologique, des traitements immunosuppresseurs associés et du délai post-transplantation d'après Brunet et al. [32]. MMF= mycophénolate mofétil ; IL-2 :interleukinee 2. 24

Tableau 3 : Classifications des stades d'évolution de la maladie rénale d'après le guide du parcours de soins - Maladie rénale chronique de l'adulte – HAS (Juillet 2021) [40]..... 26

Tableau 4 : Formule d'estimation du DFG à partir de la créatininémie et de la cystatine C sérique d'après Inker et al. [53] 28

Licence CC BY-NC-ND 3.0

Table des annexes

Annexe 1: Development of new tacrolimus C0-based metrics and their association with new onset diabetes mellitus in renal transplant patients 153

Licence CC BY-NC-ND 3.0

Abréviations :

^{51}Cr-EDTA	acide éthylène-diamine-tétra-acétique marqué au ^{51}Cr
^{99m}TC-DTPA	diéthylène-penta-acétate marqué au technétium 99m
ADME	Absorption, distribution, métabolisme, élimination
AUC	Aire sous la courbe
C0	Concentration résiduelle
CKD-EPI	Chronic Kidney Disease - Epidemiology Collaboration
Cmax	Concentration maximale
CYP3A4/CYP3A5	Cytochrome 3A4/4A5
DFG	Débit de filtration glomérulaire
EBE	Estimateur Bayésien empirique
FDA	Food and Drug Administration
FKBP-12	FK-506 binding protein-12
HAS	Haute Autorité de Santé
HLA	Human Leukocyte Antigen
HR	Hazard ratio
IL-2	Interleukine 2
IPRED	Prédictions individuelles
LSS	Stratégie de prélèvements limités
MAP-BE	Maximum a posteriori Bayesian Estimator
MARS	Multivariate Adaptive Regression Splines
MDRD	Modification of diet in renal disease
MIPD	Model-informed precision dosing
NFAT	Facteur de transcription des lymphocytes T activés
OCT2	Organic Cation Transporter 2
P-gp	Glycoprotéine P
PK	Pharmacocinétique
POPPK	Pharmacocinétique de population

Licence CC BY-NC-ND 3.0

PRED	Prédiction
RNPGx	Réseau francophone de Pharmacogénétique
SVM	support vector machine
Vd	Volume de distribution
VPC	Visual Predictive Check
Xgboost	Extreme Gradient Boosting

Licence CC BY-NC-ND 3.0

I. Introduction

Dans cette thèse, nous nous sommes intéressés à l'utilisation d'outils de modélisation et de l'intelligence artificielle afin : (i) d'estimer l'exposition au tacrolimus, (ii) d'évaluer le bon fonctionnement du rein chez des patients transplantés rénaux et (iii) d'évaluer la relation exposition au tacrolimus/survenue d'effets indésirables et notamment la survenue d'un diabète post-transplantation.

Dans une première partie, nous développerons différents points : (i) l'intérêt du suivi thérapeutique pharmacologique du tacrolimus, (ii) le débit de filtration glomérulaire et l'iohexol comme marqueurs de la fonction rénale, (iii) le développement de modèles de pharmacocinétique de population ainsi que leur utilisation dans le suivi de patients transplantés enfin (iv) l'utilisation d'approches innovantes telle que l'intelligence artificielle dans le suivi de ces patients.

Dans une seconde partie, nous présenterons les différentes études réalisées durant cette thèse de Doctorat. La première étude concerne l'utilisation de la pharmacocinétique de population afin de prédire l'exposition au tacrolimus en estimant l'aire sous la courbe chez des patients transplantés rénaux *de novo* prenant une formulation générique du Prograf®, l'Adoport® (**article 1**). Les deuxième et troisième études concernent l'évaluation du fonctionnement du rein via l'estimation du débit de filtration glomérulaire chez des patients transplantés selon 2 approches : (a) une approche de pharmacocinétique de population et le développement d'un estimateur Bayésien basé sur une stratégie de prélèvements limités (**article 2**) (b) une approche hybride combinant un modèle de pharmacocinétique de population à un algorithme de Machine Learning **(article 3**). La quatrième étude décrit les performances d'un modèle hybride dans la prédiction de l'exposition de l'isavuconazole, antifongique utilisé chez des patients transplantés (**article 4**). Enfin, la cinquième étude porte sur l'exposition longitudinale au tacrolimus et son lien avec l'apparition de diabète post-transplantation (**article 5)**.

Licence CC BY-NC-ND 3.0

I.1. Le Tacrolimus

I.1.1. Origine

Isolé en 1984 à partir du champignon *Streptomyces tsukubaensis*, le tacrolimus (FK-506) a rapidement montré une activité supérieure à celle de la ciclosporine en tant qu'inhibiteur de la calcineurine *in vitro* [1]. En 1989, le Dr Starlz a dirigé la première étude clinique utilisant le tacrolimus comme immunosuppresseur [2] puis devant la balance bénéfice/risque du tacrolimus, l'US *Food and Drug Administration* (FDA) a autorisé la mise sur le marché du tacrolimus sous la spécialité Prograf® le 8 avril 1994 comme traitement prophylactique du rejet de greffe hépatique. L'indication concernant la transplantation rénale a été octroyée 3 ans plus tard.

I.1.2. Pharmacologie du tacrolimus

I.1.2.1. Mécanisme d'action

Le tacrolimus, une fois pénétré dans le lymphocyte, forme un complexe avec une protéine appelée FK binding protein 12 (FKBP-12) (Figure 1). Ce complexe, en se liant à la calcineurine de manière non compétitive, inhibe son activité de phosphatase. L'inhibition de la calcineurine diminue la production et la sécrétion d'interleukine 2 (IL-2) par inhibition de la translocation nucléaire du facteur de transcription (NFAT) et donc de la transcription du gène de l'IL-2. Cette diminution de synthèse de l'IL-2 inhibe la prolifération des lymphocytes T par blocage du cycle cellulaire au stade G0.

Licence CC BY-NC-ND 3.0

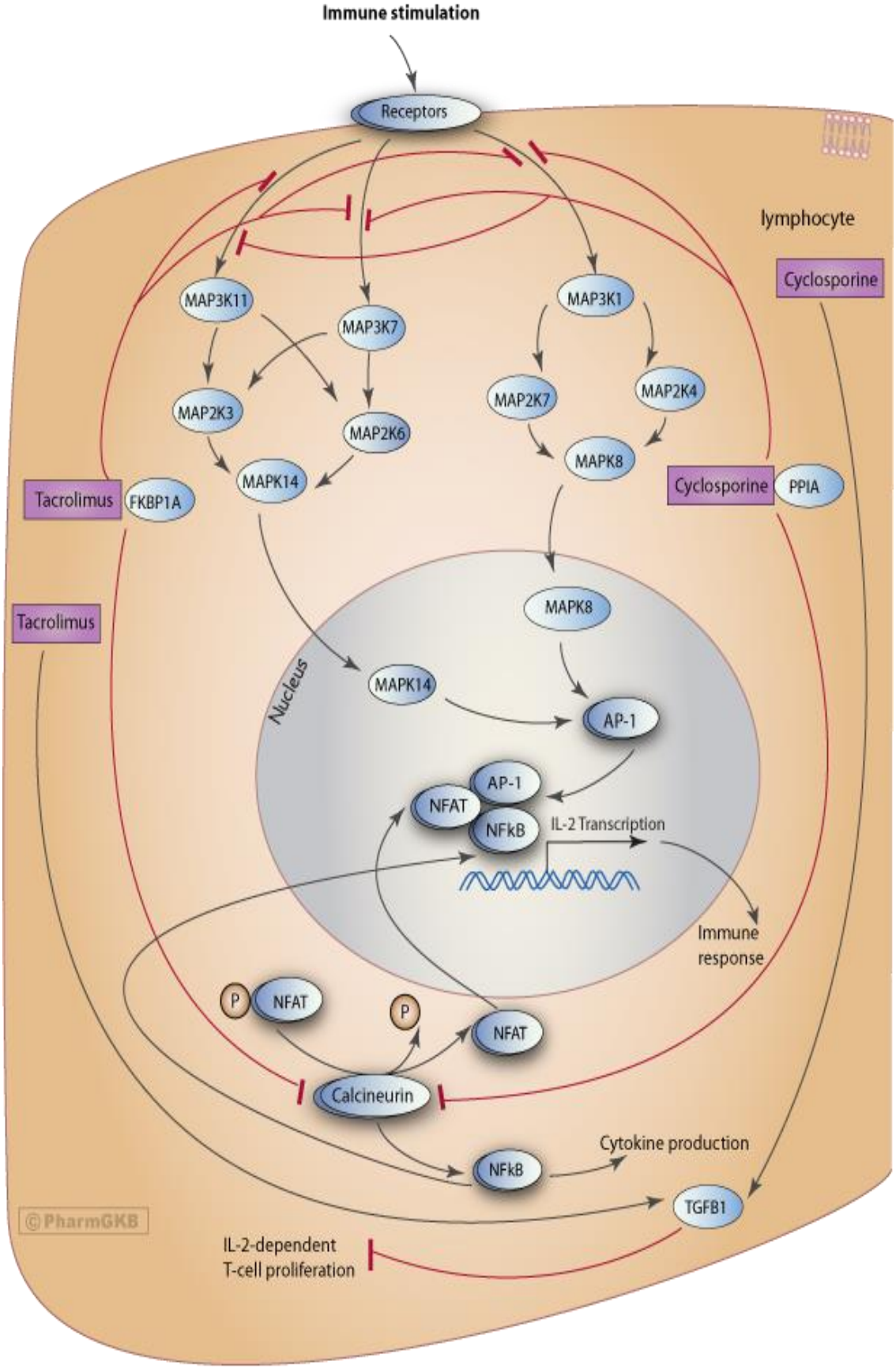

Figure 1 : Mécanisme d'action des immunosuppresseurs d'après www.pharmgkb.org

Licence CC BY-NC-ND 3.0

I.1.2.2. Pharmacocinétique et source de variabilité

Lors de la prise orale du tacrolimus, celui-ci est absorbé à partir du duodénum jusqu'au colon avec un pic d'absorption au niveau du jéjunum, environ 1h30 après sa prise [3]. Sa biodisponibilité est de l'ordre de 20-25%. Une fois absorbé, il se distribue largement (y compris dans les hématies) avec un volume de distribution (Vd) de 1300 L et se lie fortement aux protéines plasmatiques et plus particulièrement à l'albumine et à la α-1-glycoprotéine acide (>98%). Il est métabolisé au niveau hépatique via les CYP3A4/CYP3A5 et est éliminé dans les fèces avec une demi-vie de 12h.

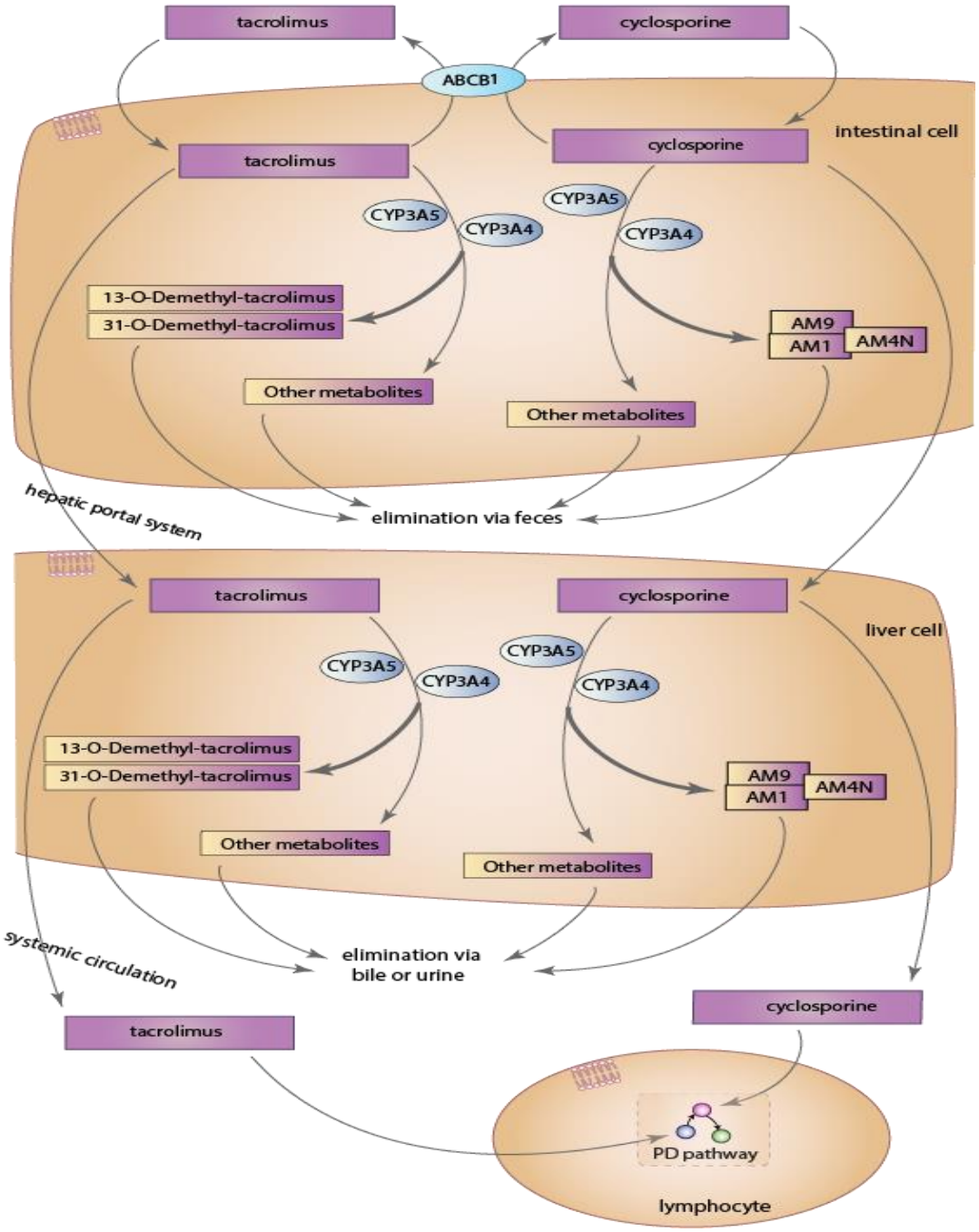

Figure 2 : Voie d'absorption et de métabolisme du tacrolimus d'après www.pharmgkb.org

Licence CC BY-NC-ND 3.0

La pharmacocinétique du tacrolimus présente une grande variabilité intra- mais également interindividuelle. De nombreux facteurs tels que l'alimentation, l'âge, le rythme circadien, les médicaments associés, le polymorphisme des transporteurs (P-gp) et des enzymes du métabolisme (CYP3A4/3A5), le délai post-transplantation ou encore l'hématocrite sont des sources de variabilités de la cinétique du tacrolimus [4].

La faible biodisponibilité du tacrolimus est en partie liée à la glycoprotéine P (P-gp) et aux cytochromes P450 3A (CYP3A4 et CYP3A5) intestinaux dont il est substrat. La biodisponibilité est également influencée par la prise concomitante d'un repas qui peut entraîner une diminution de son exposition allant de 20% à 45% [4,5].

Jacobson et al. [6] ont montré que les concentrations résiduelles (C0) de tacrolimus normalisées par le poids et la dose étaient statistiquement plus importantes chez les personnes âgées de 65 à 84 ans que chez les adultes entre 35 et 64 ans et que chez les jeunes adultes (18-34 ans) (+17% et +34%, respectivement), montrant que l'âge influence la clairance du tacrolimus : plus le sujet est âgé, plus la clairance est faible. Ainsi la dose nécessaire afin d'atteindre les cibles thérapeutiques diminue avec l'âge.

Park et al. [7] et Fontova et al. [8] ont montré l'impact du cycle circadien sur la pharmacocinétique du tacrolimus. Dans ces 2 études, les auteurs ont observé une diminution de l'exposition du tacrolimus après une prise nocturne. Fontova et al. [8] rapportent une AUC moyenne après la dose matinale augmentée de 20% par rapport à l'AUC moyenne après la dose nocturne (respectivement 115,4 h.µg/L vs 92,4 h.µg/L, $p<0.001$).

Saint-Marcoux et al. ont observé une exposition augmentée dans les premiers mois post-transplantation montrant que le délai post-transplantation était également un facteur de variabilité. Les rapports C0/dose et AUC/dose ont significativement augmenté de 2,33 à 3,44 µg/L.mg et de 43,1 à 64,2 h.µg/L.mg entre le premier et le 9e mois post-transplantation rénale [9].

Les 2 principales sources génétiques concernent les enzymes du métabolisme (CYP3A4 et CYP3A5) et les transporteurs d'influx et d'efflux (notamment la P-gp). La recherche des polymorphismes CYP3A5*3 avant l'initiation du traitement est recommandée par la Réseau National de Pharmacogénétique (RNPGx) [10] afin d'adapter la dose initiale de tacrolimus pour obtenir des concentrations résiduelles adéquats. En effet, les génotypes CYP3A5*1/*3 ou CYP3A5*1/*1 sont associés à l'expression du CYP3A5 et donc à un métabolisme accru du tacrolimus et la particularité est que seulement 7% de la population européenne exprime le

Licence CC BY-NC-ND 3.0

CYP3A5 [11]. La dose initiale est 1,5 à 2 fois plus élevée chez les expresseurs que chez les non expresseurs (patients avec un génotype CYP3A5*3/*3) dans la limite d'une dose initiale maximum de 0,30 mg/kg/jour. En ce qui concerne le CYP3A4, la recherche du *CYP3A4*22* semble intéressante dans le cas de suspicion de métabolisme lent du tacrolimus. Cette recherche doit être effectuée après élimination d'un problème d'interaction médicamenteuse ou d'absorption [10].

Concernant les transporteurs d'influx et d'efflux, Tron et al. ont effectué une revue de la littérature sur la pharmacogénétique des transporteurs du tacrolimus (Figure 2) [12]. Peu de polymorphismes décrits, présents sur les transporteurs d'influx ou d'efflux, semblent impacter l'exposition du tacrolimus ou l'apparition d'effets indésirables. Toutefois, il semble intéressant de continuer à explorer ces différents polymorphismes car il pourrait permettre une meilleure compréhension de la variabilité interindividuelle du tacrolimus surtout s'ils sont évalués en combinaison et non indépendamment [12].

Les interactions, qu'elles soient d'origine médicamenteuse ou alimentaire, constituent une importante source de variabilité de la pharmacocinétique du tacrolimus. En effet comme détaillé ci-dessus, le tacrolimus est métabolisé majoritairement par le CYP3A4 et transporté principalement par la P-gp. Ce sont 2 voies majoritairement impactées par les interactions. En effet, le CYP3A4 est situé à différents endroits comme dans les entérocytes, les hépatocytes et minoritairement dans le rein. La P-gp est, quant à elle, présente également à différents endroits dont les entérocytes, les hépatocytes et la barrière hémato-encéphalique.

Licence CC BY-NC-ND 3.0

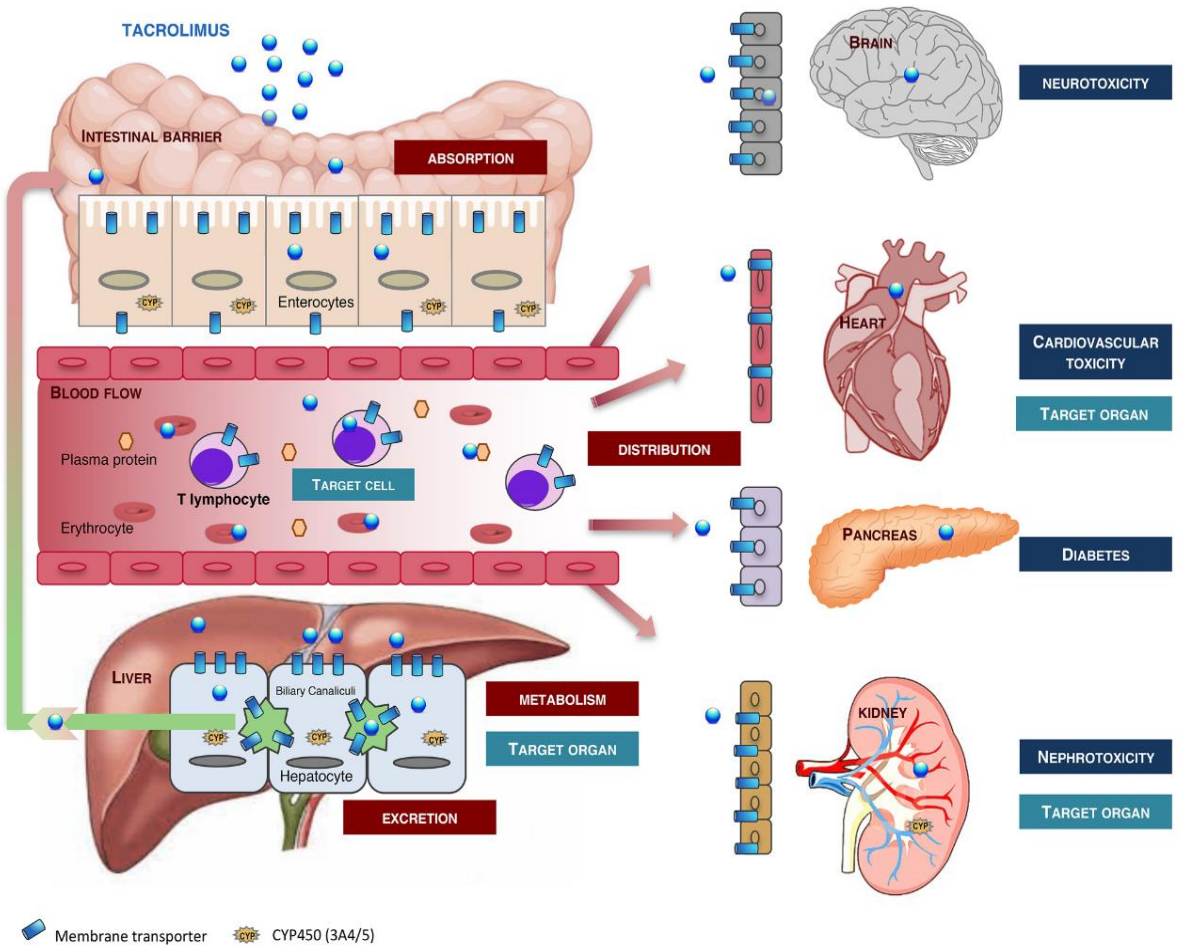

Figure 3 : Représentation graphique du métabolisme et transport du tacrolimus dans les principaux organes d'après Tron et al.[12]

I.1.3. Utilisation clinique du tacrolimus en transplantation rénale

Le tacrolimus est indiqué dans le traitement préventif contre le rejet de greffe solide (rénal, hépatique et cardiaque) ou d'allogreffe. Il est commercialisé sous différentes formulations : à libération immédiate (Prograf®, Modigraf®, Adoport®) avec une interdose de 12h ou à libération retardée/prolongée (Advagraf®, Conferoport®, Envarsus®) avec une interdose de 24h. De nos jours, il est la pierre angulaire du traitement prophylactique contre le rejet de greffe. Il est recommandé d'initier le tacrolimus dans les heures suivant la transplantation du greffon. Chez l'adulte, la posologie initiale est de 0,20-0,30mg/kg/jour en une ou deux prise(s) par jour en fonction de la spécialité. Toutefois son utilisation n'est pas sans risque, le tacrolimus possède une marge thérapeutique étroite ainsi qu'une variabilité pharmacocinétique interindividuelle importante entrainant un risque d'inefficacité et donc de rejet de greffe en cas de sous-exposition ou l'apparition d'effets indésirables comme par exemple, la neurotoxicité, la survenue de diabète post-transplantation, les infections ou encore la néphrotoxicité en cas de surexposition.

Licence CC BY-NC-ND 3.0

I.1.4. Relation exposition/effets indésirables du tacrolimus

I.1.4.1 Neurotoxicité

Les différents troubles neurologiques induits par une thérapie immunosuppressive dont le tacrolimus ont été décrits par Faravelli et al. [13] (Figure 4).

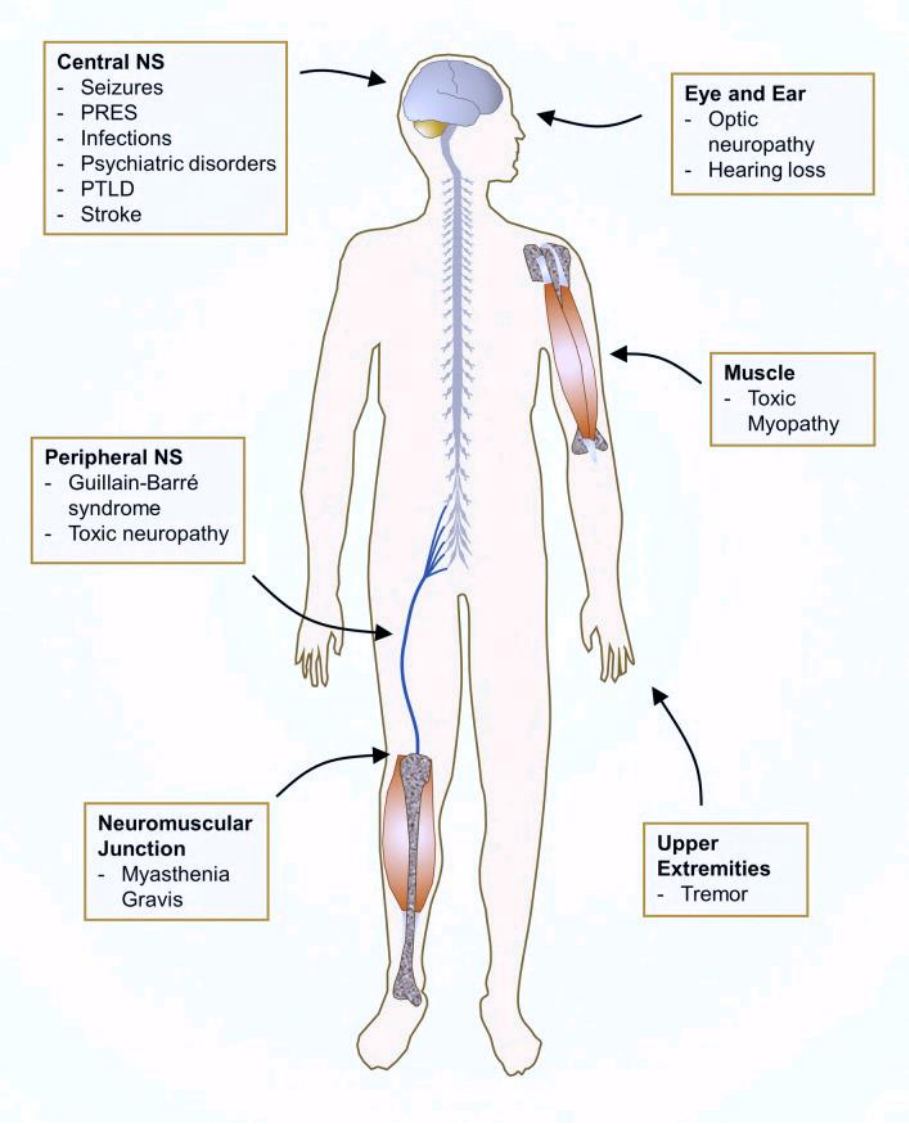

Figure 4 : Présentation des différents troubles neurologiques pouvant être induits par le tacrolimus d'après Faravelli et al. [13]

Ces troubles peuvent toucher le système nerveux central et/ou périphérique (crises d'épilepsie, troubles psychiatriques…) ou encore le système neuromusculaire (myopathie, myasthénie).

Dans cette même revue, les auteurs ont également décrit les différents mécanismes potentiels de neurotoxicité induite par le tacrolimus (Figure 3).

Licence CC BY-NC-ND 3.0

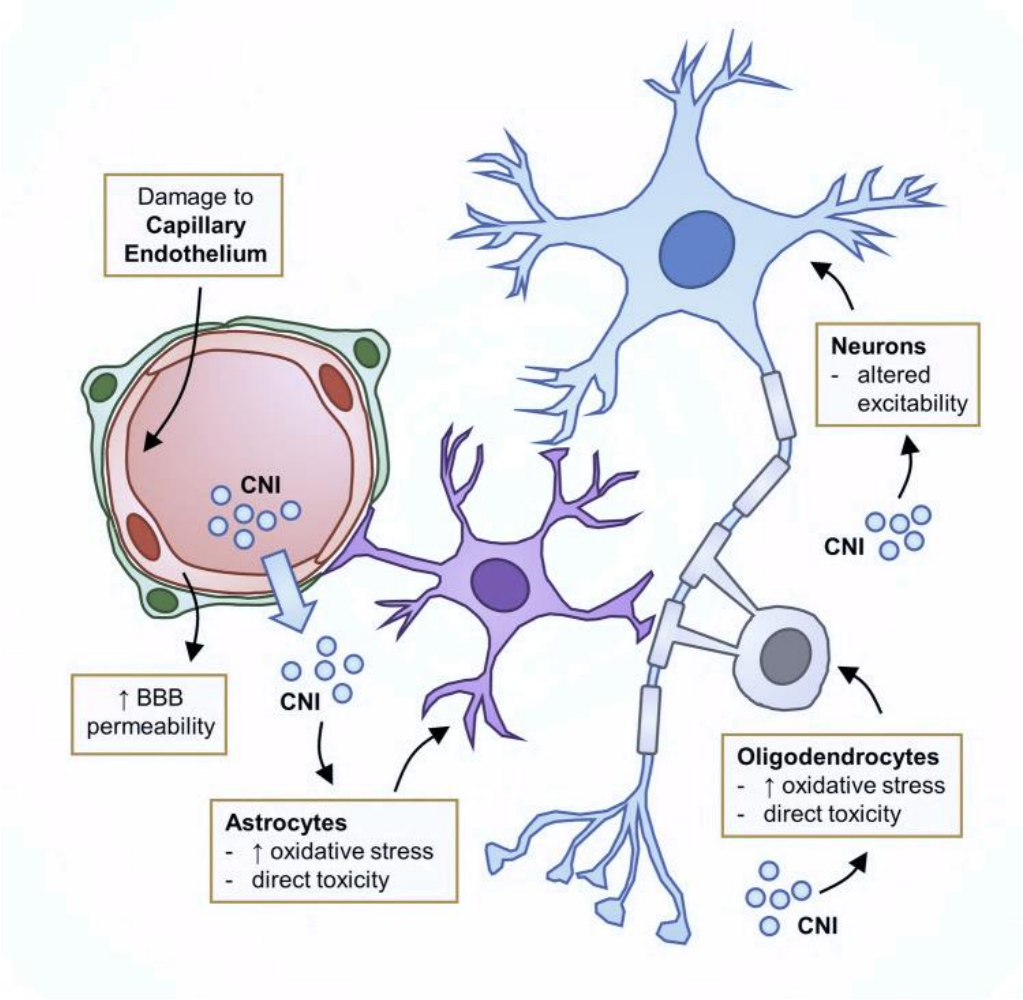

Figure 3 : Schéma explicatif des différents mécanismes de toxicité proposé par Faravelli et al.[13] ; BBB = Barrière hémato-encéphalique.

Les inhibiteurs de la calcineurine, substrats de la P-gp, sont connus pour augmenter la perméabilité de l'endothélium capillaire. Ces 2 mécanismes jouent un rôle dans l'augmentation de la concentration intracérébrale en tacrolimus. Sakamoto et al. [14,15] ont montré, chez des rats, qu'une concentration intracérébrale importante (>700µg/g) pouvait être associée à l'apparition d'effets indésirables neurologiques comme des tremblements, des crises épileptiques, de l'irritabilité ou encore des comportements violents ainsi qu'à leurs intensités (statistiquement non testée). Toutefois, une corrélation statistique ($r=0,967$, $p<0,0001$) entre les concentrations intracérébrales et concentrations sanguines de tacrolimus a été établie. Le seuil de 700 µg/g correspondant à une concentration sanguine de 20 µg/L a été retenu, confirmant les résultats de l'étude STRATO [16].

L'étude STRATO [16], conduite chez des patients transplantés rénaux, a étudié l'impact du switch de la forme à libération immédiate (Prograf®) à la libération prolongée (Envarsus®), sur les tremblements induits par exposition au tacrolimus. Cette étude a mis en évidence une

Licence CC BY-NC-ND 3.0

diminution statistique (p<0,0001) des tremblements chez les patients convertis à la forme à libération prolongée. Fructuoso et al. [17] ont également observé qu'après le switch des patients transplantés rénaux vers une forme prolongée de tacrolimus, la déclaration de tremblements avait significativement diminué (20,8% vs 11,8%, p<0,0001).

I.1.4.2. Néphrotoxicité

La néphrotoxicité induite par le tacrolimus, qu'elle soit aiguë ou chronique, peut s'expliquer par différents mécanismes (Tableau 1) :

Tableau 1 : Différents mécanismes supposés de néphrotoxicité (aiguë et/ou chronique) du tacrolimus

Forme de néphrotoxicité	Origines	Mécanismes supposés
Aiguë	Hémodynamique	- Augmentation des résistances vasculaires rénales
	Toxicité tubulaire aiguë	- Vacuolisation des cellules tubulaires induit par à une augmentation volumétrique du réticulum endoplasmique
	Microangiopathies thrombotiques	- Environnementaux ? Génétiques ?
Chronique	Lésions vasculaires (hyalinose artériolaire)	- Dépôts hyalins - Hypothétique blocage de la voie calcineurine/NFAT des muscles lisses des artérioles afférentes
	Lésions tubulo-interstitielles	- Formation de radicaux libres - Augmentation de l'expression de TGF-β favorisant la fibrose
	Lésions glomérulaires	- Sclérose glomérulaire secondaire à l'hyalinose artériolaire
	Troubles hydroélectrolytiques	- Acidose tubulaire distale - Hyperuricémie

Malgré les différents mécanismes impliqués dans la néphrotoxicité du tacrolimus, la relation entre la néphrotoxicité et les indices d'exposition au tacrolimus n'a pas été clairement démontrée [18]. Toutefois, différentes pistes ont été explorées concernant la néphrotoxicité et notamment celle du ratio concentration résiduelle/dose (C0/D) [32–36]. La survenue de néphrotoxicité est statistiquement significative (p=0,015) chez les métaboliseurs rapides (C0/D

Licence CC BY-NC-ND 3.0

< 1,05) par rapport aux métaboliseurs intermédiaires et lents [34]. Dans une étude ultérieure, les mêmes auteurs ont voulu comprendre le mécanisme de cette néphrotoxicité [33]. Ils ont étudié la relation entre ce rapport C0/D de tacrolimus et la néphrotoxicité, confirmée histologiquement. Ces derniers ont montré une vacuolisation statistiquement plus importante ainsi qu'une diminution de la production d'une protéine Fn14, protéine connue pour être impliquée dans la néphrotoxicité des inhibiteurs de la calcineurine [20], chez les patients possédant un C0/D < 1,05.

A dose constante, l'observation d'une concentration résiduelle plus faible suggère que le métabolisme du tacrolimus est plus important et donc une concentration relative en métabolites plus importante. La néphrotoxicité pourrait donc être liée à la surexposition à certains des métabolites du tacrolimus. Un début de réponse est proposé par Zegarska et al. [23] qui ont observé une faible corrélation statistiquement significative ($r=-0,244$, $p<0,05$) entre la concentration d'un des métabolites du tacrolimus, M-III, et le débit de filtration glomérulaire estimé.

I.1.4.3. Diabète post-transplantation

Le diabète post-transplantation est un des principaux effets secondaires du tacrolimus chez les patients transplantés. Le tacrolimus semble avoir différents mécanismes de toxicité sur les cellules β du pancréas dont le principal est la diminution de sécrétion d'insuline par les cellules β du pancréas [35-38]. Rodriguez-Rodriguez et al. [25] ont décrit les différentes cibles du tacrolimus dans le mécanisme de survenue du diabète (Figure 5) :

Licence CC BY-NC-ND 3.0

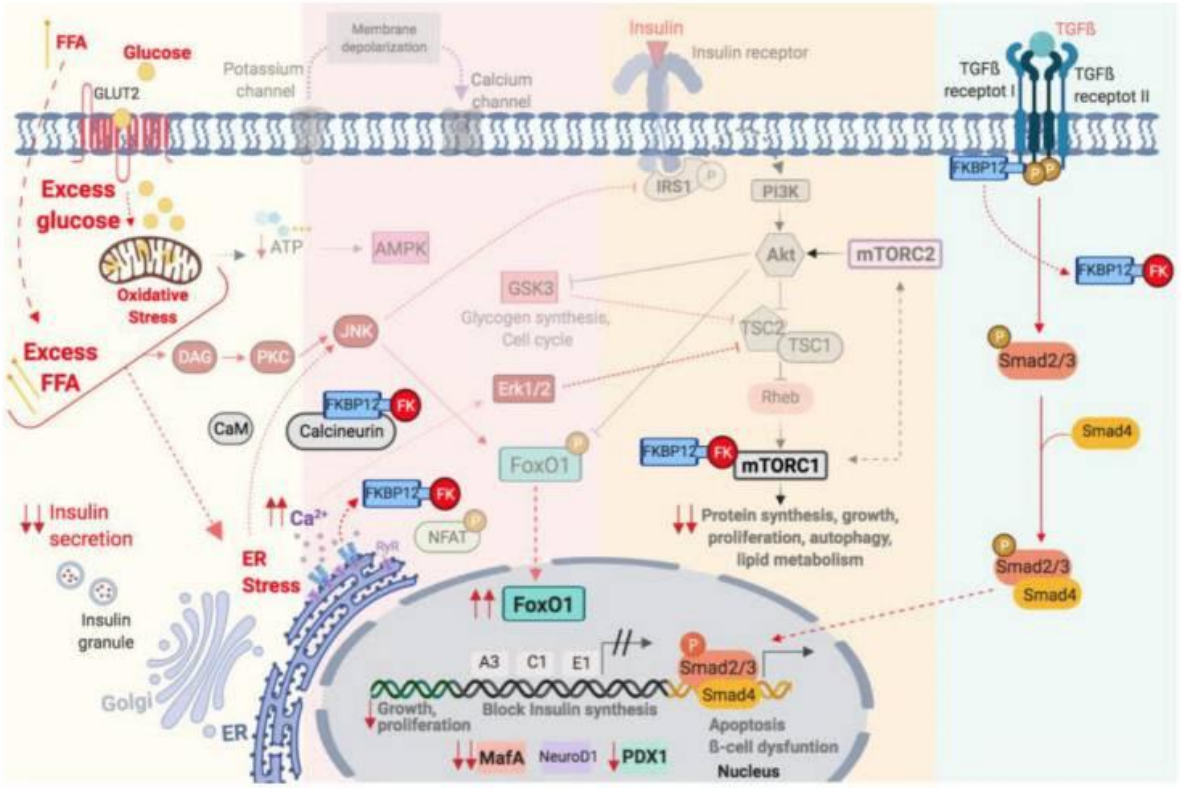

Figure 5 : Voie de toxicité du tacrolimus sur les cellules β du pancréas d'après Rodriguez-Rodriguez et al. [25]

De nombreux articles décrivent la prise d'inhibiteurs de la calcineurine comme facteur de risque de survenue de diabètes post-transplantation avec un surrisque pour le tacrolimus [26–29]. Cependant des relations divergentes ont été établies entre les indices d'exposition au tacrolimus et l'apparition de diabète. Une C0 élevée à l'initiation du traitement par tacrolimus a été montrée comme facteur de risque de développer un diabète chez des patients ayant subi une transplantation rénale [30]. *A contrario,* la C0 initiale a été démontrée comme protecteur chez des patients transplantés hépatiques [31]. Cette divergence entre les 2 études peut s'expliquer par les intervalles thérapeutiques en tacrolimus qui différent dans ces 2 indications. En effet, la transplantation rénale nécessite une exposition plus importante au tacrolimus qu'en cas de transplantation hépatique [32] (Tableau 2). Maes et al. [33] ont également étudié cette relation chez des patients transplantés rénaux. Ils ont montré un risque augmenté de survenue d'un diabète au cours de la première année lorsque les patients avaient un nombre plus important de C0 > 15 µg/L au cours du premier mois post-transplantation. Cette dernière étude semble suggérer l'existence d'une relation entre la survenue de diabète et la surexposition cumulée au tacrolimus.

Licence CC BY-NC-ND 3.0

Tableau 2 : Stratégies thérapeutique du tacrolimus dans les indications de la transplantation rénal et hépatique en fonction de l'âge, du risque immunologique, des traitements immunosuppresseurs associés et du délai post-transplantation d'après Brunet et al. [32]. MMF= mycophénolate mofétil ; IL-2 :interleukinee 2.

Organe	Population et risque immunologique	Immunosuppresseurs associés	Délai post-transplantation	Cible C0 (µg/L)
Rein	Adulte avec un risque immunologique faible	Induction par anticorps anti récepteur interleukine 2, MMF, corticoïdes	Quel que soit le délai	4-12
		Induction par antiglobulines ou anticorps anti récepteur IL-2, Evérolimus, corticoïdes	0-2 mois	4-7
			> 2 mois	2-4
	Adulte avec un risque immunologique élevé	Tous	Quel que soit le délai	10-15
Foie	Adulte	MMF ou évérolimus et corticoïdes	< 1 mois	6-10
			> 1 mois	5-8
		Monothérapie ou induction uniquement	0-3 mois	10-15
			> 3 mois	5-10
		Stratégie sans corticoïdes	Quel que soit le délai	10-15

Licence CC BY-NC-ND 3.0

I.1.4.4. Infections

En inhibant le système immunitaire (inhibition la prolifération des lymphocytes T), le tacrolimus permet d'éviter le rejet de greffe. Malheureusement, cette immunosuppression favorise les différents types d'infections virales [34], bactériennes [35] et fongiques dont l'incidence semble plus élevée chez les patients sous tacrolimus [34], comparé aux autres thérapies immunosuppressives, notamment la ciclosporine, utilisées en transplantation solide. Ceci confirme la supériorité de l'activité immunosuppressive in vitro du tacrolimus par rapport à la ciclosporine [1].

La relation entre l'exposition au tacrolimus et la survenue d'infections semble être bien établie depuis des années [37] cependant peu d'études ont étudié la relation avec les indices d'exposition au tacrolimus usuellement utilisés [38]. Devant l'absence d'évidence, la prévention des infections reste primordiale surtout en début de transplantation (< 6 mois), avec une incidence d'infection opportuniste estimée à10% [39].

I.2. Évaluation de la fonction rénale et son intérêt de le suivi du patient

I.2.1. Le débit de filtration glomérulaire

Le débit de filtration glomérulaire (DFG) permet de quantifier la fonction d'élimination du rein. Il correspond à la quantité de liquide filtrée par le glomérule par unité de temps. Il est exprimé en mL/min/1,73m2 et peut être quantifié grâce à différents composés, qu'ils soient endogènes (créatinine, cystatine C…) ou exogènes (iohexol, 51Cr-EDTA…).

La maladie rénale chronique est définie comme une diminution persistante du DFG pendant plus de 3 mois. En 2021, L'Haute Autorité de Santé (HAS) a proposé une classification des stades d'évolution de la maladie rénale (Tableau 3).

Licence CC BY-NC-ND 3.0

Tableau 3 : Classifications des stades d'évolution de la maladie rénale d'après le guide du parcours de soins - Maladie rénale chronique de l'adulte – HAS (Juillet 2021) [40]

STADE	DFG (mL/min/1,73m^2)	DEFINITION
1	≥ 90	Maladie rénale chronique* avec DFG normal ou augmenté
2	60-89	Maladie rénale chronique* avec DFG légèrement diminué
3A	45-59	Insuffisance rénale chronique modérée
3B	30-44	
4	15-29	Insuffisance rénale chronique sévère
5	< 15	Insuffisance rénale chronique terminale

*** avec marqueurs d'atteinte rénale : albuminurie, hématurie, leucocyturie, ou anomalies morphologiques ou histologiques, ou marqueurs de dysfonction tubulaire, persistant plus de 3 mois (deux ou trois examens consécutifs).**

I.2.2. Évaluation de la fonction rénale

I.2.2.1. Les composés endogènes

I.2.2.1.1. La créatinine et les formules d'estimation du débit de filtration glomérulaire

La créatinine sérique est un composé endogène de masse moléculaire de 113,1 Da. Elle est produite par dégradation de la créatine au niveau musculaire et est éliminée au niveau rénal, majoritairement par filtration glomérulaire mais également par sécrétion rénale. Cette dernière représente environ 10% de la créatinine éliminée à l'état physiologique. La créatinine possède des limites intrinsèques. En effet, il existe une variabilité interindividuelle concernant sa production qui est étroitement liée à la masse musculaire de l'individu mais aussi à d'autres facteurs tels que le sexe, l'âge, l'ethnie et le poids. Le régime alimentaire suivi par le patient ou une activité physique intense peuvent également influencer la créatinine sérique. Il existe aussi une variabilité interindividuelle de sa sécrétion rénale qui peut être modifiée par diverses interactions médicamenteuses. Par exemple, les transporteurs OCT2 (Organic Cation Transporter 2), transporteurs de nombreux médicaments sous forme cationiques (metformine…), sont inhibés par la cimétidine entraînant alors une estimation erronée du DFG [41].

Plusieurs formules ont été développées pour estimer le DFG [42] à partir de la créatininémie : la formule de Schwartz [43] dans une population pédiatrique, l'équation Modification of Diet in Renal Disease (MDRD) [44] et plus récemment Chronic Kidney Disease EPIdemiology

Licence CC BY-NC-ND 3.0

collaboration (CKD-EPI) [45]. La formule de Cockcroft & Gault, première formule développée, estime la clairance de la créatinine (mL/min) et non le DFG [46].

Chaque formule possède ses limites et ses avantages. L'équation MDRD a tendance à sous-estimer le DFG des patients quand celui est supérieur à 60 mL/min/1,73m2 [47]. La formule de CKD-EPI semble fournir une estimation plus précise mais est plus complexe à calculer. La formule de Cockcroft & Gault est simple à réaliser mais ne donne pas de résultats fiables chez les personnes âgées (sous-estimation de la fonction rénale) et chez les sujets obèses (surestimation de la fonction rénale) [48].

I.2.2.1.2. La cystatine C

La cystatine C est un peptide non glycolysé composé de 122 acides aminés pesant 13 kDa. Sa sécrétion est constante par les cellules nucléées du corps entier. Le sexe, l'âge, la masse musculaire, l'alimentation [49] et l'heure de prélèvement n'influencent pas sa production [50]. En revanche un dysfonctionnement thyroïdien peut impacter sa production (hyper- ou hypoproduction en cas d'hyper- ou hypothyroïdie respectivement) [51]. La consommation de tabac, ou une inflammation qu'elle soit aigue ou chronique, peuvent également l'augmenter [52].

Ce peptide, filtré au niveau glomérulaire, n'est pas sécrété au niveau rénal mais est réabsorbé en quasi-totalité pour être catabolisé au niveau du tube contourné distale. Ce catabolisme important de la cystatine C conduit à des concentrations urinaires de cystatine C de l'ordre de traces.

Mais l'absence de formules validées permettant d'estimer le DFG à partir de la seule concentration plasmatique de cystatine C est un frein à son utilisation en routine. En 2012, Inker et al. ont développé une formule associant, la créatinine et la cystatine C en intégrant l'âge, le sexe et l'ethnie. Cette formule, développée sur la base d'un échantillon regroupant 5352 patients issus de 13 études différentes puis validée chez 1119 patients de 5 études différentes, offre une meilleure performance que la formule CKD-EPI [53].

Licence CC BY-NC-ND 3.0

Tableau 4 : Formule d'estimation du DFG à partir de la créatininémie et de la cystatine C sérique d'après Inker et al. [53]

Basis of Equation and Sex	Serum Creatinine†	Serum Cystatin C	Equation for Estimating GFR
	mg/dl	*mg/liter*	
CKD-EPI creatinine–cystatin C equation¶			
Female	≤0.7	≤0.8	$130 \times (Scr/0.7)^{-0.248} \times (Scys/0.8)^{-0.375} \times 0.995^{Age}$ [×1.08 if black]
		>0.8	$130 \times (Scr/0.7)^{-0.248} \times (Scys/0.8)^{-0.711} \times 0.995^{Age}$ [×1.08 if black]
Female	>0.7	≤0.8	$130 \times (Scr/0.7)^{-0.601} \times (Scys/0.8)^{-0.375} \times 0.995^{Age}$ [×1.08 if black]
		>0.8	$130 \times (Scr/0.7)^{-0.601} \times (Scys/0.8)^{-0.711} \times 0.995^{Age}$ [×1.08 if black]
Male	≤0.9	≤0.8	$135 \times (Scr/0.9)^{-0.207} \times (Scys/0.8)^{-0.375} \times 0.995^{Age}$ [×1.08 if black]
		>0.8	$135 \times (Scr/0.9)^{-0.207} \times (Scys/0.8)^{-0.711} \times 0.995^{Age}$ [×1.08 if black]
Male	>0.9	≤0.8	$135 \times (Scr/0.9)^{-0.601} \times (Scys/0.8)^{-0.375} \times 0.995^{Age}$ [×1.08 if black]
		>0.8	$135 \times (Scr/0.9)^{-0.601} \times (Scys/0.8)^{-0.711} \times 0.995^{Age}$ [×1.08 if black]

Toutefois, l'utilisation de cette formule doit être faite avec prudence chez les personnes de plus de 65 ans, ou possédant un indice de masse corporelle < 20 kg/m^2 ou un DFG < 15 min/mL/1,73m2 car seulement 13%, 4% et 3% des patients faisaient respectivement partie de ces sous-populations.

I.2.2.2. Les composés exogènes

I.2.2.2.1. Les radio-isotopes

L'acide éthylène-diamine-tétra-acétique marqué au ^{51}Cr (^{51}Cr-EDTA) est une molécule uniquement filtrée par le rein et sa clairance extra-rénale est quasi inexistante. Dans sa revue de la littérature, Soveri et al. [54] ont montré que la précision d'estimation du DFG était tout à fait satisfaisante comparé à la clairance de l'inuline avec un biais moyen de -5% et 3% pour sa clairance rénale et plasmatique, respectivement. Le diéthylène-penta-acétate marqué au technétium 99m (^{99m}Tc-DTPA) est également éliminé par filtration glomérulaire. Celui-ci possède les mêmes performances d'estimation du DFG que le ^{51}Cr-EDTA [55].

Malgré leurs performances, les radio-isotopes possèdent plusieurs limites d'utilisation. En effet, ces molécules produisent un faible rayonnement γ nécessitant la mise en place de radioprotection pour le patient, l'équipe soignante et l'environnement. De plus, compte-tenu de leur demi-vie relativement faible (quelques heures), ces molécules doivent être produites extemporanément afin d'être administrées le plus rapidement possible au patient. Cette contrainte limite leur utilisation à certains centres spécialisés [56].

Licence CC BY-NC-ND 3.0

I.2.2.2.2. L'iohexol

L'iohexol est une molécule tri-iodée de masse molaire de 821,1 g/mol. Elle est non ionisée et possède un logP = -3,05, ce qui en fait une molécule hydrophile. L'iohexol est administré par voie intraveineuse et n'est pas métabolisé. Le volume de distribution de cette molécule est compris entre 0,35 à 0,85 L/kg. L'iohexol possède une demi-vie de 2h, une faible liaison aux protéines plasmatiques (<2%) et est exclusivement éliminé par filtration glomérulaire [57].
L'iohexol est commercialisé en France sous le nom d'OMNIPAQUE®. Il est utilisé comme produit de contraste dans les tomodensitométries, urographies ou angiographies que ce soit chez l'adulte ou l'enfant. Les propriétés pharmacologiques de cette molécule en font un bon candidat pour mesurer le DFG. La première étude utilisant l'iohexol comme marqueurs du DFG a été publiée en 1989. Celle-ci a montré que l'utilisation de l'iohexol plasmatique permettait d'obtenir des résultats d'estimation du DFG comparables à ceux obtenus via l'inuline avec un bias moyen de -2% [58]. Soveri et al., dans sa revue de la littérature, ont montré que d'autres études obtenaient des résultats similaires avec des biais moyen allant de -3% à 6% [54].

I.2.2. Intérêt du suivi de la fonction rénale

Le suivi de la fonction rénale chez le patient transplanté rénal est déterminant dans leur prise en charge.

Il permet d'objectiver

- la reprise du fonctionnement du greffon (absence de sténose, obstacle urétéral…)
- l'absence de rejet aigu
- une possible néphrotoxicité due aux immunosuppresseurs
- l'absence de récidive d'une glomérulopathie sur le transplant

I.3. Définition du suivi thérapeutique pharmacologique et exemple du tacrolimus

Le suivi thérapeutique pharmacologique (STP) est une activité biologique qui permet : (i) d'optimiser la posologie d'un médicament en fonction des concentrations sanguines mesurées afin de maximiser l'efficacité thérapeutique et de minimiser l'apparition d'effets indésirables médicamenteux, (ii) de vérifier l'observance du patient. Les molécules sujettes au STP doivent respecter certains critères :

- Une relation concentration/effet clairement établie

Licence CC BY-NC-ND 3.0

- Une zone thérapeutique du médicament étroite (une variation faible de la concentration peut entrainer rapidement un sous- ou surdosage conduisant à une inefficacité ou une toxicité)
- Une variabilité pharmacocinétique interindividuelle importante
- L'effet du médicament ne pouvant pas être mesuré directement (efficacité des antihypertenseurs/prise de la pression artérielle)
- Le médicament doit être mesurable analytiquement

Le tacrolimus est un bon exemple de molécule sujette au STP. En effet, le tacrolimus possède une zone thérapeutique étroite conduisant soit à un sous-dosage synonyme de rejet de greffe soit à un surdosage pouvant conduire à de nombreux effets indésirables. Il possède également une variabilité interindividuelle importante motivant le STP régulier de cette molécule. D'après les recommandations de la HAS, le suivi des immunosuppresseurs doit se faire à chaque consultation. L'HAS recommande, durant les 6 premiers mois, une consultation toutes les 2 semaines, puis une consultation mensuelle jusqu'à la fin de la première année. Pour la suite de son suivi, le patient a une consultation tous les 1 à 4 mois en fonction de son état clinique [59]. Enfin le dosage du tacrolimus est réalisable avec différentes méthodes analytiques (chromatographie couplée à une spectre de masse, analyses immuno-enzymatiques…) [60]. Le STP du tacrolimus se réalise sur un prélèvement de sang total à l'état d'équilibre c'est-à-dire environ 3-5 jours après le début du traitement. Le prélèvement doit être réalisé avant une prise, ce qui correspond à la concentration résiduelle. La concentration résiduelle doit être adaptée en fonction de différents critères (type de greffe, âge, période post-greffe, risque immunologique et enfin traitements immunosuppresseurs associés) [32]. La C0 possède une bonne association avec la prévention du rejet de greffe bien qu'une méta-analyse a montré le contraire [61]. Toutefois, le meilleur marqueur de l'exposition est théoriquement l'AUC interdose. Elle permet de décrire l'ensemble de la pharmacocinétique du tacrolimus. Mais cette AUC reste difficile à réaliser en routine (nombre de prélèvements importants). Cependant grâce à des approches de modélisation (pharmacocinétique de population, intelligence artificielle…), il est possible d'estimer cette AUC à partir d'un nombre limité de prélèvements.

I.4. La Pharmacocinétique de population

La pharmacocinétique (PK) se définit comme l'étude du devenir du médicament après son administration. La PK se définit en différentes étapes-clés : l'absorption, la distribution, le métabolisme et l'excrétion (ADME). Les différentes étapes de la pharmacocinétique d'un

Licence CC BY-NC-ND 3.0

médicament se décrivent à travers l'utilisation de paramètres PK comme sa clairance, son volume d'élimination, sa biodisponibilité ou encore sa constante d'absorption (hors administration intraveineuse).

Lorsque différents individus prennent un médicament à la même posologie, les concentrations sanguines observées peuvent varier, sous l'influence de polymorphismes génétiques, des caractéristiques physiques (sexe, âge, taille, poids), du fonctionnement des organes (foie, rein). Ces différences de concentrations observées entre les individus correspondent à la variabilité interindividuelle.

Avant les années 1970, la PK se limitait à la description des paramètres PK moyens au sein d'une population à partir des nombreux prélèvements réalisés chez des individus soit via une approche de PK non compartimentale soit via une approche en 2-étapes [62]. Ces approches, encore utilisées dans les essais de phase 1 dans le développement d'une nouvelle molécule ne permettent pas de quantifier la variabilité interindividuelle. Puis avec l'amélioration des capacités informatiques, la pharmacocinétique de population (POPPK) s'est développée. Lewis Sheiner, Stuart Beal et leur équipe ont été les premiers à décrire le principe de la POPPK [63–69]. Leur méthodologie permet, à partir de quelques échantillons prélevés chez plusieurs individus, de développer un modèle de POPPK décrivant la pharmacocinétique d'un médicament et sa variabilité interindividuelle (et intraindividuelle le cas échant) ainsi que l'erreur résiduelle. Le premier modèle de POPPK a été celui décrivant la pharmacocinétique et la variabilité de la digoxine [70].

Un modèle de POPPK est un modèle pharmaco-statistique composé de 3 parties :

- Modèle pharmacocinétique structural
- Modèle de variabilité interindividuelle
- Modèle d'erreur résiduelle

Le modèle de pharmacocinétique structural utilise souvent la notion de modèles mécanistiques c'est-à-dire que le modèle décrit de manière résumé le processus ADME du médicament sans décrire l'ensemble du processus physiologique. Les modèles mécanistiques peuvent être de 2 types : (i) modèle caténaire correspondant une chaine de compartiments interconnectés (ii) modèle mamillaire correspondant à un compartiment central interconnecté avec un nombre défini de compartiments périphériques.

Licence CC BY-NC-ND 3.0

Les caractéristiques individuelles sont responsables de cette variabilité interindividuelle et peuvent être décrites selon la formule suivante :

$$PK_i = PK_{population} \times cov_i + exp(\eta_i)$$

Avec PK_i : paramètre PK individuel ; $PK_{population}$: paramètre PK moyen dans la population ; cov_i : covariable ; η_i :erreur aléatoire .

η_i est usuellement exprimé sous forme exponentielle afin d'éviter d'obtenir un paramètre PK inférieur à 0.

Le modèle d'erreur permet de réduire la part de l'erreur inexpliquée par le modèle structural. Il permet de décrire la variabilité de la PK de la molécule. Cette variabilité se compose elle-même de 3 parties : (i) la variabilité interindividuelle (ii) la variabilité intraindividuelle, correspondant la variation de concentrations observées chez un même individu et enfin (iii) la variabilité résiduelle.

Afin de mieux expliquer la variabilité, il est usuellement réalisé une recherche de corrélation entre les paramètres PK (ou leur erreur aléatoire) et les covariables et ainsi permettre de diminuer la part non expliquée de la variabilité.

Le modèle d'erreur résiduel peut être décrit usuellement par 3 types de modèles : (i) additif (ii) proportionnel et (iii) mixte. $g(t_{ij}, \psi_i, \xi)\varepsilon_{ij}$ peut se définir soit de type $a + \varepsilon_{ij}$ (additif), soit de type $b.\varepsilon_{ij}$ (proportionnel) ou enfin de type $a + b.\varepsilon_{ij}$ (mixte). Le choix du modèle d'erreur dépend des concentrations observées et de la méthode analytique. Usuellement, le modèle additif est préféré au modèle proportionnel lorsque les concentrations de la cinétique ne varient pas de plus d'un log. Enfin le modèle mixte s'utilise usuellement lors les concentrations varient de plus d'un log et que les concentrations faibles sont proches de la limite de quantification de la méthode de dosage.

I.4.1. La pharmacocinétique de population paramétrique

La POPPK paramétrique repose sur l'hypothèse de normalité ou de log-normalité des distributions des observations, des paramètres PK et des erreurs résiduelles. La variabilité peut être soit d'origine interindividuelle soit d'origine aléatoire. Ces modèles sont donc des modèles à effets mixtes composés de paramètres fixes (paramètres PK moyens : ψ) et de variabilité interindividuelle (variance de la population : ω^2). Le paramètre individuel ψ_i est distribué

Licence CC BY-NC-ND 3.0

autour de ψ avec un effet aléatoire individuelle η_i. La POPPK paramétrique a l'avantage de reposer sur une distribution normale (ou log-normale) ce qui lui confère une puissance statistique. En revanche, elle contraint la distribution à la normalité, ce qui peut conduire à la non-détection de l'existence de sous-populations notamment dues à un polymorphisme génétique. Le modèle paramétrique ne détectera pas les sous-populations et surévaluera la population générale (Figure 6). Il existe néanmoins des moyen de prendre en compte ces sous populations (« mixed models »).

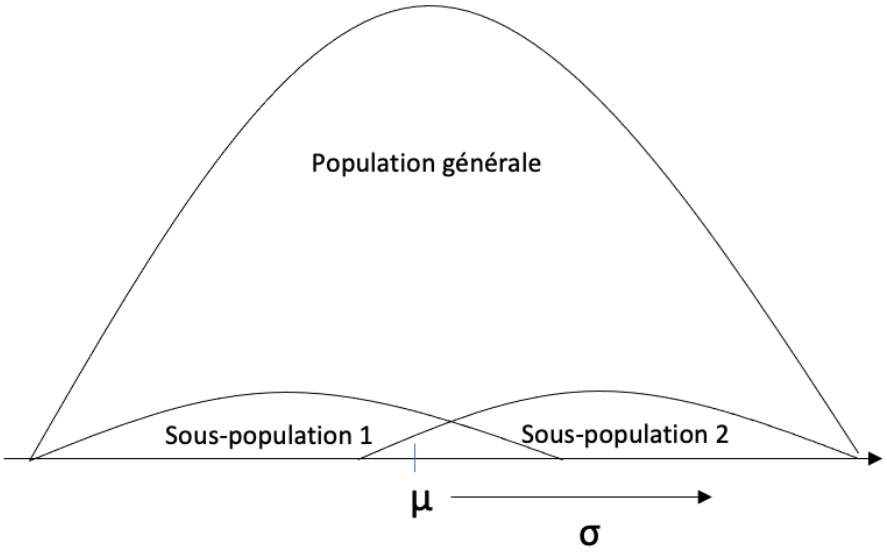

Figure 6 : Distribution normale d'un paramètre PK de moyenne μ et d'écart-type σ et problème de détection des sous-populations.

I.4.2. La pharmacocinétique de population non paramétrique

La POPPK non-paramétrique, à la différence de la POPPK paramétrique, ne repose pas sur une hypothèse de normalité ou log-normalité des paramètres PK. Leur distribution ne peut donc pas être définie par une loi dite continue. La distribution est dite discrète, c'est-à-dire que chaque valeur de paramètre PK possède une probabilité de survenue dans la population étudiée. La POPPK non-paramétrique a l'avantage de permettre de détecter les sous-populations (contrairement à l'approche paramétrique.

Licence CC BY-NC-ND 3.0

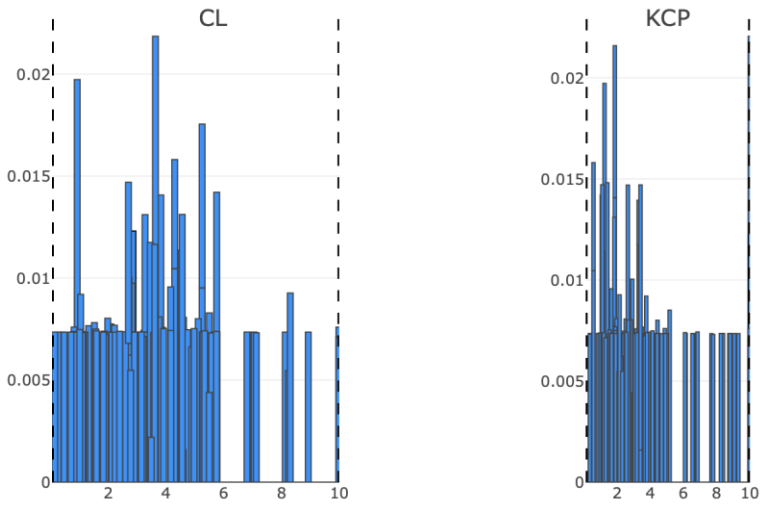

Figure 7 : Exemple de distribution des paramètres pharmacocinétiques dans un modèle de pharmacocinétique de population non-paramétrique. CL = clairance, KCP = constate d'échange entre le compartiment central vers le compartiment périphérique.

I.4.3. Définition d'un estimateur Bayésien empirique

Le théorème de Bayes est un des théorèmes les plus importants en probabilités. Il permet de calculer la probabilité qu'un évènement arrive sachant que d'autres événements se sont produits.

$$P(A|B) = \frac{P(B|A) \times P(A)}{P(B)}$$

A partir de ce théorème, 2 types d'estimateurs Bayésiens empiriques (EBE) ont été créés : (i) les estimateurs minimisant la moyenne des erreurs au carré (ii) les estimateurs *maximum a posteriori* (MAP-BE). Ce sont ces derniers qui sont usuellement utilisés, en PK, afin de prédire les paramètres PK individuels les plus probables à partir des paramètres PK populationnels et des concentrations individuelles observées. Il se décrit à partir de la formule suivante :

$$\widehat{\psi_i^{mode}} = \underset{\psi_i}{\operatorname{argmax}} p\left(\psi_i | y_i; \hat{\theta}\right)$$

Avec $\widehat{\psi_i^{mode}}$: l'espérance modale du paramètre individuel ; ψ_i : paramètre individuel ; y_i : observations individuelles ; θ : variabilité individuelle.

Une fois le paramètre PK individuel estimé, l'effet aléatoire individuel peut être déterminé, par la formule suivante :

$$\eta_i = \psi_i - \psi_{pop} - \beta \times cov, \text{ si la distribution est normale}$$

$$\eta_i = log(\psi_i) - log(\psi_{pop}) - \beta \times log(cov), \text{ si la distribution est log-normale}$$

Licence CC BY-NC-ND 3.0

Lorsque l'on développe un estimateur bayésien à partir d'un modèle de POPPK, on recherche souvent une stratégie de prélèvements limités (LSS) afin de rendre plus facile son utilisation en routine (confort du patient et des infirmières, délai de rendu plus rapide du résultat). Toutefois, la diminution de prélèvements chez un individu conduit à un manque d'informations pour l'EBE. L'information manquante sera apportée par le mode de la population de développement conduisant les paramètres PK individuels à tendre vers le mode de la population de développement, c'est ce qu'on appelle le η-shrinkage. Plus le nombre de prélèvements de la LSS est faible, plus le shrinkage sera important [71].

Ce phénomène peut être quantifié selon deux formules :

$$\eta - \text{shrinkage}_{\psi_i} = 1 - \frac{sd(\eta_i)}{\omega_{\psi_i}} \text{ [72]}$$

où $sd(\eta_i)$ est l'écart-type empirique du paramètre PK individuel ψ_i et ω_{ψ_i}est l'écart-type du paramètre ψ_i

$$\eta - \text{shrinkage}_{\psi_i} = 1 - \frac{var(\eta_i)}{\omega^2_{\psi_i}} \text{ [73]}$$

où $var(\eta_i)$ est la variance empirique du paramètre PK ψ_i et $\omega^2_{\psi_i}$est la variance du paramètre ψ_i

Le calcul du $\eta - \text{shrinkage}$ basé sur le $sd(\eta_i)$ est utilisé plus fréquemment grâce à la popularisation de cette formulation par le logiciel NONMEM [74] toutefois le rapport des variances semble plus statistiquement parlant. Un intervalle de 20-30% a été proposé pour définir si le shrinkage était trop important [75]. La présence d'un shrinkage important peut révéler ou masquer à tort la présence ou l'absence d'une corrélation entre les η_i et une covariable [75].

I.5. Utilisation de la pharmacocinétique de population et des estimateurs Bayésiens dans le suivi du patient

Depuis leur avènement, les modèles de POPPK et les EBE sont utilisés pour l'individualisation des traitements des patients par différents moyens. Ils peuvent être utilisés :

- *A priori* : c'est-à-dire à partir de données utilisés dans le modèle comme des données clinico-biologiques du patient, le modèle est capable de prédire les paramètres individuels pharmacocinétiques du médicament et donc de pouvoir proposer un schéma d'administration du traitement (posologie, durée d'administration si administration intraveineuse, et fréquence de prise). Le modèle peut également être utilisé a priori pour déterminer des *probability of*

Licence CC BY-NC-ND 3.0

target attainment (PTA) [76,77]. Ces PTA permettent de comparer les chances d'atteindre une cible déterminée en fonction de posologies différentes. Les PTA peuvent également être réalisées en fonction d'une covariable (sexe, poids ou encore polymorphisme génétique) en maximisant la probabilité d'atteindre la cible déterminée (Figure 8).

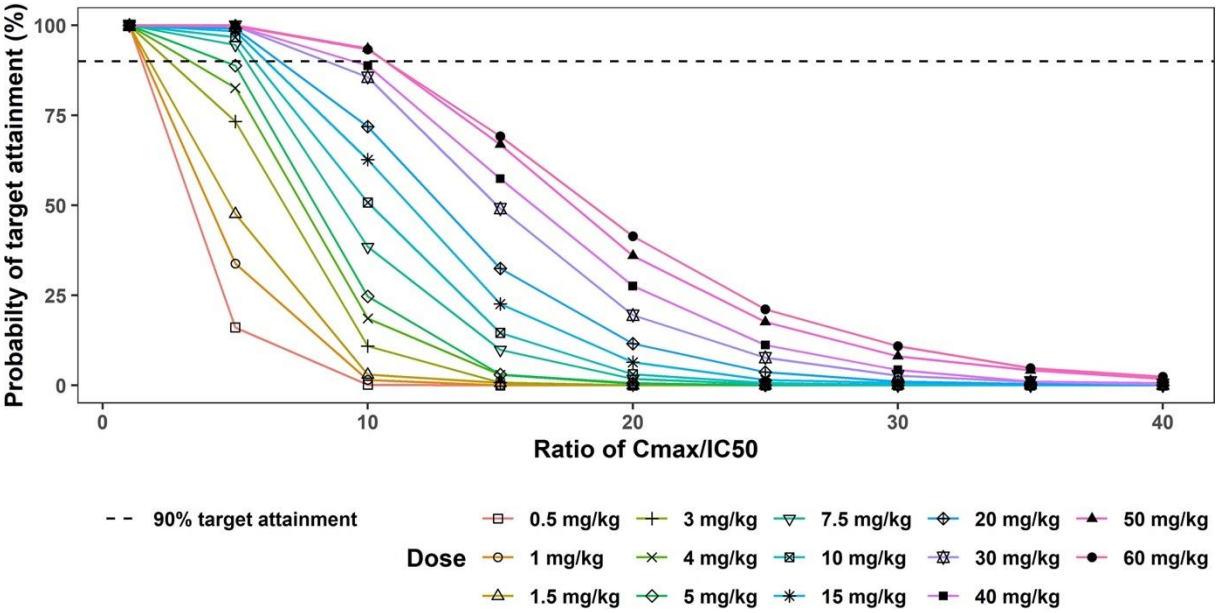

Figure 8 : Exemple de *probability of target attainment* de l'oxfendazole en fonction de différentes posologies d'après Bach et al. [78]

- *A posteriori* : En se basant sur les données individuelles observées (covariables et surtout les concentrations à un instant t) l'estimateur Bayésien basé sur le modèle de POPPK propose une estimation des paramètres PK individuels plus vraisemblables pour le patient.

- A partir des modèles de POPPK il est également possible de réaliser des simulations. Ces simulations peuvent être utilisés de différentes façons :

(i) diminuer le nombre de patients utilisés dans les essais cliniques [79]. Une étude clinique *in silico,* visant à étudier l'avantage de différents posologies d'insuline administré par inhalation sur le contrôle de la glycémie postprandial, a été mise en place [80]. Les résultats de cette étude ont contribué à l'acceptation de l'autorisation de mise sur le marché de ce traitement par la FDA.

(ii) développer d'autres modèles (pharmacocinétique de population, intelligence artificielle) [81–83]. En effet, de nombreuses études ont utilisé des simulations afin de développer des modèles plus performants sans augmenter le nombre de patients, quelle que soit la méthodologie utilisée (pharmacocinétique de population ou intelligence artificielle).

Licence CC BY-NC-ND 3.0

I.6. L'intelligence artificielle

L'intelligence artificielle peut être définie de différentes manières en fonction du point de vue de chacun. Marvin Lee Minsky, un des créateurs du concept de l'intelligence artificielle, définit celle-ci comme « une application capable de traiter des tâches qui sont, pour l'heure, réalisées de manière plus satisfaisante par des êtres humains dans la mesure où elles impliquent des processus mentaux de haut niveau comme l'apprentissage perceptuel, l'organisation de la mémoire et l'esprit critique ». Cette définition semble obsolète compte tenu que l'algorithme de Deep Learning AlphaGo a été capable de battre des humains au jeu chinois Go à 2 reprises (2015 et 2017). L'intelligence artificielle est un vaste domaine scientifique en constante évolution dont l'objectif est de créer des algorithmes de plus en plus complexes, se rapprochant de plus en plus du raisonnement humain, afin de réaliser une tâche.

I.6.1. Les différents types d'apprentissage et algorithmes dans l'intelligence artificielle

En intelligence artificielle, il existe 4 approches d'apprentissage des algorithmes de machine learning :

- Non supervisée
- Semi-supervisée
- Par renforcement
- Supervisée

L'approche non supervisée est nommée ainsi car la variable à prédire n'est pas définie préalablement. L'algorithme apprend à partir des données. Les données sont soit regroupées en fonction de leurs similarités (clustering de données comme avec les algorithmes k-means) soit en réduisant la dimensionnalité (analyse en composante principale). Ce type d'algorithme est utilisé dans différents domaines comme l'identification de groupes de clients par les entreprises ou encore l'identification de signaux de sécurité de pharmacovigilance [84].

L'approche semi-supervisée permet l'utilisation conjointe des approches supervisée et non supervisée. Différentes méthodologies peuvent être utilisées dans cette approche comme par exemple, celle du *self-training*. Dans un premier temps, l'algorithme non supervisé permet de résumer les données en les classifiant en groupes. Dans un second temps, les prédictions de l'étape non supervisée servent de variables prédictives pour l'algorithme supervisé.

L'apprentissage par renforcement, similairement à l'apprentissage d'un humain, permet à un algorithme d'affiner ses prédictions via ses expériences accumulés au cours du temps. En

Licence CC BY-NC-ND 3.0

fonction des actions menées, l'algorithme (ici nommé « agent ») reçoit des récompenses ou des pénalités. L'agent sait retenir les actions qui l'ont mené aux récompenses, jusqu'à atteindre son objectif final. L'agent ne reçoit aucune indication sur la manière de réaliser sa tâche, seule son expérimentation lui permettra d'apprendre. Il existe 2 principaux types, (i) le *temporal difference learning* (ou TD learning) et le (ii) Q-learning.

Dans l'approche supervisée, à l'inverse de l'approche non supervisée, la variable à prédire est étiquetée (exemple : prédiction de la catégorie « malade » / « non malade ») et l'algorithme recherche une solution à partir des autres variables disponibles. Les algorithmes supervisés permettent de résoudre des problèmes de régression (prédiction d'une variable quantitative) ou de classification (prédiction d'une variable qualitative).

En fonction du type d'algorithmes choisis, la solution pour prédire la variable étiquetée peut être de type linéaire (régression linéaire simple ou multiples), plan linéaire (SVM linéaires) ou encore sous forme d'arbres décisionnels (forets aléatoires [85] ou extreme Gradient Boosting (Xgboost) [86]).

Différents types d'algorithmes peuvent être utilisés afin de résoudre ces types de problèmes mais nous pouvons les classer en 3 grandes classes : (i) les modèles linéaires, (ii) les modèles basés sur les arbres, (iii) les réseaux de neurones.

- Les modèles linéaires généralisés permettent de prédire une variable à expliquer à partir de variables explicatives en utilisant des fonctions linéaires ou des plan linéaires. Il existe différents modèles linéaires ou plan linéaires : (i) la régression linéaire simple ou multiples permettant de résoudre principalement un problème de régression, (ii) la régression logistique, dérivée de la régression linéaire par l'intermédiaire d'une fonction logit où la fonction dépendante est binaire, afin de résoudre un problème de classification, (iii) les algorithmes de *support vector machine* (SVM) [87] ou *multivariate adaptative regression splines* (MARS) [88] permettent de résoudre des problèmes de classification en déterminant soit un plan linéaire simple soit multiple.
- Les modèles basés sur les arbres peuvent également résoudre les 2 types de problèmes (régression et classification). Il est parfois difficile d'interpréter ces types d'algorithmes car on ne connait pas la composition de la multitude d'arbres établis lors de l'apprentissage. Il existe 3 grands types d'algorithmes : (i) arbre de décision, l'algorithme va essayer de prédire en formant un arbre où chaque nœud correspondra à une variable prédictive. Une des limites de ces types d'algorithme est qu'il est

Licence CC BY-NC-ND 3.0

particulièrement sujet au sur-apprentissage [89], c'est-à-dire que l'algorithme apprend de manière optimale à prédire la variable étiquetée dans la base d'entrainement mais est difficilement généralisable, (ii) *random forest*, l'algorithme est composé de plusieurs arbres décisionnels entrainés successivement sur des sous-groupes de la population entière afin de prédire la variable d'intérêt. La prédiction est réalisée par vote majoritaire à partir des différents arbres (les différents arbres travaillent en parallèle). (iii) *gradient boosting*, à la différence du *random forest,* les arbres décisionnels ne sont pas utilisés en parallèle mais plutôt en série. Chaque arbre corrige les erreurs résiduelles des arbres précédents agrégés.

- les réseaux de neurones sont utilisés pour résoudre des problèmes difficiles comme reconnaitre une musique, l'animal sur une photo… Afin d'être performant, les réseaux de neurones nécessitent un nombre important de données ainsi qu'un temps important d'apprentissage. Il existe des réseaux de neurones en multicouches. La couche initial ou input layer en anglais permet de traiter initialement l'information comme digérer l'information apportée par chaque pixel d'une photo montrant un vase. Les couches intermédiaires de ces réseaux vont recevoir les informations de l'input layer. Chaque neurone va prédire une probabilité et transmettra le résultat à la couche suivante. Cette information se verra attribuer une fonction d'activation permettant de moduler la prédiction de ce neurone par rapport aux couches précédentes si le biais est trop important et ainsi de suite. Enfin chaque neurone de la dernière couche va prédire la probabilité de déterminer si l'objet est un vase ou non puis l'algorithme donnera une probabilité globale. Afin de maximiser l'apprentissage de l'algorithme, il existe un phénomène appelé rétropropagation du gradient ou « backpropagation ». C'est cette « backpropagation » qui va nuancer la fonction d'activation d'un neurone pour diminuer ou augmenter le poids de ses prédictions.

I.6.2. Utilisation de l'intelligence artificielle en model-informed precision dosing

Les algorithmes de machine learning sont de plus en plus utilisés en médecine [90] et la pharmacocinétique ne fait pas exception. A la date du 5 Septembre 2022 et depuis 2000, 2043 articles traitant de la pharmacocinétique et du machine learning ont été publiés. Le nombre de nouveaux articles publiés est d'ordre exponentiel.

Différentes méthodes d'utilisation du machine learning en *model-informed precision dosing* (MIPD) existent. En effet, les algorithmes peuvent faciliter le développement de modèles de POPPK avec notamment le choix du modèle structural [91,92], la détermination des covariables

Licence CC BY-NC-ND 3.0

significativement pertinentes pour le modèle [93] ou l'existence de sous-population réagissant différemment aux médicaments [94]. Ils peuvent également être utilisés pour établir des prédictions *a priori* en déterminant la dose initiale [95,96] ou pour prédire l'interdose d'administration d'un traitement [97]. Enfin une utilisation des algorithmes *a posteriori* a déjà été décrite pour prédire l'exposition à un médicament [81,98,99].

Depuis peu et devant l'opacité des algorithmes, certains auteurs développent des modèles hybrides composés d'un modèle de pharmacocinétique de population et d'un algorithme de population capable de réestimer les paramètres PK [100], de diminuer l'erreur d'estimation [83] ou de développer un algorithme permettant de choisir entre l'estimation du MAP-BE ou des *flatten prior* (diminution de la part des connaissances a priori) [101] ou de « de-shrinker les estimations des MAP-BE [83].

Le tacrolimus est donc une molécule possédant de nombreuses sources de variabilité ainsi qu'un intervalle thérapeutique étroit, nécessitant la mise en place d'un STP. Une faible variation de l'exposition du tacrolimus peut entrainer de nombreuses conséquences, soit une inefficacité en cas de sous-exposition, soit l'apparition d'effets indésirables en cas de surexposition comme une néphrotoxicité, neurotoxicité, diabète…

Concernant l'efficacité du tacrolimus, il existe une bonne corrélation avec la C0 toutefois le meilleur marqueur d'exposition au tacrolimus est l'AUC [32]. Ce qui rend sa mise en place en routine difficile. Pour ce qui est des effets indésirables, le choix des marqueurs d'exposition au tacrolimus afin prédire l'apparition de ceux-ci fait encore débat. Devant l'absence de consensus, il semble pertinent de suivre l'exposition au tacrolimus mais également d'autres marqueurs biologiques comme le DFG afin de prévenir l'apparition de néphrotoxicité.

L'utilisation d'outils comme la POPPK ou le machine learning peuvent faciliter le STP du tacrolimus et mais également le suivi du fonctionnement d'autres organes ou de l'exposition à un autre médicament comme l'isavuconazole afin de minimiser l'impact de ses effets indésirables.

Licence CC BY-NC-ND 3.0

Partie II. Résultats

II.1. IMPAKT Study: Clinical Pharmacokinetics and Bayesian Estimators for the Individual Dose Adjustment of a Generic Formulation of Tacrolimus in Adult Kidney Transplant Recipients

Articles publiés dans *Clinical Pharmacokinetics*

Ces travaux sont issus de l'étude IMPAKT (NCT03076151). La pharmacocinétique de l'Adoport®, formulation générique du Prograf® a été étudiée chez 29 patients ayant reçu une transplantation rénale *de novo*. Un modèle de pharmacocinétique de population ainsi qu'un estimateur Bayésien basé sur le *maximum a posteriori* (MAP-BE) utilisant une stratégie de prélèvement limités ont été développés. Les performances de ce nouvel MAP-BE ont été comparées aux performances du MAP-BE développé précédemment pour la formulation princeps [9].

Après avoir bénéficié d'une transplantation rénale *de novo*, 29 patients ont reçu de l'Adoport® comme un des traitements immunosuppresseurs. Trois cinétiques ont été réalisées chez ces 29 patients à J7, M1 et M3 post-transplantation. Chaque cinétique était composée de 9 prélèvements (0min, 20min, 40min, 1h, 2h, 3h, 4h, 6h et 9h). Un modèle de pharmacocinétique ainsi qu'un MAP-BE ont été développés pour chaque période.

Les résultats obtenus ont montré une très bonne estimation des concentrations individuelles (IPRED) ainsi qu'une distribution homogène des résidus pondérés quelle que soit la période post-transplantation (J7, M1 et M3). Toutefois, une légère surestimation des concentrations prédites par le modèle (PRED) est observée chez les patients expresseurs du CYP3A5. Six stratégies de prélèvements limités comprenant des prélèvements compris entre 0min et 6h après la prise de l'Adoport® ont été évaluées. Trois combinaisons différentes de 3 points ont montré des résultats similaires (0-1-2h ; 0-1-3h et 0-2-4h) quel que soit le statut génétique concernant le CYP3A5, avec toutefois une imprécision légèrement plus faible pour la stratégie 0-1-3h.

Enfin, ces résultats, obtenus grâce à ces nouveaux MAP-BEs, ont été comparés à ceux développés précédemment pour la spécialité Prograf®. Les MAP-BEs développés pour le Prograf® ou l'Adoport® ont montré des résultats similaires. Ces résultats confirment les résultats de bioéquivalence entre le Prograf® et son générique, l'Adoport®. Les résultats obtenus peuvent questionner sur l'utilisation généralisée des modèles de POPPK et MAP-BEs développés avec le princeps chez des patients prenant la formulation générique. Dans une étude de

Licence CC BY-NC-ND 3.0

bioéquivalence, Robertsen et al. ont montré, une discordance entre l'exposition obtenue avec le princeps (Prograf®) et un de ses génériques chez les patients transplantés âgés de plus de 60 ans [102]. Les auteurs observaient une surexposition lors de l'utilisation de la forme générique avec un rapport AUC générique/princeps= 1,17 ainsi qu'un délai plus court pour atteindre la concentration maximale. Ainsi la prudence est de mise concernant l'utilisation de modèles de POPPK chez des patients prenant une formulation générique et la similarité des paramètres PK obtenus (AUC, Cmax, Tmax) entre les 2 formulations doit être vérifiée avant toute utilisation.

Dans le modèle développé, aucune covariable n'a été retenue et la question de leur influence sur les prédictions individuelles peut être posée. En effet, de très bonnes performances d'estimation des concentrations individuelles ou de l'AUC ont été obtenues. Ces résultats confirment les propos de Sheiner et al.[70] qui explique que dès lors qu'un prélèvement individuel est disponible, l'information apportée est plus importante que celle apportée par l'ajout de n'importe quelle covariable.

Licence CC BY-NC-ND 3.0

Clinical Pharmacokinetics
https://doi.org/10.1007/s40262-020-00959-y

ORIGINAL RESEARCH ARTICLE

Clinical Pharmacokinetics and Bayesian Estimators for the Individual Dose Adjustment of a Generic Formulation of Tacrolimus in Adult Kidney Transplant Recipients

Pierre Marquet[1,2] · Alexandre Destère[1,2] · Caroline Monchaud[1,2] · Jean-Philippe Rérolle[2,3] · Matthias Buchler[4] · Hakim Mazouz[5] · Isabelle Etienne[6] · Antoine Thierry[7] · Nicolas Picard[1,2] · Jean-Baptiste Woillard[1,2] · Jean Debord[1,2]

Accepted: 30 October 2020
© Springer Nature Switzerland AG 2020

Abstract

Background Tacrolimus has a narrow therapeutic range and requires dose adjustment, usually based on the trough blood concentration but preferably on the area under the concentration–time curve over 12 h post-dose ($AUC_{0–12h}$). The single-arm, multicentre, clinical study IMPAKT aimed: (i) to develop, in de novo kidney transplant recipients, pharmacokinetic models and maximum a-posteriori Bayesian estimators for a generic, immediate-release, oral formulation of tacrolimus to estimate tacrolimus $AUC_{0–12h}$ at different post-transplant periods using a limited sampling strategy, and considering the *CYP3A5*3* polymorphism as a covariate and (ii) to compare the performance of these Bayesian estimators to those previously developed for the original formulation.

Methods Thirty patients were enrolled and 29 provided nine blood samples over 9 h at day 7 and months 1 and 3 post-transplant. Tacrolimus blood profiles measured with liquid chromatography-tandem mass spectrometry were modelled using one-compartment, double gamma absorption, linear elimination models developed in-house. Different limited sampling strategies of three time-points within 4 h post-dose were tested for the maximum a-posteriori Bayesian estimator of tacrolimus $AUC_{0–12h}$. The models and estimators were validated internally and their performance compared to that of models previously developed for the original formulation.

Results The concentration–time curves, $AUC_{0–12h}$/dose and trough blood concentration/dose exhibited wide inter-individual variability. The covariate-free pharmacokinetic models developed for the three post-transplant periods closely fitted the individual profiles. Maximum a-posteriori Bayesian estimators based on three different limited sampling strategies and no covariate yielded accurate $AUC_{0–12h}$ estimates, including for the five cytochrome P450 3A5 expressers and for the four patients without corticosteroids. The 0–1 h–3 h strategy finally chosen had very low bias (– 4.0 to – 2.5%) and imprecision (root mean square error 5.5–9.2%). The maximum a-posteriori Bayesian estimators previously developed for the reference product fitted the generic profiles with similar performance.

Conclusions We developed original pharmacokinetic models and accurate maximum a-posteriori Bayesian estimators to estimate patient exposure and adjust the dose of generic tacrolimus, and confirmed that the robust tools previously developed for the original formulation can be applied to this generic.

Electronic supplementary material The online version of this article (https://doi.org/10.1007/s40262-020-00959-y) contains supplementary material, which is available to authorized users.

✉ Pierre Marquet
pierre.marquet@unilim.fr

Extended author information available on the last page of the article

Published online: 24 November 2020

Adis

Licence CC BY-NC-ND 3.0

Key Points

This paper reports the first population pharmacokinetic models and Bayesian estimators developed for Adoport®, a generic oral formulation of tacrolimus

A one-compartment, double gamma absorption, linear elimination model closely fitted the individual profiles

Bayesian estimators combined with the 0–1 h–3 h limited sampling strategy yielded accurate and precise estimation of the area under the concentration–time curve over 12 h post-dose

Pharmacokinetic models and Bayesian estimators previously developed for the original formulation fitted Adoport® profiles and estimated the inter-dose area under the concentration–time curve as well as the ad hoc tools

These tools are now available to the kidney transplant community through the ISBA expert system: https://pharmaco.chu-limoges.fr

1 Introduction

The bioequivalence of generic drugs with the reference product has to be demonstrated in healthy volunteers on the basis of the area under the concentration–time curve (AUC) and maximal concentration of the concentration–time profile, generally after a single drug dose. This standard scheme cannot guarantee that the generic formulation will yield the same pre-dose concentration at steady state, i.e. after repeated dosing, even less so in patients. This may be of concern for narrow therapeutic index drugs, in particular those requiring therapeutic drug monitoring, which is often based on the drug pre-dose blood concentration. The fact that some of these drugs can be dose adjusted based on their inter-dose AUC can be reassuring in this respect, as the AUC is one of the bioequivalence criteria, but it still raises the question of the applicability of the tools developed for AUC estimation of the reference product to generic formulations.

Tacrolimus is a calcineurin inhibitor widely used for the prevention of allograft rejection in solid organ transplantation, as well as in other indications across the world [1]. It is characterised by a narrow therapeutic index and large inter-individual pharmacokinetic (PK) variability. Therapeutic drug monitoring is recommended for tacrolimus (and is even compulsory in many countries) to minimise the risk of acute rejection and the occurrence of adverse effects (mainly nephrotoxicity and, to a lesser extent, neurotoxicity) and it is generally based on trough whole blood tacrolimus concentrations (C_0). However, retrospective studies showed that C_0 was not [2–4], or was only slightly [5], associated with acute graft rejection in kidney or liver transplant recipients. In contrast, a few papers reported that tacrolimus AUC was significantly associated with acute rejection [6, 7]. The recent consensus report of a consortium of European experts on tacrolimus therapeutic drug monitoring recommended using the inter-dose AUC over 12 h post-dose ($AUC_{0–12h}$), as it is expected to be the best marker of tacrolimus exposure [1]. Actually, tacrolimus monitoring based on the full $AUC_{0–12h}$ is difficult to set up routinely, owing to clinical constraints and the necessity of multiple samples. Our and other groups previously reported PK models and Bayesian estimators to calculate tacrolimus inter-dose AUC using a limited sampling strategy (LSS), i.e. a few blood samples collected in the first hours post-dose, for three different tacrolimus formulations in different transplant settings [8–15]. We have proposed them to the transplant community though a free website since 2007 and reported the results obtained in hundreds of patients [16, 17].

One of the most important sources of inter-individual variability in tacrolimus pharmacokinetics is a single nucleotide polymorphism within intron 3 of cytochrome P450 (CYP) 3A5, a metabolic enzyme expressed in the intestinal mucosa and the liver highly involved in the oral tacrolimus first-pass effect. Patients who carry at least one *CYP3A5*1* allele (CYP3A5 expressers, about 12% of the white European population [18]) show a 1.5- to two-fold higher tacrolimus oral clearance than *CYP3A5*3/*3* carriers (non-expressers) [1]. Corticosteroids that induce CYP450s and P-glycoprotein might also affect tacrolimus pharmacokinetics [19].

Adoport® (Sandoz, Levallois-Perret, France) is a generic, twice-daily, immediate-release formulation of tacrolimus, whose pharmaceutical equivalence and bioequivalence with the reference product Prograf® (Astellas Pharma, Levallois-Perret, France) was demonstrated in healthy volunteers as well as in a kidney transplant population [20]. However, it has never been demonstrated that the PK tools (including Bayesian estimators) developed and used in a clinical setting for an original formulation can also be used for its generics. For instance, the LSSs used with maximum a posteriori Bayesian estimation (MAP-BE) generally include sampling points on both sides of the peak, i.e. before and after the time to maximum concentration (T_{max}), while bioequivalence studies cannot guarantee that T_{max} is similar between formulations (no statistical tests are required by the regulatory agencies for T_{max}). This question is of particular importance for patient security and our liability in the context of the ISBA expert system (as well as similar web services), where on the one hand, one cannot guarantee that all patients are actually on the original formulation and,

Licence CC BY-NC-ND 3.0

on the other hand, one cannot continue to refuse patients on generic formulations.

The objectives of the present clinical study were: (i) to develop, in de novo kidney transplant recipients on this generic formulation, population PK models and Bayesian estimators enabling the assessment of tacrolimus $AUC_{0–12h}$ at different post-transplant periods, on the basis of a limited number of samples collected during the first few hours post-dose, and considering the *CYP3A5*3* polymorphism and corticosteroid cotreatment as covariates, if possible and useful, and (ii) to compare the performance of these MAP-BEs and LSSs to those we previously developed for the original formulation.

2 Material and Methods

2.1 Study Design and Patient Population

The "Pharmacokinetic Study of Adoport® (Tacrolimus) in Patients With de Novo Kidney Transplantation" (IMPAKT) study was sponsored by Limoges University Hospital, funded by Sandoz France, authorised by the Ethics Committee CPP16-058 on 8 December, 2016 and registered on ClinicalTrials.gov (Identifier: NCT03076151, registered on 6 March, 2017). We enrolled 30 kidney transplant recipients on immunosuppression regimes including Adoport®, from five French kidney transplant centres (university hospitals of Amiens, Clermont-Ferrand Limoges, Poitiers and Tours). Patients had to be aged > 18 years, male or female, recipients of a first kidney graft, transplanted for less than 7 days at the time of enrolment, affiliated to a health insurance system and they had to sign the study informed consent form. The exclusion criteria were: all contraindications to tacrolimus according to the summary of product characteristics; patients with pre-transplant, donor-specific, anti-human leukocyte antigen antibodies; recipients of any allograft other than the kidney; pregnant (positive β-HCG test) or lactating women; women without any method of contraception, except for those with no childbearing potential (according to the guidelines of the Clinical Trial Facilitation Group, related to contraception and pregnancy tests in clinical trials) [21]; patients participating in any other interventional clinical study; patients under judicial protection; and patients unable to understand the purposes and risks of the study, who could not provide written informed consent or who were unwilling to comply with the study protocol.

Each patient had to participate in three PK investigations, at 7 ± 3 days (D7), 1 month ± 1 week (M1) and 3 months ± 1 week (M3) post-transplantation. During each of these study visits, nine blood samples were collected in EDTA tubes, just before (C0) and then 20 and 40 minutes, 1, 2, 3, 4, 6 and 9 h after the morning dose of generic tacrolimus administration.

2.2 Tacrolimus Determination and Pharmacokinetic Modelling

Tacrolimus blood determination was centralised at the Laboratory of Pharmacology-Toxicology of Limoges University Hospital (CHU Limoges) and performed using a fully validated, liquid chromatography–tandem mass spectrometry technique, as previously described [11]. Briefly, after precipitation of 100 µL of whole blood with 25 g/L of zinc sulphate in water/methanol (70:30, v/v), tacrolimus was extracted and separated using two-dimension high-performance liquid chromatography and detected using tandem mass spectrometry in the positive-ion, selected reaction monitoring mode. [^{13}C,D_2]-Tacrolimus was employed as the internal standard. The lower limit of quantification was 1 ng/mL, the method was linear between 1 and 100 µg/L (r > 0.99) and the intra- and inter-day coefficients of variation (CV%) were < 18%.

Pharmacokinetic modelling was performed using a parametric approach in the iterative two-stage individual modelling software (developed locally by one of us, JD). We used a single-compartment model with linear elimination, and biphasic absorption, as previously described for other formulations of tacrolimus in different transplant settings [8, 10, 14, 15].

In this model, the absorption rate at time t is described as the sum of two gamma distributions:

$$V_{abs}(t) = F \times D[r \times f_1(t) + (1-r) \times f_2(t)]$$

With

$$fi(t) = \frac{b^{a_i}}{\Gamma(a_i)}.t^{a_i-1}.\exp(-b_i.t)$$

The estimated population parameters were: $\hat{C}_0$, the model-estimated trough concentration after administration of a theoretical dose D_0 = 1000 mg (the real trough concentration can be calculated by dividing this value by 1000 and multiplying by the patient dose); MAT1 and MAT2, the mean absorption times of the two absorption phases (defined as $\frac{a_i}{b_i}$); SDAT1 and SDAT2, the standard deviations of absorption times (defined as $\frac{\sqrt{a_i}}{b_i}$); r, the fraction of the dose absorbed by the faster method; $FA_{IV} = F \times D_0/V_d$, where F is the bioavailability factor, A_{IV} is the intravenous coefficient, V_d is the volume of distribution, and b is the elimination constant. The error model used was $0.0001 + 0.05 \times C$ (C = drug concentration). Different sets of parameters were estimated for the different post-transplantation periods (D7, M1 and M3). The robustness of the model was checked using the

Licence CC BY-NC-ND 3.0

traditional predicted vs observed and individually predicted vs observed concentrations, and the weighted residuals vs time. The stability of the results was investigated using iterative random splitting of the database (circular permutation) to obtain at each round one group for model development (75% of the concentration vs time profiles) and another group for model validation (the remaining 25% profiles). Additionally, the final models were evaluated using visual predictive checks after 1000 Monte-Carlo simulations and extraction of their 90% prediction intervals, using the vpc R package (https://CRAN.R-project.org/package=vpc).

The optimal combinations of sampling times for Bayesian estimation were obtained by comparing the accuracy and precision of tacrolimus $AUC_{0–12h}$ estimates obtained with several combinations of three sampling times within the first few hours post-dose, as compared to the reference tacrolimus $AUC_{0–12h}$ obtained using all available time-points. In addition, we evaluated the ability of Bayesian estimators previously developed for the reference product [16] to predict tacrolimus AUCs measured in patients on the generic formulation in the present study.

2.3 Cytochrome P450 3A5 Genotyping

Genotyping of *CYP3A5*3* was also centralised in the Department of Pharmacology-Toxicology at Limoges University Hospital. DNA was isolated from EDTA-treated blood and genotyped for CYP3A5 rs776746 (CYP3A5*1/*3 allele) using a validated TaqMan allelic discrimination assay on a Rotor Gene Q® (Qiagen, Courtaboeuf, France), as previously described [22].

2.4 Statistical Analysis

The performance of the population PK models was evaluated by linear regression of measured vs estimated concentrations in the validation set (successive subgroups of 25% patients not involved in model development). The performance of the models in the subgroups of CYP3A5 expressers and patients without corticosteroids was checked by visually comparing them on the diagnostic plots with the predominant group of non-expressers on corticosteroids.

We used a two-way analysis of variance (patients*LSS) followed by the Dunnett's multiple comparison test to compare the different LSS for MAP-BE of tacrolimus $AUC_{0–12h}$ with the reference $AUC_{0–12h}$ obtained using all time-points. For those providing estimates not statistically different from the references, we calculated the relative mean prediction error, or bias, and the relative root mean square error (RMSE). For the LSS finally selected, we computed the correlation and difference (Bland–Altman) plots with the reference, the minimum and maximum differences, the bias, RMSE and the number of differences out of the ± 20% acceptable range. The performance of the Bayesian estimators in patients carrying the minor CYP3A5*1 allele or receiving no corticosteroids was assessed visually on the correlation and Bland–Altman plots, but no statistical test was performed because of their small numbers in our population.

3 Results

One patient was withdrawn from the study owing to numerous severe adverse events (AEs), before any PK profile was collected. The other 29 patients completed the study and their characteristics are described in Table 1. Twenty-three patients received tacrolimus in combination with mycophenolate mofetil and 26 with corticosteroids at one study visit at least, whereas only two received tacrolimus as a monotherapy over the whole study period. The average tacrolimus daily dose decreased from 9.4 mg on day 7 to 6.2 mg at month 3 (with up to eight-fold variability across the study population at M1 and M3), while C_0 and $AUC_{0–12h}$ tended to increase at M1 and decrease at M3. Plasma creatinine, haematocrit and haemoglobin improved over time (Table 1). The AEs reported by the investigators are reported in Table 1 of the Electronic Supplementary Material (ESM). All patients except for one had at least one AE, with a total of 260 AEs reported, 24 of which were considered as serious AEs. However, none of these serious AEs was deemed attributable to tacrolimus by the investigators and the Clinical Trial Pharmacovigilance Unit of Limoges University Hospital. Three acute graft rejection episodes were reported in three patients, two of which were confirmed by a biopsy (both categorised as acute T-cell-mediated rejection, grade 1b). These acute rejection episodes occurred 2 weeks, 3 weeks and 3 months post-transplantation.

A total of 87 PK profiles of tacrolimus were analysed. The concentration–time curves of Adoport® exhibited large inter-individual variability at each time period, and so did C_0 (CV% = 38%, 35% and 26% at D7, M1 and M3, respectively) and $AUC_{0–12h}$ (CV% = 32%, 31% and 26%, respectively). The variability was even larger for C_0/dose (CV% = 47%, 76% and 43%, respectively) and $AUC_{0–12h}$/dose (CV% = 41%, 65% and 40%, respectively). In contrast, the AUC/C_0 ratio showed much lower inter-individual variability (CV% = 21%, 18% and 18%, respectively) and intra-individual variability over the first 3 months post-transplant (CV% = 14%).

Reasonable correlation was found between morning C_0 and the reference $AUC_{0–12h}$ at all post-transplant periods (r^2 = 0.6857 at D7, 0.7912 at M1 and 0.6441 at M3) (Fig. 1). Accordingly, the $AUC_{0–12h}/C_0$ ratio varied mildly with time and between patients: mean (inter-individual CV%) = 18.58 h (21.31%) at D7, 18.17 h (18.36%) at M1 and 18.28 h (17.89%) at M3. The mean $AUC_{0–12h}/C_0$ ratio was

Licence CC BY-NC-ND 3.0

Table 1 Demographic characteristics of the per-protocol population ($n = 29$), laboratory test results, and tacrolimus dose and exposure

Characteristic	Value
Patient characteristics at enrolment ($n = 29$)	
Age (years)	59 (30–76)
Sex, *n*)	
Male	22
Female	7
Bodyweight (kg)	78 (61.1–116)
CYP3A5 genotype (*n*)	
*1/*1	2
*1/*3	3
*3/*3	19
Unknown	5
Day 7 ($n = 29$)	
Tacrolimus daily dose (mg)	9.4 (4–14)
Tacrolimus morning C_0 (mg/L)	9.3 (3.1–16.3)
Tacrolimus $AUC_{0-12\,h}$ (h mg/L)	166 (80–313)
Hematocrit (%)	27.8 (21.3–36.7)
Hemoglobin (g/dL)	9.2 (7.1–12.1)
Creatinine (μmol/L)	320 (94–1021)
Co-medications (*n*)	
MMF	23
Corticosteroids	26
Month 1 ($n = 29$)	
Tacrolimus daily dose (mg)	9.2 (2–19)
Tacrolimus morning C_0 (mg/L)	10.4 (5.1–23.0)
Tacrolimus $AUC_{0-12\,h}$ (h·mg/L)	186 (111–371)
Hematocrit (%)	33.1 (23.1–43.0)
Hemoglobin (g/dL)	10.7 (7.6–13.3)
Creatinine (μmol/L)	170 (80–325)
Co-medications (*n*)	
MMF	22
Corticosteroids	25
Month 3 ($n = 29$)	
Tacrolimus daily dose (mg)	6.2 (2–15)
Tacrolimus morning C_0 (mg/L)	8.0 (1.5–10.7)
Tacrolimus AUC_{0-12h} (h·mg/L)	141 (36.9–203.6)
Hematocrit (%)	37.8 (23.0–49.7)
Hemoglobin (g/dL)	12.2 (6.9–16.4)
Creatinine (μmol/L)	153 (77–384)
Co-medications (*n*)	
MMF	22
Corticosteroids	25

AUC_{0-12h} area under the concentration–time curve over 12 h post-dose, *C_0* trough blood concentration, *CYP* cytochrome P450, *MMF* mycophenolate mofetil

not different in CYP3A5 expressers and/or patients not on steroids, as compared with the other patients (20.5 h vs 18.8 h, respectively) and the datapoints of these patients were not further apart in the AUC_{0-12h} vs C_0 regression lines than the

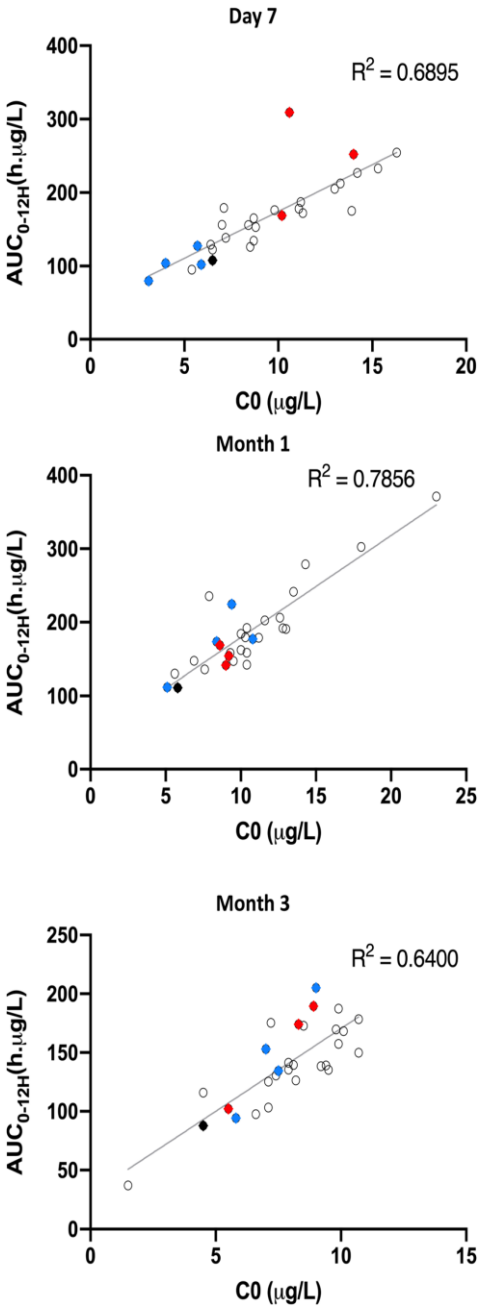

Fig. 1 Linear regression and correlation between tacrolimus C_0 and AUC_{0-12h} at the different post-transplant periods. The 4 patients carrying the *CYP3A5*1* allele (i.e. CYP3A5 expressers) and who received corticosteroids are represented with blue diamonds, the only CYP3A5 expresser without steroids with black diamonds and the CYP3A5 non-expressers (or presumably so, for one) without steroids with red diamonds

Licence CC BY-NC-ND 3.0

others (Fig. 1). One of the five CYP3A5 expressers experienced T-cell-mediated graft rejection on day 21 post-transplant, i.e. 2 weeks after the D7 visit where the tacrolimus AUC was 108 h·µg/L and 1 week before the M1 visit where the AUC was 111 h·µg/L (as compared to mean values of 166 and 186 h·µg/L in the study population, respectively). However, the other two rejection episodes were reported in non-expressers, one at week 2 just after a very high AUC value (247 h·µg/L) and the other at M3 with AUC = 137 h·µg/L (for a population average of 141 h·µg/L).

The three PK models developed (one for each of the three post-transplant periods) adequately described the data, as shown by the goodness-of-fit plots (Fig. 2). The model-predicted concentrations were clearly overestimated in the five CYP3A5 expressers, whether on corticosteroids ($n = 4$) or not ($n = 1$), but the individually predicted concentrations were as tightly fitted by the model as those of the dominant group of non-expressers on corticosteroids ($n = 23$) and the weighted residuals were very similar. The three other patients not on steroids were CYP3A5 non-expressers (or presumably so for one of them who was not genotyped) and their model-predicted concentrations were not significantly different from, and the individually predicted concentrations and Weighted residuals (WRES) as good as, those of the other non-expressers, confirming that corticosteroids had no significant influence on tacrolimus pharmacokinetics in this study. The visual predictive checks showed that the simulated data matched the observed concentration–time profiles for the three post-transplant periods (Fig. 3).

Bayesian AUC estimates obtained with six different three-point LSSs were compared with the reference AUC values using a two-way analysis of variance (patients*LSS),

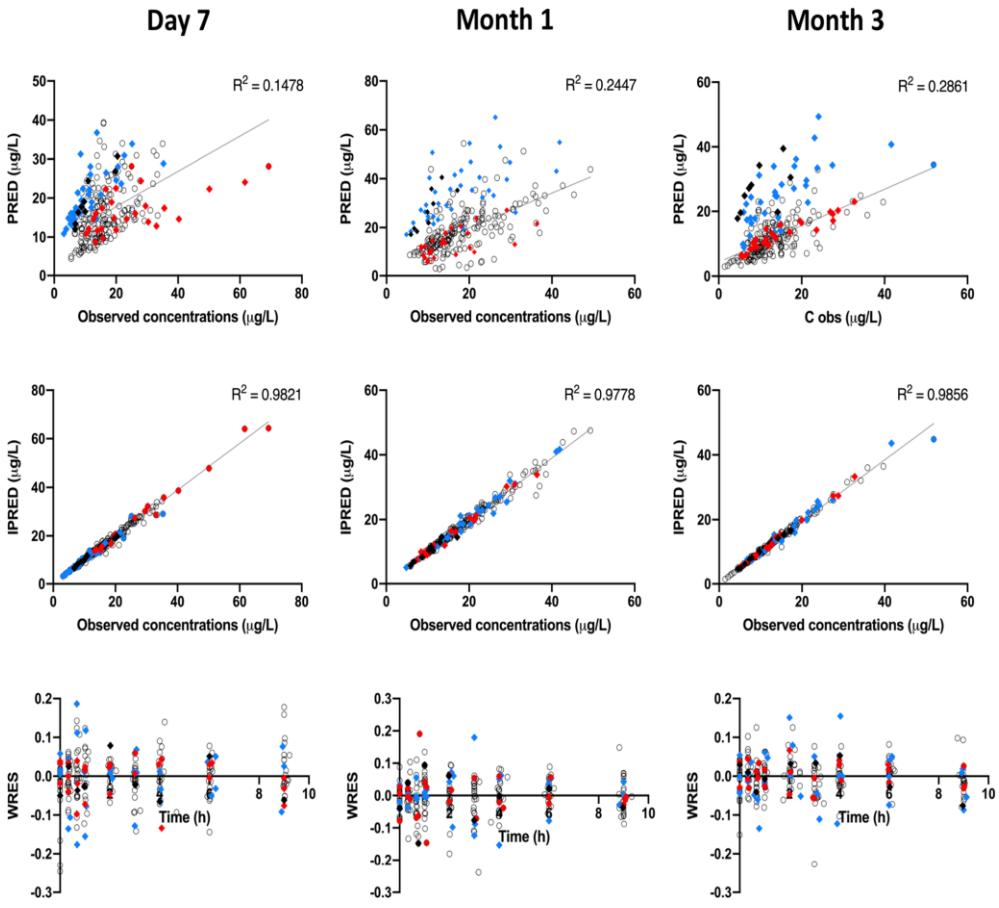

Fig. 2 Diagnostic plots of the population pharmacokinetic models. The 4 patients carrying the *CYP3A5*1* allele (i.e. CYP3A5 expressers) and who received corticosteroids are represented with blue diamonds, the only CYP3A5 expresser without steroids with black diamonds and the CYP3A5 non-expressers (or presumably so, for one) without steroids with red diamonds

Licence CC BY-NC-ND 3.0

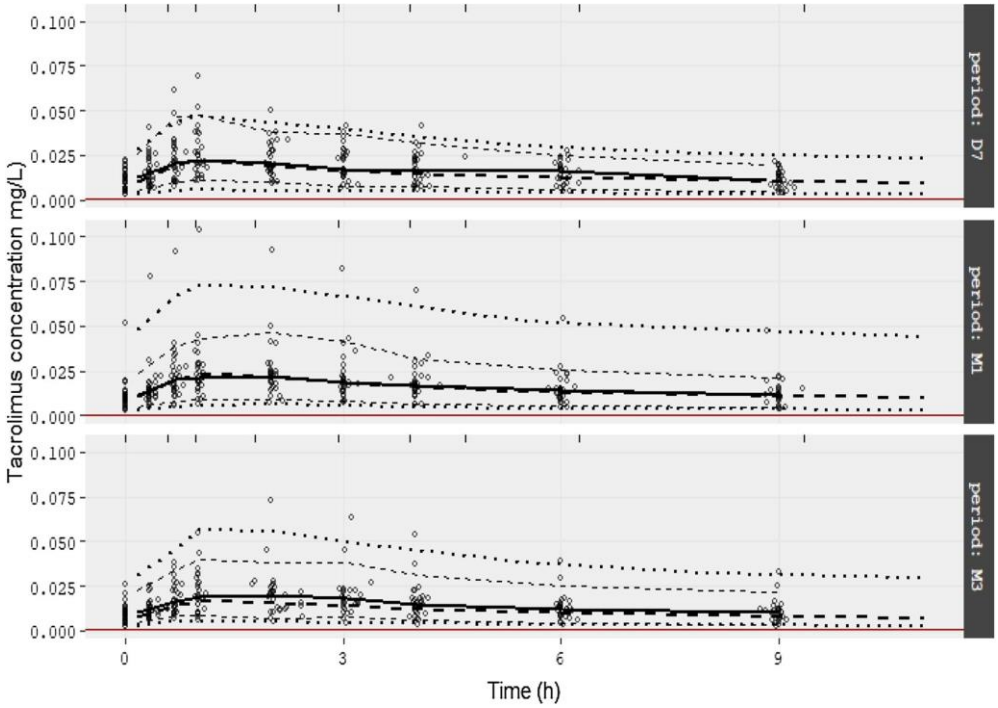

Fig. 3 Visual predictive checks of the PK models developed for generic tacrolimus for the three different post-transplant periods (day 7, month 1 and month 3)

Table 2 Dunnett's multiple comparison tests of the accuracy of different limited sampling strategies as compared to the reference area under the concentration–time curve values

Limited sampling strategy	Mean difference	Adjusted *p* value
All points vs 3 points 0–1 h–2 h	− 0.001614	0.8426
All points vs 3 points 0–1 h–3 h	− 0.003189	0.2317
All points vs 3 points 0–2 h–3 h	− 0.004431	0.0409
All points vs 3 points 0–2 h–4 h	− 0.002116	0.6360
All points vs 3 points 0–3 h–4 h	− 0.004166	0.0622
All points vs 3 points 0–3 h–6 h	− 0.004346	0.0470

h hours

showing significant between-patient variability ($p < 0.0001$) but only a trend for differences among the LSSs ($p = 0.0641$). Dunnett's multiple comparisons showed that the 0–1 h–2 h, 0–1 h–3 h and 0–2 h–4 h LSS yielded estimates not statistically different from the reference AUCs (Table 2). The Bland–Altman plots (Fig. 4) and the very similar mean prediction error (1.1%, 2.0% and 1.2%, respectively) and RMSE (9.2%, 7.8% and 8.6%, respectively) suggest that these strategies are equally acceptable, including for the patients carrying the CYP3A5*1 allele and/or without corticosteroids. Owing to its better Bland–Altman plot (Fig. 4) and lower RMSE, and for the sake of consistency with the LSS used routinely for the original formulation, we finally chose the 0–1 h–3 h LSS for the rest of this study. The AUC estimates obtained in the validation set obtained by circular permutation showed a bias between 0.2 and 3.6%, and imprecision RMSE between 6.0% and 8.6%, depending on the post-transplant period. Only one AUC value at M1, and two at M3, were estimated with inaccuracy >20% (Table 3). The best and worst AUC estimates at each post-transplant period are presented in Fig. 5. The PK models and Bayesian estimators previously developed for the reference product were able to fit closely the full concentration–time profiles obtained with the generic formulation Adoport® (Figs. 1 and 2 of the ESM), as well as to estimate accurately the $AUC_{0–12h}$ using the same LSS (Table 3).

4 Discussion

We conducted a PK study of Adoport®, a generic formulation of tacrolimus in adult kidney transplant recipients and developed PK models and Bayesian estimators, with the aim of estimating, at early (day 7) and more stable (months 1 and 3) post-transplant periods, tacrolimus $AUC_{0–12h}$ on the basis of a limited number of samples collected during the first few

Licence CC BY-NC-ND 3.0

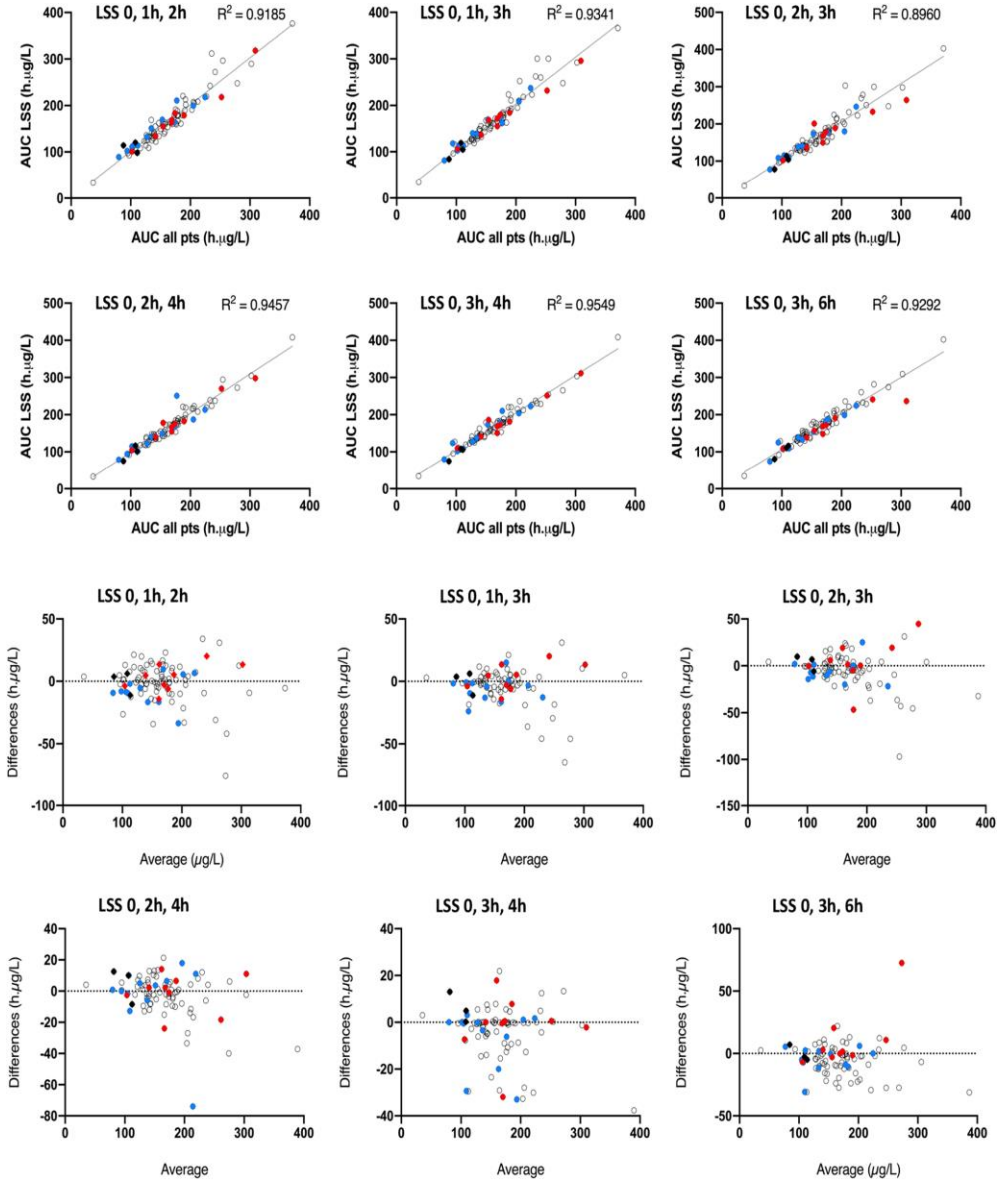

Fig. 4 Linear regression and Bland-Altman plots showing the correlation and the relative difference between reference AUCs and Bayesian AUCs obtained using different 3-point strategies (limited to the first 4 hours post-dose). The 4 patients carrying the *CYP3A5*1* allele (i.e. CYP3A5 expressers) and who received corticosteroids are represented with blue diamonds, the only CYP3A5 expresser without steroids with black diamonds and the CYP3A5 non-expressers (or presumably so for one) without steroids with red diamonds

hours post-dose. The PK models obtained showed excellent fit with the observed profiles. In addition, the Bayesian estimators and the LSS previously developed in a similar population for Prograf®, the reference product, showed almost identical performance in this study. It is important to acknowledge that, in addition to being bioequivalent with Prograf®, the generic formulation tested in this study yields very similar T_{max} values, as previously shown in a bioequivalence study in kidney transplant recipients [20], which may represent favourable conditions for the application of our initial Bayesian estimators. The question as to whether this can be extrapolated to all generic formulations of immediate-release tacrolimus, particular those with a shift in T_{max} or more variable T_{max}, should be further investigated. However,

Licence CC BY-NC-ND 3.0

Table 3 Overall performance of the Bayesian estimation of tacrolimus area under the concentration–time curve over 12 hours post-dose using the 0–1h–3h limited sampling strategy (LSS) and the models developed for the generic formulation in the current study (internal validation by circular permutation) or the models previously developed for the original formulation drug (cross-validation)

	MAP-BE developed for the generic formulation with the LSS 0–1 h–3 h			MAP-BE previously developed for the original formulation with the LSS 0–1 h–3 h		
Post-transplant period	Day 7	Month 1	Month 3	Day 7	Month 1	Month 3
MPE, or bias, %	2.1	0.2	3.7	− 2.8	− 2.1	− 4.0
Min/max errors, %	− 8.0/18.1	− 11.5/27.5	− 8.0/25.3	− 18.0/5.8	− 19.3/11.7	− 23.2/13.3
RMSE, %	6.0	8.6	8.5	6.2	7.3	9.5
No. of patients with error outside the acceptable range of ± 20%	0	2	1	0	0	1

h hour, *MAP-BE* maximum a posteriori Bayesian estimation, *max* maximum, *Min* minimum, *MPE* mean prediction error, *RMSE* root mean square error

several LSSs yielded equivalent performance for $AUC_{0–12h}$ estimation in the present study, confirming that Bayesian estimation is flexible with respect to sampling times and suggesting that it can cope with situations where T_{max} is not framed by the time-points (such as with the 0–2 h–4 h LSS for instance, where all time-points are after the peak for most patients). Altogether, the present results are very reassuring with regard to the thousands of individual dose adjustment requests posted on the ISBA website (https://pharmaco.chu-limoges.fr). Indeed, even if it was clearly stated that the tools available were only valid for the reference product and that the drug brand had to be completed on the request form, we could not be sure that all patients actually received the original formulation.

Similar to all the other formulations of tacrolimus, Adoport® oral administration in kidney transplant patients resulted in wide inter-individual variability of the concentration–time curves at each time period. Even in this rather small patient cohort, dose-standardised $AUC_{0–12h}$ varied five-fold on day 7, 11-fold at month 1 and eight-fold at month 3 post-transplantation, owing to the individual dose adjustments required to obtain exposure in a narrower range. Remarkably, the AUC/C_0 ratio varied much less between patients (only two-fold at all time periods) and was very stable with time (intra-individual CV% = 14%). We have recently recommended using this metrics to determine individual C_0 targets based on AUC and C_0 determination at least twice, in the early and stable post-transplant periods [1, 17, 23]. The current findings are in favour of the robustness of the AUC/C_0 ratio and also show that the individual relationship between C_0 and AUC does not vary much over time.

Three rejection episodes were reported in the per-protocol population of 29 patients, one of whom was a CYP3A5 expresser and had rather low tacrolimus exposure, whereas the other two had normal or high AUCs. No clear conclusion can be made about the exposure–efficacy relationship, so much so that the study was not powered for this.

Owing to a 12% frequency in the White European population, about four carriers of the CYP3A5*1 allele were expected in this study, and we found five expressers out of 25 patients whose genotype was available. The AUC vs C_0 regression, AUC/C_0 ratio, PK models and Bayesian estimators developed were specifically evaluated in this subgroup, showing equivalent behaviour and performance as compared to the rest of the population. Similarly, only four patients did not receive steroids over the course of the study (except a bolus of methylprednisolone on day 21 for one of them), one of whom carried the CYP3A5*1 allele. The model-predicted concentrations were not different in this small subgroup from those of the dominant group of non-expressers on corticosteroids ($n = 23$) and their AUC vs C_0 regression, AUC/C_0 ratio, and Bayesian estimators showed equivalent behaviour and performance, suggesting that the influence of corticosteroids on tacrolimus was negligible in this study. This prevented us from trying to develop specific PK models and Bayesian estimators for this subpopulation, or even to use the CYP3A5 genotype or treatment with corticosteroids as covariates in the models or estimators. More importantly, this study confirms that robust PK models and Bayesian estimators can accurately estimate the inter-dose AUC of a drug with high inter-patient PK variability without considering covariates as strong as the CYP3A5 genotype (that doubles tacrolimus oral clearance in expressers). With our strategy of designing models and Bayesian estimators for each combination of transplanted organ, age group (paediatrics or adults), post-transplant period (early or stable) and analytical method [24], and with the three-point LSS employed, we never found additional covariates that could improve Bayesian AUC estimation or help to reduce the number of sampling points [8–15]. This confirms the reference demonstration made more than 40 years ago by Sheiner et al. for digoxin that "information from plasma concentrations is far more valuable for forecasting than that from observable patient features-sex, age, and the like; use of all

Licence CC BY-NC-ND 3.0

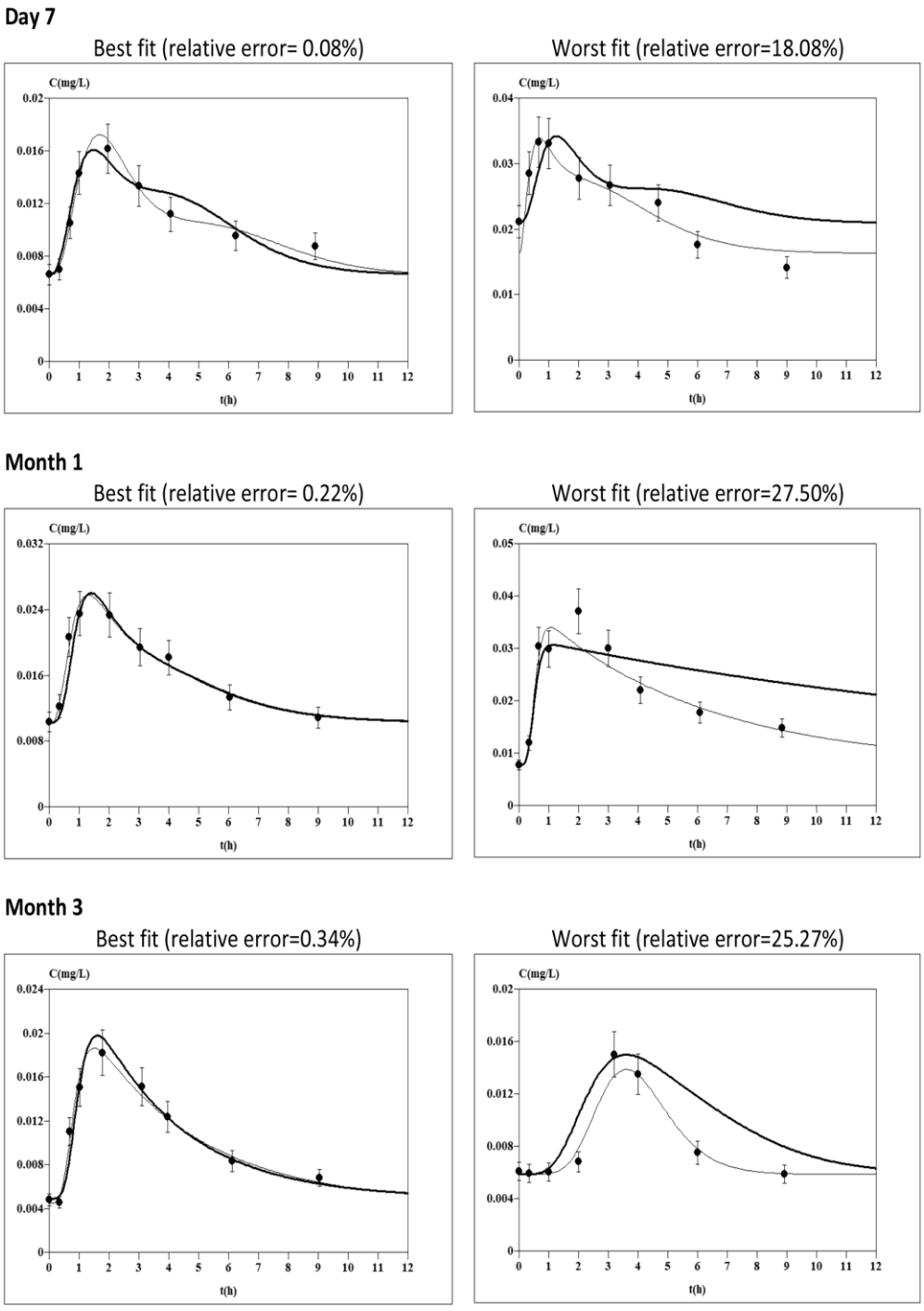

Fig. 5 Best and worst $AUC_{0-12\ h}$ estimates in the internal validation population at each post-transplant period using Bayesian estimation and the pre-dose, 1 h and 3 h limited sampling strategy. The profiles estimated using all sampling times are in thin lines, the 3-point Bayesian estimates in thick lines

Licence CC BY-NC-ND 3.0

the latter information does not improve accuracy and precision as much as only 1 plasma concentration" [25].

5 Conclusions

We developed population PK models and Bayesian estimators for Adoport®, one of the most prescribed generic formulation of tacrolimus, which tightly fitted the data without the need for covariates, not even the CYP3A5 genotype, and we confirmed that Bayesian estimators previously developed for the original formulation had very similar performance. These models and MAP-BE (now all available on the ISBA website) can also cope with different combinations of sampling times, suggesting that they are applicable to other generic formulations with a different distribution of T_{max} values (as T_{max} is not statistically compared in bioequivalence studies). We also consider that the model developed for the latest post-transplant period here (M3) is also suited for the steady-state situation, despite subtle changes that may occur in tacrolimus pharmacokinetics up to 1-year post-transplant.

Acknowledgements We thank Sandoz France and Limoges University Hospital for funding this study and providing the study drug; Hélène Roussel for writing the study protocol and overseeing the investigation sites; Alexandre Garnier for excellent study data management; Chloé Barny for handling patient samples; Naïma Tafzi and the laboratory technicians of the Department of Pharmacology, Toxicology and Pharmacovigilance for tacrolimus determination; Hélène Arnion for pharmacogenetic analyses; and Karen Poole for revising the manuscript.

Declarations

Funding This study was funded by Sandoz France and Limoges University Hospital.

Conflicts of interest/Competing Interests Pierre Marquet received consulting fees and travel grants from Sandoz, Chiesi, Pfizer, and BMS and research grants from Sandoz and Chiesi. Caroline Monchaud received an honorarium from Chiesi to participate in a board of experts. Matthias Buchler received a travel grant to attend an international congress from Sandoz. Jean-Baptiste Woillard received speaker fees from Chiesi and Gilead and travel grants to attend symposia or congresses from Chiesi and Gilead, VIIV, Astellas and Abbvie. Alexandre Destere, Jean-Philippe Rérolle, Hakim Mazouz, Isabelle Etienne, Antoine Thierry, Nicolas Picard and Jean Debord have no conflicts of interest that are directly relevant to the content of this article.

Ethics approval This study was approved by the National Research Ethics Committee CPP16-058 on 8 December, 2016 and was performed in accordance with the ethical standards as laid down in the 1964 Declaration of Helsinki and its later amendments.

Consent to participate Informed consent was obtained from all participants included in the study.

Consent for publication Not applicable.

Availability of data and material Raw data are available on request from the authors.

Code Availability Not applicable.

Author Contributions PM designed and was the principal investigator of the study, participated in result analysis and interpretation, and is the main author of the manuscript. AD participated in data analysis and participated in manuscript writing. CM participated in the study design, supervised the clinical research team, data collection and cleaning, and participated in manuscript writing. J-PR enrolled patients in the study and critically reviewed the manuscript. MB enrolled patients in the study and critically reviewed the manuscript. HM enrolled patients in the study and critically reviewed the manuscript. IE enrolled patients in the study and critically reviewed the manuscript. AT enrolled patients in the study and critically reviewed the manuscript. NP supervised pharmacogenetic testing and critically reviewed the manuscript. J-BW participated in the pharmacokinetic modelling and manuscript writing. JD performed most of the pharmacokinetic modelling and Bayesian estimation and participated in manuscript writing.

References

1. Brunet M, van Gelder T, Åsberg A, Haufroid V, Hesselink DA, Langman L, et al. Therapeutic drug monitoring of tacrolimus-personalized therapy: second consensus report. Ther Drug Monit. 2019;41(3):261–307.
2. Bouamar R, Shuker N, Hesselink DA, Weimar W, Ekberg H, Kaplan B, et al. Tacrolimus predose concentrations do not predict the risk of acute rejection after renal transplantation: a pooled analysis from three randomized-controlled clinical trials. Am J Transplant. 2013;13(5):1253–61.
3. Rodríguez-Perálvarez M, Germani G, Darius T, Lerut J, Tsochatzis E, Burroughs AK. Tacrolimus trough levels, rejection and renal impairment in liver transplantation: a systematic review and meta-analysis. Am J Transplant. 2012;12(10):2797–814.
4. Daher Abdi Z, Prémaud A, Essig M, Alain S, Munteanu E, Garnier F, et al. Exposure to mycophenolic acid better predicts immunosuppressive efficacy than exposure to calcineurin inhibitors in renal transplant patients. Clin Pharmacol Ther. 2014;96(4):508–15.
5. Israni AK, Riad SM, Leduc R, Oetting WS, Guan W, Schladt D, DeKAF Genomics Investigators, et al. Tacrolimus trough levels after month 3 as a predictor of acute rejection following kidney transplantation: a lesson learned from DeKAF Genomics. Transpl Int. 2013;26(10):982–9.
6. Undre NA, van Hooff J, Christiaans M, Vanrenterghem Y, Donck J, Heeman U, et al. Low systemic exposure to tacrolimus correlates with acute rejection. Transplant Proc. 1999;31(1–2):296–8.
7. Kuypers DR, Claes K, Evenepoel P, Maes B, Vanrenterghem Y. Clinical efficacy and toxicity profile of tacrolimus and mycophenolic acid in relation to combined long-term pharmacokinetics in de novo renal allograft recipients. Clin Pharmacol Ther. 2004;75(5):434–47.
8. Saint-Marcoux F, Knoop C, Debord J, et al. Pharmacokinetic study of tacrolimus in cystic fibrosis and non-cystic fibrosis lung transplant patients and design of Bayesian estimators using limited sampling strategies. Clin Pharmacokinet. 2005;44:1317–28.
9. Benkali K, Prémaud A, Picard N, Rérolle JP, Toupance O, Hoizey G, et al. Tacrolimus population pharmacokinetic-pharmacogenetic analysis and Bayesian estimation in renal transplant recipients. Clin Pharmacokinet. 2009;48(12):805–16.

Licence CC BY-NC-ND 3.0

10. Saint-Marcoux F, Debord J, Undre N, Rousseau A, Marquet P. Pharmacokinetic modeling and development of Bayesian estimators in kidney transplant patients receiving the tacrolimus once-daily formulation. Ther Drug Monit. 2010;32(2):129–35.
11. Benkali K, Rostaing L, Premaud A, Woillard JB, Saint-Marcoux F, Urien S, et al. Population pharmacokinetics and Bayesian estimation of tacrolimus exposure in renal transplant recipients on a new once-daily formulation. Clin Pharmacokinet. 2010;49(10):683–92.
12. Woillard JB, de Winter BC, Kamar N, Marquet P, Rostaing L, Rousseau A. Population pharmacokinetic model and Bayesian estimator for two tacrolimus formulations: twice daily Prograf and once daily Advagraf. Br J Clin Pharmacol. 2011;71(3):391–402.
13. Monchaud C, de Winter BC, Knoop C, Estenne M, Reynaud-Gaubert M, Pison C, et al. Population pharmacokinetic modelling and design of a Bayesian estimator for therapeutic drug monitoring of tacrolimus in lung transplantation. Clin Pharmacokinet. 2012;51(3):175–86.
14. Woillard JB, Debord J, Monchaud C, Saint-Marcoux F, Marquet P. Population pharmacokinetics and Bayesian estimators for refined dose adjustment of a new tacrolimus formulation in kidney and liver transplant patients. Clin Pharmacokinet. 2017;56(12):1491–8.
15. Riff C, Debord J, Monchaud C, Marquet P, Woillard JB. Population pharmacokinetic model and Bayesian estimator for 2 tacrolimus formulations in adult liver transplant patients. Br J Clin Pharmacol. 2019;85(8):1740–50.
16. Saint-Marcoux F, Woillard JB, Jurado C, Marquet P. Lessons from routine dose adjustment of tacrolimus in renal transplant patients based on global exposure. Ther Drug Monit. 2013;35(3):322–7.
17. Marquet P, Bedu A, Monchaud C, Saint-Marcoux F, Rérolle JP, Etienne I, et al. Pharmacokinetic therapeutic drug monitoring of Advagraf in more than 500 adult renal transplant patients, using an expert system online. Ther Drug Monit. 2018;40(3):285–91.
18. HapMap project. https://www.ncbi.nlm.nih.gov/probe/docs/projhapmap/. Accessed 7 May 2020.
19. Lam S, Partovi N, Ting LS, Ensom MH. Corticosteroid interactions with cyclosporine, tacrolimus, mycophenolate, and sirolimus: fact or fiction? Ann Pharmacother. 2008;42(7):1037–47.
20. Alloway RR, Sadaka B, Trofe-Clark J, Wiland A, Bloom RD. A randomized pharmacokinetic study of generic tacrolimus versus reference tacrolimus in kidney transplant recipients. Am J Transplant. 2012;12(10):2825–31.
21. Heads of Medicines Agencies, Clinical Trial Facilitation Group (CTFG). Recommendations related to contraception and pregnancy testing in clinical trials. https://www.hma.eu/fileadmin/dateien/Human_Medicines/01-About_HMA/Working_Groups/CTFG/2014_09_HMA_CTFG_Contraception.pdf. Accessed 7 May 2020.
22. Le Meur Y, Djebli N, Szelag JC, et al. CYP3A5*3 influences sirolimus oral clearance in de novo and stable renal transplant recipients. Clin Pharmacol Ther. 2006;80(1):51–60.
23. Marquet P, Albano L, Woillard JB, Rostaing L, Kamar N, Sakarovitch C, et al. Comparative clinical trial of the variability factors of the exposure indices used for the drug monitoring of two tacrolimus formulations in kidney transplant recipients. Pharmacol Res. 2018;129:84–94.
24. Saint-Marcoux F, Debord J, Parant F, et al. Development and evaluation of a simulation procedure to take into account various assays for the Bayesian dose adjustment of tacrolimus. Ther Drug Monit. 2011;33(2):171–7.
25. Sheiner LB, Beal S, Rosenberg B, Marathe VV. Forecasting individual pharmacokinetics. Clin Pharmacol Ther. 1979;26(3):294–305.

Affiliations

Pierre Marquet[1,2] · Alexandre Destère[1,2] · Caroline Monchaud[1,2] · Jean-Philippe Rérolle[2,3] · Matthias Buchler[4] · Hakim Mazouz[5] · Isabelle Etienne[6] · Antoine Thierry[7] · Nicolas Picard[1,2] · Jean-Baptiste Woillard[1,2] · Jean Debord[1,2]

1 Department of Pharmacology, Toxicology and Pharmacovigilance, CHU Limoges, University Hospital of Limoges, CBRS, Limoges, France

2 IPPRITT, Université de Limoges, INSERM, Limoges, France

3 Department of Nephrology, Dialysis and Transplantation, CHU Limoges, Limoges, France

4 Department of Nephrology and Clinical Immunology, University Hospital, Tours, France

5 Department of Nephrology, Dialysis and Transplantation, University Hospital, Amiens, France

6 Department of Nephrology, University Hospital, Rouen, France

7 Department of Nephrology, Jean Bernard Hospital, University Hospital, Poitiers, France

Adis

Licence CC BY-NC-ND 3.0

II.2. A single Bayesian estimator for iohexol clearance estimation in ICU, liver failure and renal transplant patients

Article publié dans le *British Journal of Clinical Pharmacology*

Dans ces travaux, un modèle de pharmacocinétique de population puis un MAP-BE basé sur une LSS ont été développés afin d'estimer le débit de filtration glomérulaire dans des populations hétérogènes de patients (patients stables et instables de réanimation, patients insuffisants hépatiques et patients transplantés rénaux) à partir de la clairance de l'iohexol.

Lors du développement d'un modèle de pharmacocinétique de population celui-ci est utilisable dans une indication précise. En effet, les paramètres PK moyens ainsi que leur variabilité interindividuelle peuvent être influencés par la pathologie (troubles hémodynamiques, stase, insuffisance hépatique…) . L'originalité de ce travail est d'avoir tenu compte de la pathologie comme potentielle covariable catégorielle permettant l'utilisation de ce modèle dans différentes indications. En effet, les modèles de POPPK décrivant la pharmacocinétique de l'iohexol précédemment publiés ont été développés dans des populations spécifiques [103–107].

Dans ce travail, un modèle a été développé chez 81 patients de réanimation instables hémodynamiquement, 64 patients ayant reçu une transplantation rénale, 21 patients de réanimation stables et 9 patients insuffisants hépatiques (n total=175). Le modèle a été validé par VPC ainsi que sur des patients réels (n=36). Un estimateur bayésien dérivé du modèle de POPPK basé sur une stratégie de prélèvements limités a été développé. Différentes stratégies de prélèvements limités ont été évaluées en comparant le biais moyen, l'imprécision ainsi que le pourcentage de patients en dehors de l'intervalle de ± 20% de biais. Une comparaison avec la formule de Bröchner-Mortensen a également été réalisée.

Les performances globales du MAP-BE basé sur la LSS sont satisfaisantes quelle que soit la population d'évaluation. Toutefois, seul un patient insuffisant hépatique se trouvait dans le groupe de validation et les résultats dans cette sous population devront être confirmés.

En conclusion, l'utilisation d'une covariable catégorielle sur le type de pathologie peut permettre la création d'un seul modèle de pharmacocinétique de population et d'un MAP-BE utilisable sur différentes populations tout en gardant une précision satisfaisante.

Licence CC BY-NC-ND 3.0

Received: 30 April 2021 | Revised: 9 December 2021 | Accepted: 13 December 2021

DOI: 10.1111/bcp.15197

ORIGINAL ARTICLE

A single Bayesian estimator for iohexol clearance estimation in ICU, liver failure and renal transplant patients

Alexandre Destere[1,2] | Charlotte Salmon Gandonnière[3] | Anders Åsberg[4,5] | Véronique Loustaud-Ratti[1,6] | Paul Carrier[6] | Stephan Ehrmann[3,7] | Chantal Barin-Le Guellec[1] | Pierre Marquet[1,2] | Jean-Baptiste Woillard[1,2]

[1]Pharmacology & Transplantation, INSERM U1248, Université de Limoges, Limoges, France

[2]Department of Pharmacology, Toxicology and Pharmacovigilance, University Hospital of Limoges, Limoges, France

[3]Médecine Intensive Réanimation, INSERM CIC 1415, CRICS-TriggerSep Research Network, CHRU de Tours, Tours, France

[4]Department of Transplantation Medicine, Oslo University Hospital Rikshospitalet, Oslo, Norway

[5]Department of Pharmacy, University of Oslo, Norway

[6]Department of hepato-gastro-enterology, University Hospital of Limoges, Limoges, France

[7]Centre d'Etude des Pathologies Respiratoires INSERM, U1100, Faculté de médecine, Université de Tours, Tours, France

Correspondence
Jean-Baptiste Woillard, PharmD, PhD, Univsity of Limoges, INSERM U1248 IPPRITT, 2 rue du Pr Descottes, F-87000 Limoges, France.
Email: jean-baptiste.woillard@unilim.fr

Aims: Iohexol clearance has been proposed to estimate the glomerular filtration rate (GFR). A population pharmacokinetics (popPK) model was developed from heterogeneous patients. A Bayesian estimator (MAP-BE) based on a limited sampling strategy (LSS) was derived and evaluated in external patients.

Methods: Full pharmacokinetic data (7–12 samples) from 172 patients receiving iohexol for measurement of their GFR (unstable and stable ICU patients, liver failure patients and kidney transplant patients) were split into development ($n = 136$) and validation ($n = 36$) datasets. A PopPK model was developed in Monolix and was used to develop MAP-BE based on LSS. Its performance for GFR estimation was evaluated in the validation set.

Results: A two-compartment model with first-order elimination best described the data. The final model included the type of patients on volume of distribution (Vd), clearance and intercompartmental constants, serum creatinine on clearance and body weight on Vd. The best LSS included samples at 0.1–1-9 h exhibiting a relative mean prediction error (MPE) (RMSE) = −3.7% (14.3%) and better performance than the Bröchner-Mortensen formula (−3.0%/17%). Split by type of patients, the highest interindividual variability and imprecision was observed in unstable ICU patients (MPE (RMSE) = 3.7% (18.8%)) while the best performances were obtained for renal transplant patients (MPE (RMSE) = 1.0% (5.8%)). All LSS that included samples before 9 hours for the third sample were associated with an increased imprecision.

Conclusion: A single MAP-BE of iohexol based on a three-sample LSS for four heterogeneous populations was developed and allowed accurate estimation of GFR in kidney transplant patients, slightly biased in stable ICU patients and slightly imprecise in unstable ICU patients.

KEYWORDS
Bayesian estimator, glomerular filtration rate, ICU, iohexol, liver failure, population pharmacokinetics, renal transplantation

The authors confirm that the Principal Investigators for this paper are Charlotte Salmon Gandonnière and Véronique Loustaud-Ratti and that they had direct clinical responsibility for the patients.

 © 2022 British Pharmacological Society

Alexandre Destere | Thèse de doctorat | Université de Limoges | 2022
Licence CC BY-NC-ND 3.0

1 | INTRODUCTION

Iohexol has been approved in France as a contrast agent. It is used mainly for computed tomography scans, urograms or angiographies, for both children and adults. Iohexol exhibits interesting pharmacokinetic characteristics that make it the most used exogenous tracer for the measurement of the glomerular filtration rate (GFR).[1] Bröchner-Mortensen,[2] Ng et al.[3] and others used this tracer with samples collected only in the second elimination slope (beyond 120 min), with fixed correction for the distribution phase. In routine care, GFR is usually estimated using serum creatinine, an endogenous compound produced mostly by muscle fibres, filtered and secreted by the kidneys.[4] However, patients hospitalised in intensive care units (ICU) may present with conditions that modify the production and elimination of creatinine (fever, liver failure, change in water balance, rhabdomyolysis, etc.) rendering GFR estimation formulas based on this marker less accurate.[5] Liver failure patients and especially decompensated liver failure patients often have kidney injuries. One such specific condition is hepatorenal syndrome, characterised by a high mortality rate. It is often associated with subclinical renal lesions that in turn significantly worsen the liver prognosis. The prognostic value of the kidney function (as indirectly assessed by serum creatinine) during cirrhosis is included in the MELD (model for end-stage liver disease) score, a predictive model of 3-month mortality. Finally, combined liver-kidney transplantation, which requires precise GFR estimation in order to reliably prioritise patients on the waiting list, should be considered if the GFR decreases below 30 mL/min.[6] In kidney transplant patients, GFR monitoring is routinely used for the detection of acute rejection, as well as for evaluating the progressive loss of graft function.

Some studies have developed popPK models for iohexol in specific populations (kidney transplant or elderly patients) using different structural models (e.g. with two or three compartments)[7–9] and more recently a popPK model for ICU patients using a three-compartment structural model.[10] Estimating the pharmacokinetics parameters of a compound in an individual requires drawing many blood samples, which is not easy to apply in routine care. Limited sampling strategies (LSS) and maximum a posteriori Bayesian estimators (MAP-BE) can be derived from popPK models to estimate exposure based on a reduced number of concentration–time points, and possibly of covariates.

In this context, the objective of this study was to develop a population pharmacokinetics model and a MAP-BE based on an LSS for intravenous iohexol, allowing accurate measurement of GFR in four heterogeneous populations (stable and unstable ICU patients, kidney transplant patients and liver failure patients).

What is already known about this subject

- Iohexol is used to measure the glomerular filtration rate (GFR).
- Only a few models are available to estimate GFR based on an iohexol administration and a limited blood sampling strategy.
- They were developed in a single homogeneous population.

What this study adds

- A maximum a posteriori Bayesian estimator that estimates GFR over 24 h with only three points (0.1–1-9 h) was developed.
- It was developed from four heterogeneous populations (stable and unstable ICU patients, liver failure and kidney transplant patients).
- Performances were accurate in kidney transplant patients, slightly biased in stable ICU patients and slightly imprecise in unstable ICU patients.

2 | METHODS

2.1 | Patients

The dataset was made up of clinical and pharmacokinetic data from 172 patients composed of haemodynamically unstable (average of eight samples per patient) and stable (average of eight samples per patient) ICU patients, liver failure patients with advanced liver disease and with different grades of ascites (average of 11 samples per patient)[11] and kidney transplant patients (average of 12 samples per patient) from a previously published study.[12]

In all these studies, 3235 mg (i.e., 5 mL) of iohexol was injected as an intravenous bolus. Iohexol plasma concentration was measured using a high-performance liquid chromatography with diode-array detection (HPLC-DAD) method with a lower limit of quantification (LLOQ) of 10 mg/L for the ICU patients (unstable or stable), or a liquid Chromatography with tandem mass spectrometry (LC–MS/MS) method (LLOQ = 1 mg/L) for the liver failure and kidney transplant patients. Concentrations below the LLOQ were kept as such.

2.2 | Model development and covariate analysis

The population pharmacokinetic model was developed in Monolix (version 2019R1; Antony, France: Lixoft SAS, 2019. http://lixoft.com/products/monolix/).

Random data splitting stratified on the type of patients (unstable ICU, stable ICU, renal transplant and liver failure) was first performed allocating 75% ($n = 136$) to model development and 25% ($n = 36$) to its evaluation. The structural model was chosen after comparing one-, two- or three-compartment models with linear elimination, based on the Akaike information criterion (AIC), goodness-of-fit plots and adjustment performances. The interindividual variability (IIV) was

Licence CC BY-NC-ND 3.0

described using an exponential model and covariance between random effects was investigated. Different error models (additive, proportional or combined) to describe the residual error were also compared.

The influence of potential covariates (weight, age, BMI, serum albumin, uremia, serum creatinine, type of patients) was then investigated using GGally R packages,[13] through their statistical association with the eta of PK parameters, using correlation analysis for continuous covariates or Mann–Whitney tests for binary covariates. Covariates with $r > 0.4$ or pMW < 0.05 were included using a power function, coded as follows for continuous covariates:

$$\theta 1 \times \left(\frac{\text{Cov}}{\text{median cov}}\right)^{\theta 2}$$

where θ1 is the typical value for a median patient and θ2 is the power coefficient of the covariate; and for binary covariables:

$$\theta 1 \times \theta 2^{\text{cov}}$$

where θ1 is the typical value for a patient with cov = 0 and θ2 is the fold-change in the parameter for patients with cov = 1. The COSSAC (COnditional Sampling use for Stepwise Approach based on Correlation tests) used in Monolix was applied to select the covariates retained in the final model and their relevance was assessed by the resulting decrease in IIV. The final model was evaluated by simulation using overall and stratified by type of patient visual predictive checks (VPC).

2.3 | Limited sampling strategies (LSS) and maximum a posteriori Bayesian estimation (MAP-BE)

The different points eligible for an optimal LSS for Bayesian estimation were determined from the inflexion points in the log scale spaghetti plot (Figure S1 in the Supporting Information). Three 3-point strategies were compared, with samples taken at: 0.1, 1 and 3 hours; 0.1, 1 and 6 hours; and 0.1, 1 and 9 hours. The reference CL was obtained by MAP-BE and the popPK model with all iohexol concentrations available for a given patient. The CL parameter calculated by the model was used. In the validation dataset, post-hoc iohexol CL estimates using these 3-point LSSs were compared to the reference CL by calculating the relative bias (mean prediction error, MPE), relative imprecision (root mean square error, RMSE) and the percentage of patients with a relative MPE outside the ±20% interval.

2.4 | Validation of Bayesian estimation of iohexol clearance in the validation set

In the validation set, regrouping the different independent populations (stable ICU patients, liver failure patients, kidney transplant patients), the performance of MAP-BE CL estimation using the three 3-point LSSs was assessed using the metrics described above.

In kidney transplant patients, because the PK profiles were limited to 6 hours post-dose, the concentrations at 9 and 12 hours had to be estimated using the popPK model and MAP-BE using all the available concentration–time points (these extrapolated samples were used to estimate the reference CL and the corresponding three samples of LSS).

Due to the low number of patients, there was only one patient in the validation test of the liver population.

VPCs were performed to compare the distribution of evaluation set concentrations in the model simulations. Bland–Altman plots were built to investigate the precision of GFR measurement based on the LSS on each type of patient.

2.5 | Comparison with the Bröchner-Mortensen (BM) formula

The BM formula[2] was calculated using at least four samples in the elimination phase (between 2 and 5 hours) in renal transplant recipients and liver failure patients (Supplemental method). As ICU patients only had two samples (at 2 and 5 h), the BM formula could not be calculated. The performance of the BM formula was evaluated in comparison to the reference clearance, as for those of MAP-BE.

3 | RESULTS

The characteristics of the patients included in each study are presented in Table 1. Some differences concerning demographic characteristics or laboratory test results were observed across these populations, probably due to the different recruitment settings (ICU patients in a more critical condition, younger kidney transplant patients, etc.).

The logarithmic representation of observed concentrations (mg/L) as a function of time (h) in the development population is shown in the Figure S1 in the Supporting Information. At $t = 0.1$ h, the observed concentrations were largely spread out with a median [min–max] of 328.0 [91.7–951.0] mg/L. According to the two elimination slopes observed for plasma iohexol, a two-compartment model was finally retained based on its AIC (one compartment: 28257.6; two compartments: 10744.3; three compartments: 10857.3).

The AIC of additive, proportional and combined residual error models were 11080.4, 11117.4 and 10744.3, respectively, leading us to retain the last one. Covariance was included between CL, V1, k12 and k21. η CL was influenced by serum creatinine and urea and the η volume of distribution (V1) by body weight with $r = -0.60$, -0.60 and 0.45, respectively (Figure S2 in the Supporting Information). Serum creatinine and urea had a similar effect on CL (Figure S2 in the Supporting Information) and exhibited a strong correlation between them ($r = 0.77$) which made us avoid retaining both in the same model and to select serum creatinine for its availability in routine care.

Finally, the best final covariate model after COSSAC included body weight and type of patient on the volume of distribution, serum

Licence CC BY-NC-ND 3.0

TABLE 1 Patient characteristics

Variable	Unstable patients data	Stable ICU patients validation data	Liver failure patients (LIVER) study validation data	Kidney transplant recipients
N	86	21	9	64
Weight (kg) (mean [SD])	82.3 (20.4)	78.3 (17.5)	98 (21.3)	70.8 (19.3)
Body mass index (kg/m^2) (mean [SD])	28.7 (7.0)	27.9 (5.9)	33.3 (6.9)	24.3 (4.9)
Body surface area (m^2) (mean [SD])	2.0 (0.3)	1.9 (0.2)	2.1 (0.2)	1.8 (0.3)
Age (years) (mean [SD])	64.9 (13.2)	66.9 (10.8)	61.7 (8.5)	41.9 (2.2)
Sex female (%)	31 (36.0)	9 (42.9)	0 (0)	19 (22.3)
Haematocrit (%) (mean [SD])	31.8 (6.1)	NA	32.4 (5.2)	NA
Proteinemia (g/L) (mean [SD])	53.1 (7.8)	65.4 (10.2)	NA	NA
Albuminemia (g/L) (mean [SD])	28.5 (5.8)	NA	32.4 (4.1)	NA
Serum creatinine during iohexol sampling (μM) (median [IQR]	121 [74.0–186.0]	63.0 [26.0–113.0]	95.0 [62.0–128.0]	125 [100.0–157.0]
Blood urea during iohexol sampling (median [IQR])	11.1 [7.2–16.0]	7.2 [2.4–16.7]	6.7 [3.8–12.9]	NA

NA: not available.

creatinine and type of patient on CL and type of patient on the k12 and k21 (Table 2). The correlation matrix of model parameters for the final model is presented in Table S1 in the Supporting Information. The typical PK parameters split by type of patient are presented in Table 3.

Diagnostic plots of the final covariate model are shown in Figure 1. The observed concentrations were estimated with excellent accuracy (Figure 1A). The population predicted concentrations were distributed homogeneously on either side of the linear regression line (Figure 1B) and the weighted residuals (Figure 1C) were homogeneously and normally distributed, regardless of the level of the predicted concentrations.

The VPCs split by study type are presented in Figure 2. The observed concentrations are distributed homogeneously between the 10th and 90th percentiles of the data simulated and the variability was reasonably estimated in development dataset. In the validation set, the observed concentrations are distributed homogeneously between the 10th and 90th percentiles of the data simulated in kidney transplant patients and unstable ICU patients, while the observed concentrations of stable ICU patients were included in the 10th and 50th percentiles of the simulations.

The 0.1, 1 and 9 hour limited sampling strategy was associated with the best results (Table 4) in terms of accuracy (relative MPE) and imprecision (RMSE) in comparison to the two other LSSs and also exhibits better results than the BM formula (Table 4). The Bland Altman split by type of patient in the validation set is presented in Figure 3.

4 | DISCUSSION

In this study, a parametric popPK model was developed based on rich sampling in different types of heterogeneous patients. A maximum a posteriori Bayesian estimator based on a 3-point LSS was derived from this model to allow GFR measurement.

The patient type covariate reflecting the patient group (ICU, liver failure or kidney transplantation) was included on V1, CL, k12, k21, allowing us to take into account the heterogeneity of these patients. Indeed, ICU patients are associated with strong modifications of PK parameters[10] and liver failure patients also strongly differ from renal transplant patients. Accordingly, we observed an increase in V1 in liver failure patients in comparison to the other populations that could correspond to the distribution of iohexol in ascites. We also observed a decrease of CL in unstable ICU patients that could correspond to pathological states (e.g., cardiogenic shock following sepsis). As expected, the IIV of the PK parameters and the imprecision in clearance estimation were the highest in unstable ICU patients. Of note, some parameters for patient type or correlation between PK parameters are of minimal impact and estimated with extreme imprecision (e.g., the 10% impact of beta_V1_STUDY_ICU_unstable (178% RSE) and the 10% impact of beta_CL_STUDY_liver (377% RSE), the 20% of beta_k12_STUDY_ICU_unstable (86% RSE), and correlation k12 V1 (−0.09, 113% RSE). These values are due to an unimportant or zero effect of these covariates or correlations and can be neglected.

This strategy was evaluated in a validation set and the split VPC showed that the model seems to performed well for renal transplant recipients and unstable ICU patients, while an overprediction was observed for stable ICU patients with all observations below the median of the simulated concentrations. Concerning the liver failure, the data splitting has assigned a single patient in the evaluation dataset, which makes the interpretation of the results difficult. This was also observed in the performance in terms of relative bias and imprecision in the Bland Altman split by type of patient. Indeed, it showed accurate prediction in kidney transplant patients, high relative bias in stable ICU patients and high imprecision in the unstable ICU patients, probably due to the clinical instability of these patients.

Licence CC BY-NC-ND 3.0

However, even if the relative bias was quite high for the stable ICU patients, the prediction in terms of raw bias was still clinically acceptable with a mean difference of 3.8 mL/min as observed in the Bland Altman plot. Indeed, the use of relative metrics in the case of small groups is largely sensitive to one extreme value. In this case the largest difference was an estimation of 38 mL/min instead of 31 mL/min, which still remains clinically acceptable.

Throughout this article, the reference GFR used for evaluation of our LSS was obtained using the model and all the available time-points, which has previously been regarded as an accurate estimation of the "true" iohexol CL and the "true" GFR itself.[1]

Riff et al.[9] described the pharmacokinetics of iohexol with a parametric two-compartment structural model in a population of 151 kidney transplant patients. They also developed a MAP-BE based on a 3-point LSS (T_{30min}, T_{120min} and T_{270min}), which was able to accurately estimate iohexol CL (mean error [ME] = 0.47%, RMSE = 3.42%). However, their reference CL values were derived from iohexol AUC calculated using the trapezoidal rule and six plasma concentrations between 5 and 270 min. We think that samples between at least 7 and 14 hours are required to correctly describe iohexol elimination (half-life = 1–2 h in healthy individuals). Accordingly, in our study, the shortest LSS, with the last sample drawn at 3 hours, yielded the worst estimates.

Åsberg et al.[12] also described the kinetics of iohexol in kidney transplant recipients using a two-compartment model (although with a non-parametric approach) and they estimated iohexol CL using four samples (T_{10min}, T_{30min}, T_{120min} and T_{300min}) with satisfactory precision (ME (%): – 0,9 ± 4.5; RMSE (%): 2.8 ± 3.6), and only 2% of CL estimates differing by more than 10% from the Brochner-Mortensen[14] value chosen as reference.[12] The major difference from the previous reports is the time of blood sampling, as in the study by Åsberg et al. samples were collected until 6 hours (similar to the Brochner-Mortensen formula). In the present study we developed the popPK model using samples collected until 24 hours (except for renal transplant patient data who are the ones in the study by Åsberg et al.), while all others collected samples until max 360 min. It seems that the later the last sample is drawn, the better the performance when compared to full iohexol profiles. In our study, including the sample collected at 9 hours improved CL estimation in comparison collection at 6 hours. This may be due to the nychthemeral variations of GFR, which is associated with a large intra-day variability. Iohexol clearance evaluation using the conventional 6-hour-based formula does well when compared to the 6-hour full sample reference, but the performance declines when compared to the 24-hour sample reference. Collecting late plasma samples is not a concern for ICU patients and it should be facilitated by home microsampling devices for kidney transplant patients and liver failure patients.[15]

TABLE 2 Final model parameter estimates

PK parameters	Final model	RSE (%)
V1 (L)	6.8	6.5
beta_V1_STUDY_liver	0.7	26.4
beta_V1_STUDY_ICU_unstable	0.1	178
beta_V1_STUDY_ICU_stable	0.4	33.8
beta_V1_WT	0.5	16.4
CL (L/h)	3.3	7.7
beta_CL_STUDY_liver	0.1	377
beta_CL_STUDY_ICU_unstable	−0.5	22
beta_CL_STUDY_ICU_stable	−0.4	38.5
beta_CL_SCR	−0.8	9.7
K12 (h^{-1})	1.6	12.9
beta_k12_STUDY_liver	−1.2	31.4
beta_k12_STUDY_ICU_unstable	0.2	86.5
beta_k12_STUDY_ICU_stable	−0.7	37.8
K21 (h^{-1})	1.7	8.2
beta_k21_STUDY_liver	−0.7	34.6
beta_k21_STUDY_ICU_unstable	−0.4	26.4
beta_k21_STUDY_ICU_stable	−0.8	22.5
IIV V1	0.4	6.3
IIV CL	0.5	6.2
IIV K12	0.9	6.7
IIV K21	0.5	7.9
a	2.5	7.4
b	0.04	6.3
Corr_V1_CL	0.41	19.9
Corr_K12_CL	−0.10	87.8
Corr_k12_V1	−0.09	113
Corr_K12_V1	−0.75	5.35
Corr_K21_V1	−0.51	15.3
Corr_k12_k12	0.79	4.9

Abbreviations: a, additive residual error; b, proportional residual error; beta_Y_X, influencial factor of X on PK parameters Y; CL, clearance; ICU, intesive care unit; IIV, interindividual variability; Corr_X_Y, correlations between PK parameters X and Y; k12: transfer constant from central to peripheric compartment; k21, transfer constant from peripheric to central compartment; SCR, serum creatinine; V1, central volume of distribution; WT, weight.

TABLE 3 Typical median [min–max] PK parameters in development data overall and split by type of patients

	Overall (median[min–max])	Liver failure (median[min–max])	Kidney transplanted patients	Stable ICU	Unstable ICU
V1 (L)	7.3 [2.4–33.4]	16.2 [8.4–21.6]	6.5 [2.4–15.1]	11.5 [2.4–18.8]	6.9 [2.6–33.4]
CL (L/h)	3.1 [0.3–10.9]	4.1 [3.2–7.1]	3.4 [0.8–8.8]	4.7[1.3–8.0]	2.1 [0.3–10.9]
K12 (h^{-1})	1.7 [0.2–14.7]	0.5[0.2–1.5]	1.7 [0.3–5.7]	1.7 [0.3–5.7]	2.2 [0.2–14.7]
K21 (h^{-1})	1.3 [0.2–4.1]	0.8 [0.5–2.0]	1.8 [0.6–3.5]	1.8 [0.6–3.5]	1.8 [0.2–4.1]

Licence CC BY-NC-ND 3.0

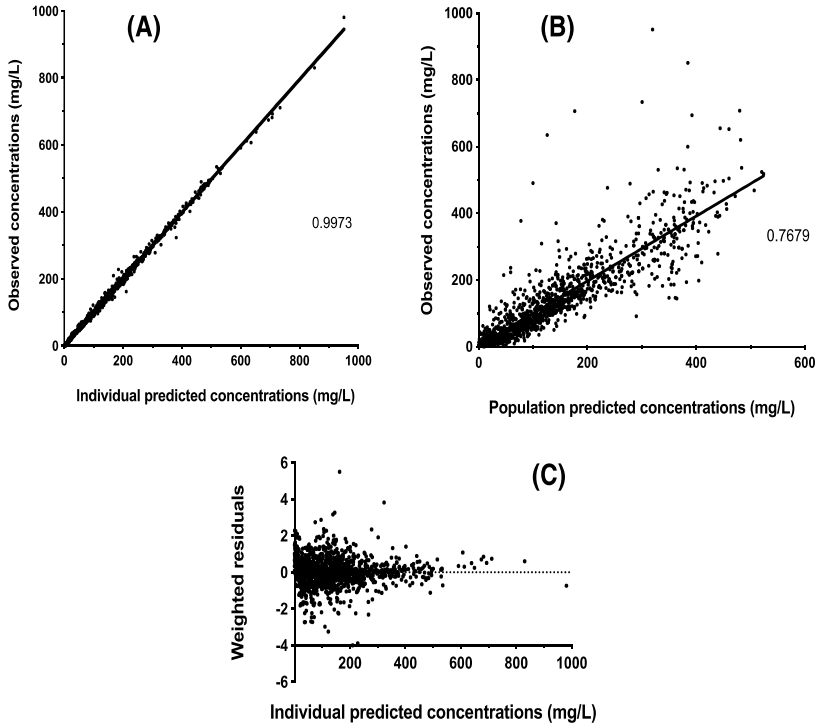

FIGURE 1 Diagnostic plots of the final model with the observed concentrations as a function of individual predicted concentrations (A), observed concentrations as a function of population predicted concentrations (B) and weighted residuals as a function of individual predicted concentrations (C)

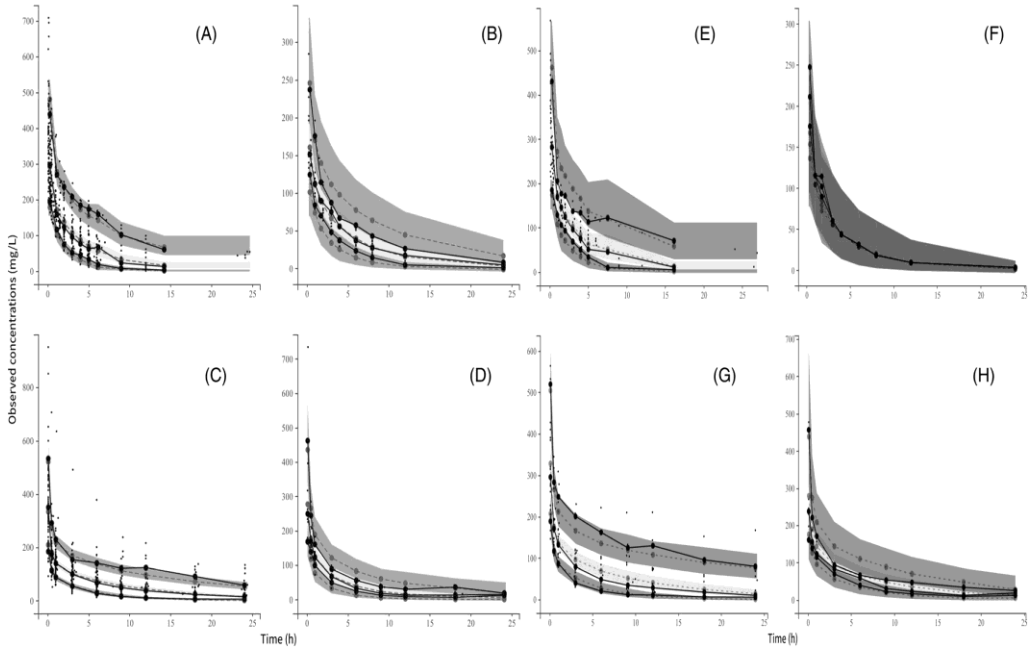

FIGURE 2 Visual predictive checks of the final model split by type of patient in the development population: (A) kidney transplants; (B) liver failure; (C) unstable ICU; (D) stable ICU; and the validation dataset split by type of patient: (E) kidney transplants; (F) liver failure; (G) unstable ICU; (H): stable ICU

Licence CC BY-NC-ND 3.0

TABLE 4 Evaluation of the three limited sampling strategies in the validation dataset overall and split by type of patient

	Relative MPE (%)		CL all pts *vs* CL 3 pts RMSE validation (%)	Percentage of patients with a bias out of the ± 20% interval
Overall	0.1–1-3 h	7.4	35.6	29.5
	0.1–1-6 h	3.9	19.8	15.9
	0.1–1-9 h	3.7	14.3	13.9
	Bröchner-Morten formula	3.0	17.0	20
Liver failure	0.1–1-3 h	4.5	4.5	0.0
Kidney transplant patients		12.1	30.2	14.3
Stable ICU		1.6	36.8	66.7
Unstable ICU		6.3	39.2	27.2
Liver failure	0.1–1-6 h	0.7	0.7	0.0
Kidney transplant patients		4.7	17.4	13.3
Stable ICU		3.8	14.7	20.0
Unstable ICU		3.6	22.9	18.2
Liver failure	0.1–1-9 h	3.3	3.4	0.0
Kidney transplant patients		1.0	5.8	0.0
Stable ICU		8.6	10.5	16.7
Unstable ICU		3.7	18.8	22.2

The best performances were observed for kidney transplant patients, especially when using a 0.1, 1 and 9 hour LSS. However, as mentioned in the Methods section, the actual iohexol plasma concentration dataset for these patients is limited to 0–6 hours and concentration at 9 hours has been extrapolated using the popPK model, making the strong assumption that the 9 hour concentration was the true iohexol concentration. Moreover, the reference CL has been estimated using these extrapolated concentrations. Consequently, the three-point GFR estimates compared to reference are likely to be overoptimistic and this is a major shortcoming of this study. The performances obtained have to be confirmed in further studies including a sample at 9 hours.

Using four plasma samples per patient at 10, 30, 120 and 240 (or 300) minutes after the injection of iohexol, Ng et al.[3] reported two phases ("fast area" and "slow area") in the kinetics of iohexol in 527 HIV seropositive men and 514 children with chronic renal disease. The use of early time points (0.1 and 1 h) is important to accurately estimate iohexol C_{max}, given the large spread of the data. This spread can probably be partly explained by the uncertainty in the 6 minute sampling time and the very rapid decrease in plasma concentrations following intravenous injection corresponding to a fast distribution. This illustrates the need for precise and accurate information about sampling times.

Model concentration estimates deviated from measured concentrations at the lower end of the concentration range. Late samples, mainly the points at T_{18h} and T_{24h}, often showed concentrations below the analytical limit of quantitation (LOQ). However, these samples provide information on the last phase of iohexol elimination, which led us to keep the first value below the LOQ (if any) for each patient. Anyway, plasma iohexol concentrations near the LOQ had a higher CV than higher values (Figure S3 in the Supporting Information), and this is clearly a limitation of this study. We can raise two hypotheses about this deviation: (i) the analytical method (HPLC with ultraviolet detection) used at that time had limited sensitivity and we have since developed a tandem-mass spectrometry technique with 10-fold better sensitivity[16]; or (ii) a third compartment exists for iohexol in these patients. The AIC was lower for the 2cp which is in favour of the LOQ hypothesis.

However, we observed that even if the low concentrations, near or below the LOQ, were poorly estimated with the two-compartment model, the effect on GFR estimation was negligible.

The comparison with the BM formula that uses samples in the second slope and correction for the first slope require an additional sample and showed worse performance in comparison to our MAP-BE. However, due to the low number of samples available within the second slope, this estimation could not be performed in the ICU patients.

GFR measurement based on serum creatinine is highly unreliable in intensive care patients, due to the delay between GFR and creatinine variations.[17] In our patients, iohexol clearance was measured using a 24-hour sampling schedule, delivering the mean GFR over 24 hours, encompassing all GFR variations (whether physiological, pathological—in unstable patients—or therapeutic) during this period. Nevertheless, in a previous work, Salmon-Gandonnière et al. demonstrated that the plasma iohexol concentration decay was steady within 24 hours in most patients and the fluid infusion volume or the use of catecholamines did not influence the iohexol pharmacokinetic parameters.[18] They also compared iohexol clearance calculated over 24 hours and over 6 hours and found that the variability of iohexol

Licence CC BY-NC-ND 3.0

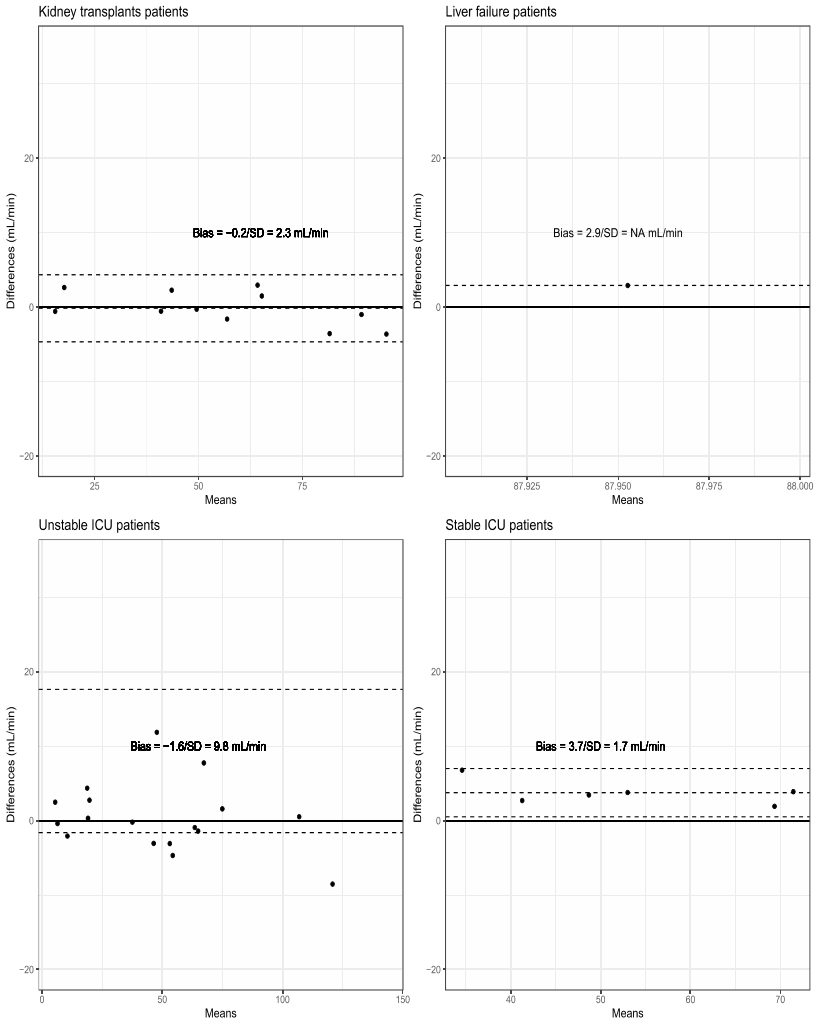

FIGURE 3 Bland-;Altman of clearance obtained using MAP-BE from all samples versus 3 samples split by type of patients in the validation dataset

clearance over 24 hours was moderate (from 5 to 55%), suggesting that aggressive therapeutic interventions in the early period of ICU hospitalisation were not accompanied by parallel and rapid fluctuations of GFR. As a comparison, the coefficient of variation of creatinine clearance in healthy individuals can be as high as 35–45%, due to variability in both creatinine production and creatinine excretion.[19]

In conclusion, we developed a popPK model and Bayesian estimator able to estimate GFR in stable or unstable intensive care patients, liver failure patients and kidney transplant patients. Performance is accurate in renal transplant patients while the model slightly overestimates in stable ICU patients and exhibits the largest imprecision in unstable ICU patients. In liver failure patients, the performance has to be further evaluated.

ACKNOWLEDGEMENTS

We thank Karen Poole for manuscript editing. No funding was received for this study.

COMPETING INTERESTS

The authors have no competing interests to declare in relation to this work.

CONTRIBUTORS

A.D. and J.B.W. were involved in the conceptualisation, methodology, formal analysis and writing of the paper. C.S.G., A.A., V.L.R., S.E. and P.C. were involved in the investigation and project administration. P.M. and C.B.L.G. were involved in the supervision and resources.

Licence CC BY-NC-ND 3.0

DATA AVAILABILITY STATEMENT

The data that support the findings of this study are available, on reasonable request, from the corresponding author. The data are not publicly available due to privacy or ethical restrictions.

ORCID

Anders Åsberg https://orcid.org/0000-0002-0628-1769
Jean-Baptiste Woillard https://orcid.org/0000-0003-1695-0695

REFERENCES

1. Soveri I, Berg UB, Björk J, et al. Measuring GFR: a systematic review. *Am J Kidney Dis*. 2014;64(3):411-424.
2. Bröchner-Mortensen J. A simple method for the determination of glomerular filtration rate. *Scand J Clin Lab Invest*. 1972;30:271-274.
3. Ng DKS, Schwartz GJ, Jacobson LP, et al. Universal GFR determination based on two time points during plasma iohexol disappearance. *Kidney Int*. 2011;80(4):423-430.
4. Haute Autorité de Santé Evaluation du débit de filtration glomérulaire, et du dosage de la créatininémie dans le diagnostic de la maladie rénale chronique chez l'adulte—Rapport d'évaluation [Internet]. https://www.has-sante.fr/portail/jcms/c_1064297/fr/evaluation-du-debit-de-filtration-glomerulaire-et-du-dosage-de-la-creatininemie-dans-le-diagnostic-de-la-maladie-renale-chronique-chez-l-adulte-rapport-d-evaluation. Published December 28, 2011. Accessed May 7, 2019.
5. Herrera-Gutiérrez ME, Seller-Pérez G, Banderas-Bravo E, Aragón-Gonzalez C, Olalla-Sánchez R, Lozano-Sáez R. Discrepancies in the RIFLE classification are due to the method used to assess the level of derangement of kidney function. *J Crit Care*. 2011;26:572-576.
6. Eason JD, Gonwa TA, Davis CL, Sung RS, Gerber D, Bloom RD. Proceedings of Consensus Conference on Simultaneous Liver Kidney Transplantation (SLK). *Am J Transplant*. 2008;8:2243-2251.
7. Benz-de Bretagne I, le Guellec C, Halimi JM, et al. New sampling strategy using a Bayesian approach to assess iohexol clearance in kidney transplant recipients. *Ther Drug Monit*. 2012;34(3):289-297.
8. Taubert M, Ebert N, Martus P, et al. Using a three-compartment model improves the estimation of iohexol clearance to assess glomerular filtration rate. *Sci Rep*. 2018;8:17723.
9. Riff C, Besombes J, Gatault P, et al. Assessment of the glomerular filtration rate (GFR) in kidney transplant recipients using Bayesian estimation of the iohexol clearance. *Clin Chem Lab Med*. 2020;58(4):577-587.
10. Salmon Gandonnière C, Helms J, le Tilly O, et al. Glomerular hyper- and hypofiltration during acute circulatory failure: iohexol-based gold-standard descriptive study. *Crit Care Med*. 2019;47(8):e623-e629.
11. Giguet B, Carrier P, Destere A, et al. Description of the evolution of iohexol plasma and urinary concentrations in cirrhotic patients. Pilot study. The Liver Meeting Digital Experience™. AASLD; 2020;72(Supplement 1):1103-1104. Meeting Abstract.
12. Åsberg A, Bjerre A, Almaas R, et al. Measured GFR by utilizing population pharmacokinetic methods to determine iohexol clearance. *Kidney Int Reports*. 2020;5(2):189-198.
13. Schloerke B, Cook D & Larmarange J et al. GGally: Extension to "ggplot2" [Internet]. 2021. https://CRAN.R-project.org/package=GGally. Accessed December 20, 2021.
14. Jødal L, Brøchner-Mortensen J. Reassessment of a classical single injection 51Cr-EDTA clearance method for determination of renal function in children and adults. Part I: Analytically correct relationship between total and one-pool clearance. *Scand J Clin Lab Invest*. 2009;69(3):305-313.
15. Luis-Lima S, Gaspari F, Negrín-Mena N, et al. Iohexol plasma clearance simplified by dried blood spot testing. *Nephrol Dial Transplant*. 2018;33:1597-1603.
16. Lee S-Y, Chun M-R, Kim D-J, Kim JW. Determination of iohexol clearance by high-performance liquid chromatography-tandem mass spectrometry (HPLC-MS/MS). *J Chromatogr B*. 2006;839:124-129.
17. Pickering JW, Ralib A, Endre ZH. Combining creatinine and volume kinetics identifies missed cases of acute kidney injury following cardiac arrest. *Crit Care*. 2013;17:R7.
18. Salmon-Gandonnière C, Benz-de Bretagne I, Mercier E, et al. Iohexol clearance in unstable critically ill patients: a tool to assess glomerular filtration rate. *Clin Chem Lab Med*. 2016;54(11):1777-1786.
19. Greenblatt DJ, Ransil BJ, Harmatz JS, Smith TW, Duhme DW, Koch-Weser J. Variability of 24-hour urinary creatinine excretion by normal subjects. *J Clin Pharmacol*. 1976;16:321-328.

SUPPORTING INFORMATION

Additional supporting information may be found in the online version of the article at the publisher's website.

How to cite this article: Destere A, Salmon Gandonnière C, Åsberg A, et al. A single Bayesian estimator for iohexol clearance estimation in ICU, liver failure and renal transplant patients. *Br J Clin Pharmacol*. 2022;1-9. doi:10.1111/bcp.15197

Licence CC BY-NC-ND 3.0

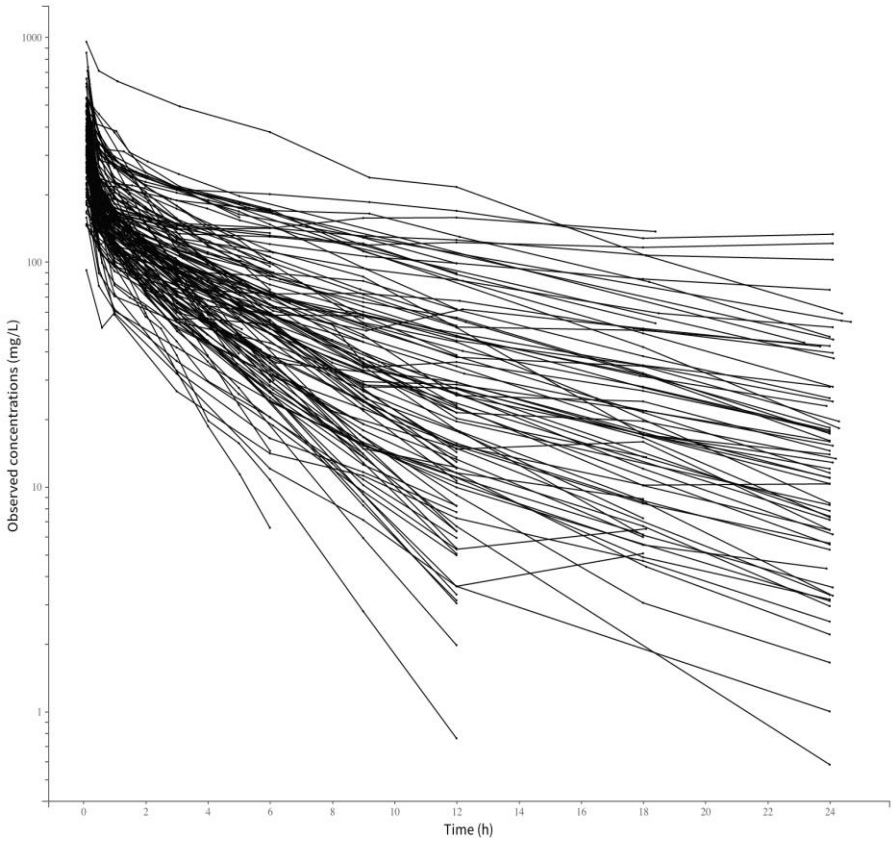

Supplemental plot 1 Log plot of iohexol plasma concentrations (mg/L) as function of time (h)

Licence CC BY-NC-ND 3.0

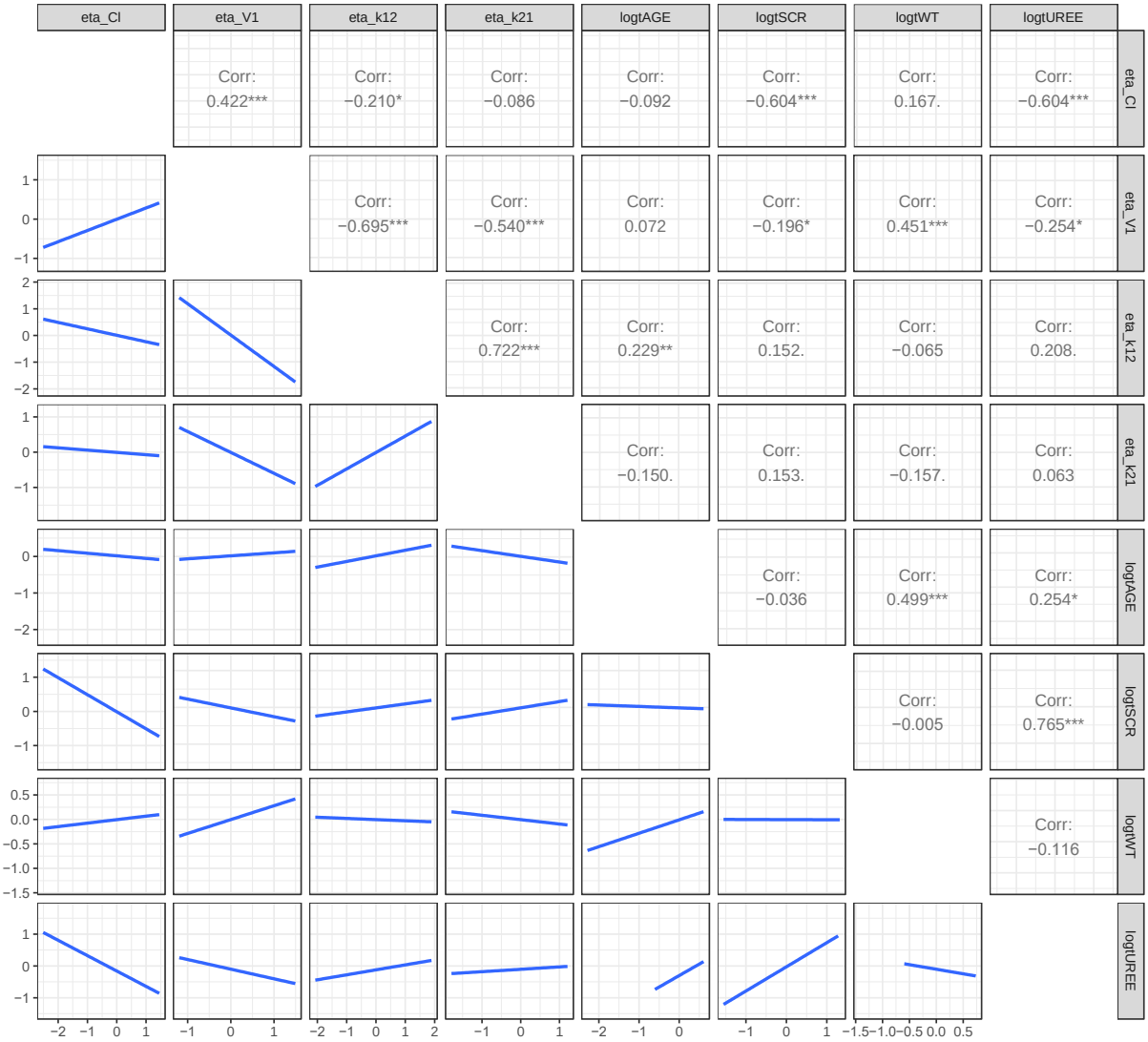

Supplemental plot 2 Correlation matrix of random effect of the PK parameters for the structural model and log of covariates.

Licence CC BY-NC-ND 3.0

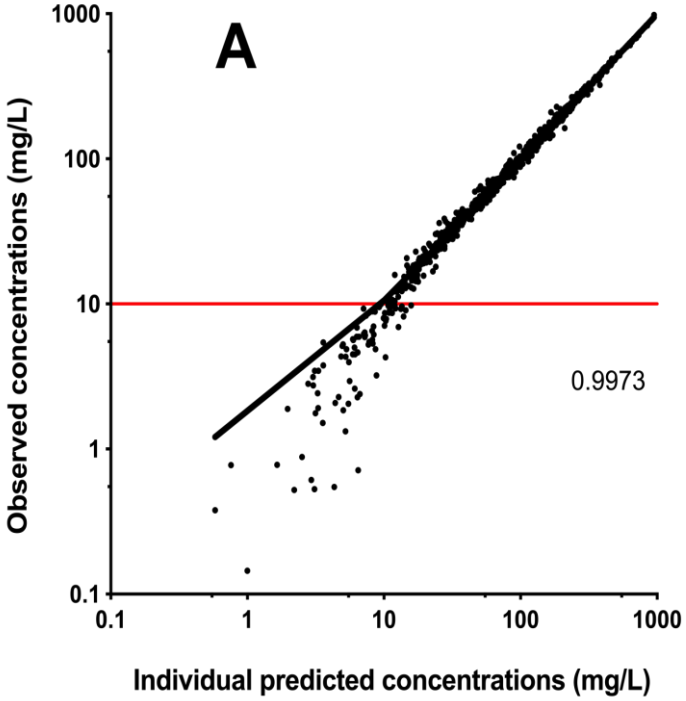

Supplemental plot 3 log10 of observed concentration as function of log10 of individual prediction highlighting deviation from abline for values near the limit of quantification (10 mg/L)

Licence CC BY-NC-ND 3.0

Supplemental method: GFR calculation using Bröchner-Mortensen formula

A linear model was applied to the 4 concentration times values for each patient to calculate the AUC using intercept and log-slope.

$$AUC = exp(intercept)/-log-slope\ CL = Dose/AUC$$

$$Cl\ BM\ Formula = 0.990778 \times CL - 0.001218 \times CL$$

$$BSA = 0.007184 \times Height^{0.725} \times Weight^{0.425}$$

$$DFG = Cl\ BM\ Formula \times 1.73/BSA$$

Licence CC BY-NC-ND 3.0

II.3. A hybrid model associating population pharmacokinetic and machine learning: a case study with iohexol clearance estimation

Article publié dans *Clinical Pharmacokinetics*

Il existe de nombreux modèles de POPPK et algorithmes de Machine Learning permettant d'estimer un ou des paramètre PK d'intérêt. Toutefois, la combinaison de ces 2 approches est assez récente et est décrite la première fois par Hughes et al. [101] puis par Tang et al. [100]. Le premier modèle hybride permet de choisir, ou non, des priors aplatis dans l'estimation Bayésienne (c'est-à-dire de diminuer l'importance de l'information a priori au profit de l'observation individuelle). Le second, réestime la clairance d'antibiotiques dans une population pédiatrique à partir de la clairance estimée par le modèle POPPK et des covariables du modèle.

Notre étude a pour objectif d'améliorer les estimations de la clairance de l'iohexol. Pour cela, au contraire de Tang et al. [100], nous avons estimé l'erreur entre la clairance obtenue à partir de tous les points de la cinétique et la clairance obtenue à partir du MAP-BE basé sur une LSS à 3 points sur des profils simulés à partir du modèle de POPPK développé précédemment [108]. Pour entrainer l'algorithme, 29 variables ont été fournies au total. Ces variables sont notamment composées des paramètres PK estimés à partir du MAP-BE, des concentrations observées et prédites par le MAP-BE, des covariables des profils simulés ainsi que des covariables informatives crées et basées sur notre connaissance expert (la création de ces covariables ainsi que les étapes de transformation des covariables comme la normalisation, le *one hot encoding* est appelée « features engineering »).

Les résultats obtenus grâce à ce modèle hybride sont assez prometteurs avec seulement 5,6% des patients ayant un biais relatif de plus de 20% entre la clairance de référence et la clairance corrigée (*versus* MAP-BE = 13,9%) ainsi qu'un biais moyen et une imprécision diminués d'environ 30%, toutes les 2 par rapport au MAP-BE utilisé seul.

Dans ce travail, nous avons comparé différents types d'algorithmes (GLMnet et Xgboost). Les résultats obtenus avec ces 2 algorithmes sont similaires. Toutefois, GLMnet semble corriger l'imprécision ainsi que le pourcentage de profils avec une erreur absolue de plus de 20% de manière plus importante que l'algorithme Xgboost.

L'amélioration des performances par notre algorithme hybride est principalement liée à la correction de l'eta-shrinkage présent dans le MAP-BE. Nous avons comparé notre méthode à celle proposée par Baklouti et al. [109] ayant pour but la correction du shrinkage du MAP-

Licence CC BY-NC-ND 3.0

BE. La correction de l'eta-shrinkage obtenue est similaire à la méthode proposée dans l'article de Baklouti et al. [109].

En complément de cette étude, cette méthodologie a été testée sur des MAP-BEs basés sur des LSS différentes en faisant varier le nombre de points. Une stratégie à 1 point augmentant le shrinkage puis une stratégie à 6 points diminuant le shrinkage ont été testées. Quelle que soit la LSS utilisée (fortement ou faiblement shrinkée), les modèles hybrides permettent d'améliorer les estimations de la clairance par rapport à l'estimation par le MAP-BE (supplemental data 2 de l'article, ci-dessous). En revanche, *a contrario* de la LSS basée sur 3 point publiée dans notre article, nous observons que le modèle hybride basé sur l'algorithme Xgboost possède de meilleures performances que celui basé sur l'algorithme GLMnet. Ce dernier point pourrait mettre en lumière que le problème étudié n'est peut-être pas linéaire.

Licence CC BY-NC-ND 3.0

Clinical Pharmacokinetics
https://doi.org/10.1007/s40262-022-01138-x

ORIGINAL RESEARCH ARTICLE

A Hybrid Model Associating Population Pharmacokinetics with Machine Learning: A Case Study with Iohexol Clearance Estimation

Alexandre Destere[1,2,3] · Pierre Marquet[1,2] · Charlotte Salmon Gandonnière[4] · Anders Åsberg[5,6] · Véronique Loustaud-Ratti[1,7] · Paul Carrier[7] · Stephan Ehrmann[4,8] · Chantal Barin-Le Guellec[1] · Aurélie Premaud[1] · Jean-Baptiste Woillard[1,2]

Accepted: 5 May 2022
© The Author(s), under exclusive licence to Springer Nature Switzerland AG 2022

Abstract

Background Maximum a posteriori Bayesian estimation (MAP-BE) based on a limited sampling strategy and a population pharmacokinetic model is frequently used to estimate pharmacokinetic parameters in individuals, however with some uncertainty (bias). Recent works have shown that the performance in individual estimation or pharmacokinetic parameters can be improved by combining population pharmacokinetic and machine learning algorithms. Objective: The objective of this work was to investigate the use of a hybrid machine learning/population pharmacokinetic approach to improve individual iohexol clearance estimation.

Methods The reference iohexol clearance values were derived from 500 simulated profiles (samples collected between 0.1 and 24.7 h) using a population pharmacokinetic model we recently developed in Monolix and obtained using all the concentration timepoints available. Xgboost and glmnet algorithms able to predict the error of MAP-BE clearance estimates based on a limited sampling strategy (0.1 h, 1 h, and 9 h) versus reference values were developed in a training subset (75%) and were evaluated in a testing subset (25%) and in 36 real patients.

Results The MAP-BE limited sampling strategy estimated clearance was corrected by the machine learning predicted error leading to a decrease in root mean squared error by 29% and 24%, and in the percentage of profiles with the mean prediction error out of the ±20% bias by 60% and 40% in the external validation dataset for the glmnet and Xgboost machine learning algorithms, respectively. These results were attributable to a decrease in the eta-shrinkage (shrinkage for a MAP-BE limited sampling strategy = 32.4%, glmnet = 18.2%, and Xgboost = 19.4% in the external dataset).

Conclusions In conclusion, this hybrid algorithm represents a significant improvement in comparison to MAP-BE estimation alone.

1 Introduction

In addition to standard therapeutic drug monitoring, population pharmacokinetic (POPPK) modeling helps to individualize the dose of drugs characterized by a large inter-individual variability and a narrow therapeutic index [1, 2]. Indeed, maximum a posteriori Bayesian estimation (MAP-BE) based on prior and observed information, often based on a limited sampling strategy and some covariates, can estimate individual pharmacokinetic (PK) parameters (e.g., distribution volume, clearance [CL]) and/or exposure indices (e.g., area

Key Points

This study investigated the ability of a hybrid model associating maximum a posteriori Bayesian estimation population pharmacokinetics with machine learning to improve individual iohexol clearance estimation.

The hybrid models developed decreased by about 30% the mean prediction error and root mean squared error in comparison to the maximum a posteriori Bayesian estimation alone.

This hybrid approach could be generalized for drugs with complex pharmacokinetics and characterized by a large error when using maximum a posteriori Bayesian estimation for individual predictions.

✉ Jean-Baptiste Woillard
jean-baptiste.woillard@unilim.fr

Extended author information available on the last page of the article

Published online: 31 May 2022

Adis

Licence CC BY-NC-ND 3.0

under the concentration–time curve) and help to derive a dose adjustment proposal. Machine-learning (ML) approaches have also recently been proposed to estimate drug exposure [3, 4]. Each approach has drawbacks: ML seems to be more accurate than a POPPK model but less flexible (for instance, with respect to sampling times), and it cannot be used to draw simulations. Recent studies proposed the combined use of a POPPK model and ML in order to choose the best POPPK structural model [5], select pertinent covariates [6], improve antibiotic CL estimation on top of POPPK estimation with covariates [7], or to select patients in whom it would be better to use flat priors than conventional MAP-BE for vancomycin [8]. Indeed, MAP-BE can suffer from a systematic deviation called shrinkage and requires the use of flat priors to correct this problem [9]. In this latter example, the ML algorithm mainly learned from the error between observations and predictions to solve a binary problem with or without the use of flattened priors. Similarly, we hypothesize that based on features, ML can learn how to decrease the error (in a regression problem) resulting from a POPPK model and MAP-BE based on a limited sampling strategy (LSS). The estimation of the glomerular filtration rate using iohexol CL could be a good case study: several POPPK models [10–14] and one ML algorithm [15] have been developed to estimate iohexol plasma CL based on LSSs. We recently published a POPPK model for iohexol CL estimation (in intensive care unit [ICU] patients and patients with liver failure or undergoing a kidney transplant) [16], the results of which are very accurate in patients undergoing a kidney transplant, but partially biased in stable ICU patients and slightly imprecise in unstable ICU patients. We made the hypothesis that such bias and imprecision could be decreased by the combination of ML and POPPK approaches. The aim of this work was to investigate the use of ML to predict the error in individual estimations resulting from MAP-BE based on a LSS (MAP-BE LSS) and on a POPPK model, to improve the individual estimation of iohexol CL and glomerular filtration rate (GFR).

2 Material and Methods

2.1 Population Pharmacokinetics

2.1.1 Data Simulation

The population parameters and relevant covariates of our recent published POPPK model [16] were used to simulate 500 patients with 250 concentration samples between 0.1 and 24.7 hours with Simulx [17]. Briefly, it consisted of a 2cp model with combined (proportional and additive) residual error and included the following: bodyweight, type of patient (stable or unstable ICU, kidney transplant, and liver failure) as covariates on the central volume; and serum creatinine and type of patient on CL. A dose of 3235 mg, generally administered in this indication, was used for the simulations. Some filters were applied to extreme values of the simulated PK parameters (central volume, CL, and transfer constant of central to peripheric volume) so as to restrict the range to that of the original publication (exclusion of 1% extreme percentiles). It is noteworthy that all simulated transfer constants of peripheric to central volume values were already in this range. The CL parameter obtained for each simulated patient by application of MAP-BE to the 250 simulated samples was considered to be the reference (refCL).

2.1.2 Estimation of the Differences between refCL and MAP-BE LSS CL

The concentrations at 0.1, 1, and 9 h (LSS selected in the original article) were extracted from the simulated concentrations and the MAP-BE LSS CL was calculated. The raw error between the refCL and MAP-BE LSS CL was calculated using the following formula:

$$\text{Error} = \text{refCL} - \text{MAPBELSSCL}.$$

Then, ML algorithms were trained to predict this error and to correct the MAP-BE LSS CL. The improvement of the iohexol CL prediction (mean prediction error [MPE] and root mean squared error [RMSE]) was evaluated.

2.2 ML Approaches

2.2.1 Preparation of the Data and Feature Engineering

Simulations were split into training (75%) and testing (25%) datasets and concentrations at 0.1, 1, and 9 h, covariates, and estimated PK parameters based on MAP-BE LSS were extracted. Feature engineering was applied by calculating: (i) the differences among the observed concentrations [OC] (OC0.1–OC1, OC0.1–OC9, and OC1–OC9); (ii) the ratios among the OC (OC1/OC0.1, OC9/OC0.1, and C9/C1); (iii) the relative ratios among the OC (OC0.1–OC1)/OC1, OC0.1–OC9/OC9, and OC1–OC9/OC9); (iv) the differences between observed and MAP-BE LSS estimated concentrations (EC) at each timepoint (OC0.1–EC0.1, OC1–EC1, OC9–EC9); and (v) the ratios between observed and MAP-BE LSS EC (OC0.1/EC0.1, OC1/EC1, OC9/EC9). Finally, a total of 29 features (PK parameters estimated by MAP-BE LSS and simulated covariates) were available for the development of the ML algorithm.

2.2.2 ML Analysis

Algorithms to predict errors between refCL and the MAP-BE LSS CL were developed using the Tidymodels framework in R [18] and two types of algorithms in parallel:

Licence CC BY-NC-ND 3.0

Xgboost [19] and penalized generalized linear regression (glmnet) [20]. A ten-fold cross-validation was applied to the training set to tune the hyperparameters and evaluate the model performances (based on the r^2). The algorithm predicted error was then added to the MAP-BE LSS to obtain the corrected CL (corCLr), as follows:

$$\text{corCL} = \text{MAPBELSSCL} + \text{algorithm predicted error}.$$

Finally, the performances of iohexol CL prediction with this hybrid model in the training dataset (using ten-fold cross-validation) and the testing dataset were evaluated by calculating the relative MPE%, the relative RMSE%, and the percentage of profiles with MPE% out of the ±20% interval between the corCl and refCL. Variable importance plots were drawn to evaluate the most important features in each algorithm.

2.2.3 External Validation

The performance of the two ML algorithms to correct the MAP-BE LSS CL were evaluated in 36 real patients of the independent validation dataset [16]. They were the same patients as those in the original article but not used in the development of the POPPK model. The study was conducted in accordance with ethical principles in the Declaration of Helsinki. All patients received verbal and written information and signed an informed consent before entering the study. Plots of the unexplained error of estimated iohexol CL obtained using MAP-BE LSS and the hybrid model in the testing and external datasets were drawn to show the improvements made by the latter.

2.2.4 Evaluation of the Shrinkage

The η shrinkage implication in the hybrid model correction was evaluated and compared to the recently published approach in Baklouti et al. [9] based on locally estimated scatterplot smoothing (LOESS).

The shrinkage of MAP-BE LSS, hybrid models, and LOESS was estimated in training, testing, and external datasets based on the formula used in Monolix [21]:

$$\text{Shrinkage} = 1 - \frac{\text{var}(\eta\text{CLx})}{\omega^2_{Cl}},$$

where x is the method used, η CL_x is the random effect of the parameter, and ω^2CL is the variance of the parameter estimate.

The random-effects correction improvement (η) for each correction method was measured using the formula proposed in Baklouti et al. [9]:

$$\text{Overall Improvement} = 1 - \frac{\sum \left[\eta\text{Cl} - \eta\text{Cl}_x\right]^2}{\sum \left[\eta\text{Cl} - \eta\text{Cl}_{\text{MAPBELSS}}\right]^2},$$

where x is the hybrid model or LOESS.

3 Results

3.1 Simulated Data

After excluding the 1% extreme percentiles of CL, central volume, and transfer constant of central to peripheric volume, 468 (out of the 500) simulated profiles from 250 samples remained. A summary of the features used as predictors in the ML algorithms is presented in Table 1. This consisted of MAP-BE estimated individual PK parameters, OCs, ECs, simulated covariates, and the 15 newly created features. No statistical difference was observed between the features used in the training and testing datasets. The distribution of MAP-BE LSS CL, and of the error between refCL and MAP-BE LSS CL are presented in Fig. 1. Glmnet and Xgboost predicted the error with r^2 ± standard deviation = 0.66 ± 0.03 and 0.64 ± 0.03 in the training set, and r^2 = 0.94 ± 0.07 and 0.70 ± 0.05 in the testing set, respectively. The performances of each hybrid algorithm (corCL) to correct the MAP-BE LSS CL are presented in Table 2. The variable importance plots of the two ML algorithms are also presented in Fig. 2. They showed that the ratio between OC and EC at 9 h that corresponds to the ratio between the concentration observed at 9 hours and that predicted by the MAP-BE LSS was found by both ML algorithms as very important, while other variables were selected only for one or another method. The unexplained errors between the MAP-BE LSS and the hybrid model with either Xgboost or glmnet in the testing set are presented in Fig. 3A, B.

3.2 Performance to Correct the MAP-BE LSS CL in Actual Data

The performances of MAP-BE LSS and the hybrid algorithms with either glmnet or Xgboost to predict the refCL in the external datasets are presented in Table 2, and the plot of the corresponding unexplained errors in Fig. 3C, D. Whatever the hybrid model chosen, the performance to predict refCL was better than MAP-BE LSS.

3.3 Evaluation of the Shrinkage and the Improvement of Prediction of Individual Random Effects (η) in Training, Testing, and External Datasets

The shrinkage of the MAP-BE, hybrid models (Xgboost and glmnet), and LOESS method is presented in Table 3. The shrinkage obtained with the Xgboost hybrid model was similar to the one obtained with the LOESS method while the one obtained with the glmnet hybrid model was

Licence CC BY-NC-ND 3.0

Table 1 Characteristics of the simulated profiles in the training and testing subsets

	Overall	Training	Testing	Student test *p* value
n	468	351	117	
OC0.1, mean (SD)	373.56 (147.12)	375.03 (145.61)	369.13 (152.09)	0.707
EC0.1, mean (SD)	373.05 (144.96)	374.43 (143.36)	368.91 (150.20)	0.722
OC1, mean (SD)	164.28 (64.33)	163.59 (62.41)	166.34 (70.03)	0.69
EC1, mean (SD)	163.56 (62.73)	162.92 (60.95)	165.47 (68.04)	0.704
OC9, mean (SD)	52.24 (37.52)	52.66 (37.53)	50.96 (37.61)	0.671
EC9, mean (SD)	51.91 (36.88)	52.34 (36.89)	50.64 (36.97)	0.666
MAP-BE CL, mean (SD)	2.98 (1.84)	2.97 (1.88)	2.99 (1.72)	0.927
MAP-BE V1, mean (SD)	8.54 (4.07)	8.44 (3.94)	8.85 (4.45)	0.341
MAP-BE k12, mean (SD)	1.64 (0.89)	1.65 (0.87)	1.60 (0.93)	0.595
MAP-BE k21, mean (SD)	1.25 (0.51)	1.24 (0.45)	1.27 (0.64)	0.518
Serum creatinine, mean (SD)	132.07 (76.43)	131.22 (75.43)	134.65 (79.63)	0.675
Weight, mean (SD)	77.43 (19.83)	77.63 (19.95)	76.85 (19.54)	0.714
Type of patients, *n* (%)				0.801
Liver failure	22 (4.7)	17 (4.8)	5 (4.3)	
Unstable ICU	235 (50.2)	180 (51.3)	55 (47.0)	
Stable ICU	56 (12.0)	42 (12.0)	14 (12.0)	
Kidney transplant	155 (33.1)	112 (31.9)	43 (36.8)	
OC0.1–OC1 difference, mean (SD)	209.28 (107.64)	211.44 (107.26)	202.79 (108.99)	0.452
OC0.1–OC9 difference, mean (SD)	321.32 (140.39)	322.37 (138.94)	318.17 (145.22)	0.78
OC1–OC9 difference, mean (SD)	112.04 (55.13)	110.93 (52.96)	115.38 (61.31)	0.45
OC0.1/OC1 ratio, mean (SD)	2.35 (0.69)	2.37 (0.69)	2.29 (0.68)	0.291
OC0.1/OC9 ratio, mean (SD)	18.07 (41.65)	17.13 (35.73)	20.90 (55.85)	0.397
OC1/OC9 ratio, mean (SD)	6.65 (11.84)	6.40 (10.72)	7.38 (14.75)	0.441
OC0.1/OC1 relative ratio, mean (SD)	1.35 (0.69)	1.37 (0.69)	1.29 (0.68)	0.291
OC0.1/OC9 relative ratio, mean (SD)	17.07 (41.65)	16.13 (35.73)	19.90 (55.85)	0.397
OC1/OC9 relative ratio, mean (SD)	5.65 (11.84)	5.40 (10.72)	6.38 (14.75)	0.441
OC0.1–EP0.1 difference, mean (SD)	0.51 (3.64)	0.60 (3.60)	0.22 (3.74)	0.33
OC0.1–EP0.1 difference, mean (SD)	0.72 (2.87)	0.68 (2.69)	0.87 (3.37)	0.526
OC0.1–EP0.1 difference, mean (SD)	0.33 (1.29)	0.33 (1.28)	0.32 (1.34)	0.976
OC0.1–EP0.1 ratio, mean (SD)	1.00 (0.0.1)	1.00 (0.0.1)	1.00 (0.0.1)	0.297
OC1/EC1 ratio, mean (SD)	1.00 (0.02)	1.00 (0.02)	1.00 (0.02)	0.921
OC9/EC9 ratio, mean (SD)	0.99 (0.07)	0.99 (0.07)	0.99 (0.07)	0.833

CL clearance, *ECx* estimated concentrations at x hours, *ICU* intensive care unti, *k12* transfer constant of central to peripheric volume, *k21* transfer constant of peripheric to central volume, *OCx* observed concentrations at x hours, *SD* standard deviation, *V1* central volume

decreased. Regarding the improvement of prediction of random effects (η) in the training and testing datasets, glmnet obtained the best results (33.6% and 82.5%) in comparison to Xgboost (33.8% and 4.2%) and the LOESS method (17.3% and −12.9). Similar results were observed in the external dataset as the glmnet had the highest improvement (45.5%) compared with the Xgboost hybrid model (33.4%) and the LOESS method (20.1%). The performances in terms of RMSE and MPE or profiles outside the ±20% interval were still better for both ML approaches in comparison to the LOESS method in the training, testing, and external datasets.

4 Discussion and Conclusions

In this study, we developed a hybrid model that associates MAP-BE LSS backed on a POPPK model on the one hand with a ML algorithm on the other hand, to improve the performance of individual estimation of iohexol plasma CL mainly by correcting the shrinkage. We observed a decrease in MPE%, RMSE%, and the percentage of profiles out of the ±20% MPE interval with the hybrid models vs MAP-BE LSS alone. The advantage of this approach is that the use of a hybrid model allows interpretability of the predictions to be conserved contrary to ML algorithms alone, while

Licence CC BY-NC-ND 3.0

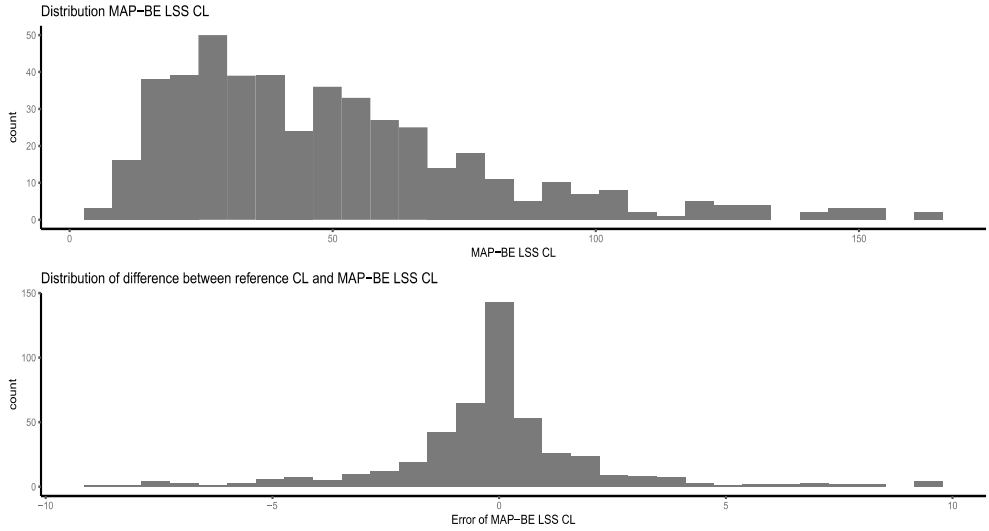

Fig. 1 Histogram of maximum a posteriori Bayesian estimation (MAP-BE) of iohexol plasma clearance (CL) based on the 0.1-h, 1-h, and 9-h limited sampling strategy and difference (error) between the reference CL and MAP-BE CL in the simulated dataset

benefiting from the powerful data-driven reduction in error brought by ML.

The glmnet algorithm yielded the best results in terms of the percentage of estimations out of the ± 20% bias interval, while the imprecision was almost similar to the Xgboost and this latter had a lower mean bias. That led us to select the penalized glmnet because of the lower percentage of profiles out of the ± 20% bias interval.

The performance of refCL estimation was highly improved when using the hybrid models with about a 30% decrease in MPE% and RMSE% in the external dataset in comparison to the standard MAP-BE approach. The shrinkage observed after correction in the external dataset, whatever the methods used (LOESS recently developed by Baklouti et al. [9] [23%], the glmnet hybrid model [18.2%], or the Xgboost hybrid model [19.4%]), was improved in comparison to the MAP-BE approach (Table 3). However, although the decrease in shrinkage is similar between the methods, the overall improvement and the performances in terms of individual predictions (MPE, RMSE, and percentage of bias out of the ± 20% interval) were higher with the hybrid models in comparison to LOESS. The shrinkage and improvement evaluate different aspects: the first evaluates the spread of the estimated parameter while the second evaluates the precision of the random effect of the parameter estimation in comparison to that of the MAP-BE. Finally, the MPE and RMSE evaluated the performance of the prediction in the PK parameter itself.

Performance improvement with hybrid ML and POPPK algorithms has previously been reported by other studies. Hughes and Keizer developed a hybrid model to choose whether flat priors must be applied for MAP-BE and they observed a decrease in RMSE of 12–22% (5–18% for the two-feature ML algorithm) vs MAP-BE alone. Tang et al. recently developed an extra tree regressor to predict an individual CL based on individual covariates and MAP-BE CL predicted by POPPK models and individual concentrations for six antibiotics. They found a mean decrease in mean residual error up to 71.3% in comparison to POPPK alone. This work has similarities to the present study. However, the authors directly predicted the CL using the ML approach but not the error and they did not include the other post-hoc PK parameters in the predictors (except CL) and no feature engineering was performed [7]. We chose on the contrary to predict the error between refCL and MAP-BE LSS CL estimates because it provides direct access to the amount of correction brought by the ML algorithm. Additionally, feature engineering allowed an improvement in prediction as highlighted by the VIP plot that shows that the OC/EC ratio of 9 hours has a strong importance in error prediction whatever the ML algorithm used. As the algorithms are different (glmnet is derived from regression and Xgboost from boosting), this explains why the features selected are varied. The ratio between OC and EC at 9 hours between the observed concentration and that predicted by the POPPK model provides useful information about the difference between the true and estimated CL.

Shrinkage is intrinsically linked to MAP-BE based on LSS. The level of shrinkage depends on the amount of individual information provided. We wanted to determine whether the hybrid approach corrects for low shrinkage and increases the estimation accuracy for different LSS

Licence CC BY-NC-ND 3.0

Table 2 Performance of the different models to predict reference clearance in the training, testing, and external datasets

	MAP-BE LSS	Training			MAP-BE LSS	Testing			MAP-BE LSS	External		
		Hybrid model Xgboost	Hybrid model GLMnet	LOESS		Hybrid model Xgboost	Hybrid model GLMnet	LOESS		Hybrid model Xgboost	Hybrid model GLMnet	LOESS
MPE%	−2.0	−0.3	−0.3	−0.3	−1.0	0.7	0.2	0.8	−3.7	−2.2	−3.7	−2.6
RMSE%	10.1	7.5	7.2	8.7	6.2	5.7	2.4	6.3	14.3	10.9	10.2	12.3
Profiles with MPE% outside the ±20% interval (%)	4.0	2.8	2.9	3.1	1.7	0.9	0	1.7	13.9	8.3	5.6	11.1

LOESS locally estimated scatterplot smoothing, *LSS* limited sampling strategy, *MAP-BE* maximum a posteriori Bayesian estimator, *MPE* mean prediction error, *RMSE* root mean squared error

scenarios. We evaluated this by simulating different LSSs (one and six samples) and evaluating their performances. We observed that LOESS, Xgboost, or glmnet hybrid models still decreased the shrinkage and improved the individual predictions in comparison to MAP-BE, even if only to a smaller extent (Electronic Supplementary Material).

The benefit of applying such a ML approach to real data would allow learning from features that were not present during model building or that are more complex to implement in a POPPK context, or a systemic bias in a clinical setting that simulations did not allow. However, this is very rarely possible because of the limited number of data available in PK studies.

Interestingly, we observed in the testing dataset, but not in real patients, that the corrections tend to be the highest for small values of iohexol CL that are also characterized by a large bias when using MAP-BE alone (Fig. 3). These values are the most critical in routine care as they are used to characterize renal failure severity categories and, when needed, to trigger the renal replacement procedure. The highest errors, even after corrections, were observed in the testing set and in real patients for the hyper-CL, which in contrast are less critical in routine care. In this study, only the MAP-BE LSS CL was corrected by predicting the error between refCL and MAP-BE LSS. The correction was only applied to the iohexol CL as it is the surrogate for the GFR estimate. We agree that the correction of only one parameter leads to a change in the relationship with the other PK parameters as they are estimated simultaneously in a patient. However, the corrected parameter is not re-implemented in the POPPK model or used to perform simulations but only used in this case to estimate the GFR or more generally to calculate the area under the concentration–time curve of a drug using the dose/CL formula. The simultaneous correction of every PK parameter would require the use of deep learning approaches, allowing work on a vector of parameters, but is not suited in the present case given the amount of available data. This deserves further investigation.

We chose to use the POPPK model that we recently developed for the same dataset [16] instead of models already published, for many reasons. First, we had the full structure including the PK parameter correlation matrix, allowing more precise simulations. Second, this model fits diverse target populations including ICU patients, patients with liver failure, and patients undergoing a kidney transplant.

To improve the reliability of simulations, we chose to filter out the extreme values (one percentile) of the PK parameters, i.e., those that were distributed out of the original range [16]. We observed an improvement in performance in comparison to the hybrid algorithm developed when keeping all the PK parameter values (data not shown). Probably, the amount of data to be filtered out depends on the quality of the initial POPPK model and should be adjusted accordingly.

Licence CC BY-NC-ND 3.0

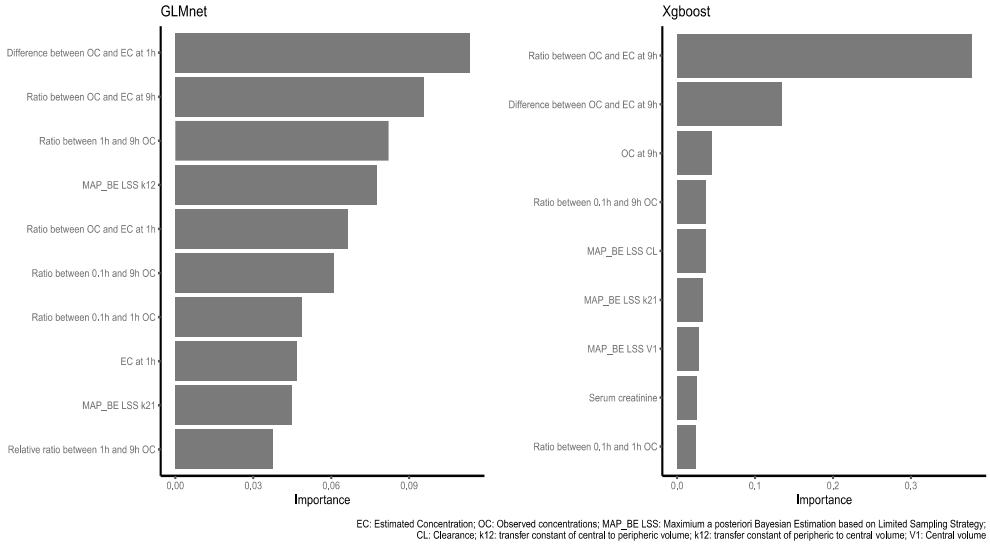

Fig. 2 Variable importance plots of the glmnet and Xgboost machine learning algorithms. *CL* clearance, *EC* estimated concentration, *h* hours, *k12* transfer constant of central to peripheric volume, *k12* transfer constant of peripheric to central volume, *MAP_BE LSS* maximium a posteriori Bayesian estimation based on a limited sampling strategy, *OC* observed concentrations, *V1* central volume

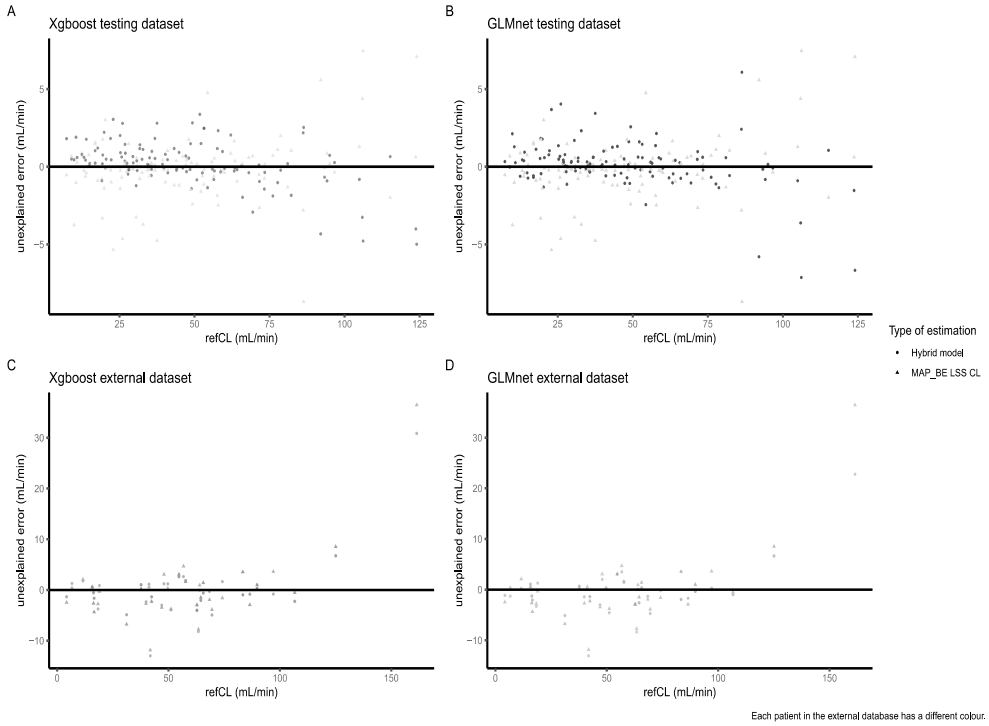

Fig. 3 Plots of the unexplained error of maximium a posteriori Bayesian estimation (MAP-BE) and hybrid models vs reference iohexol plasma clearance (CL) in the testing and external datasets for Xgboost and glmnet algorithms. *LSS* limited sampling strategy, *refCL* reference clearance

Licence CC BY-NC-ND 3.0

Table 3 Shrinkage evaluation for machine learning algorithms and the method described in Baklouti et al. [9] in comparison with MAP-BE LSS

	Training	Testing	External
MAP-BE LSS	17.6	32.1	32.4
Hybrid model Xgboost	7.1	25.4	19.4
Hybrid model glmnet	−2.4	26.7	18.2
LOESS method [9]	6.7	22.9	23.0

LOESS locally estimated scatterplot smoothing, *MAP-BE LSS* maximum a posteriori Bayesian estimator based on a limited sampling strategy

In our case, the simulated CL range was between 3.9 and 183.4 mL/min, which is enough to cover most of the GFR values observed in routine care.

From a practical point of view, these hybrid models can be implemented in dedicated computer or mobile apps (including MAP-BE and ML residue correction) to be used in routine practice. The overall procedure and code of the method developed here are shown in the ESM.

In the present study, we selected an accurate POPPK model to simulate PK profiles from which the ML algorithms could learn. A biased model would have led to the development of a biased hybrid model, hence poor generalizability and poor performance in independent datasets, which was obviously not the case here. Finally, this approach seems promising and needs to be investigated for other drugs with POPPK models with a large residual error (e.g., mycophenolic acid, characterized by complex pharmacokinetics) [22]. It is of note that the performances of forecasting concentrations into future occasions was not evaluated in this study as iohexol is administered only once. The ability of such an approach to forecast future occasions needs to be investigated in further studies. In this case, the intra-individual variability will have to be learnt in addition to the inter-individual variability, which is quite complicated based on simulations.

In conclusion, we developed a hybrid model associating MAP-BE that relies on a POPPK model with ML algorithms, yielding an improved estimation of individual iohexol plasma CL mainly owing to the decrease of η shrinkage of MAP-BE based on the LSS. The results obtained with this hybrid algorithm show a strong improvement in comparison toh MAP-BE alone and a good improvement in comparison to a recently published approach that deshrinks individual random effects [9].

Supplementary Information The online version contains supplementary material available at https://doi.org/10.1007/s40262-022-01138-x.

Acknowledgements The authors acknowledge Karen Poole for her manuscript editing.

Declarations

Funding No funding was received for the conduct of this study or the preparation of this article.

Conflicts of interest/competing interests None of the authors has any conflicts of interest that are directly relevant to the content of this study.

Ethics approval Ethics approval was obtained.

Consent to participate The patients included in the validation set had participated in clinical trials for which they had given their consent and they signed informed consent regarding publishing their data.

Availability of data and material The data that support the findings of this study can be obtained from Alexandre Destere on reasonable request (alexandre.destere@gmail.com).

Code availability The code is available as Electronic Supplementary Material.

Author contributions AD, JBW, PM, and AP contributed to the study conception and design. Material preparation and data collections were performed by CSG, AA, VLR, PC, SE, and CBLG and the analysis was conducted by AD and JBW The first draft of the manuscript was written by AD, JBW, and PM and all authors read and commented on the previous versions of the manuscript.

References

1. Leger F, Debord J, Le Meur Y, Rousseau A, Buchler M, Lachatre G, et al. Maximum a posteriori Bayesian estimation of oral cyclosporin pharmacokinetics in patients with stable renal transplants. Clin Pharmacokinet. 2002;41:71–80.
2. Marquet P, Destère A, Monchaud C, Rérolle J-P, Buchler M, Mazouz H, et al. Clinical pharmacokinetics and Bayesian estimators for the individual dose adjustment of a generic formulation of tacrolimus in adult kidney transplant recipients. Clin Pharmacokinet. 2021;60:611–22.
3. Guo W, Yu Z, Gao Y, Lan X, Zang Y, Yu P, et al. A machine learning model to predict risperidone active moiety concentration based on initial therapeutic drug monitoring. Front Psychiatry. 2021;12: 711868.
4. Woillard J, Labriffe M, Debord J, Marquet P. Tacrolimus exposure prediction using machine learning. Clin Pharmacol Ther. 2021;110:361–9.
5. Sibieude E, Khandelwal A, Girard P, Hesthaven JS, Terranova N. Population pharmacokinetic model selection assisted by machine learning. J Pharmacokinet Pharmacodyn. 2022;49:257–70.
6. Koch G, Pfister M, Daunhawer I, Wilbaux M, Wellmann S, Vogt JE. Pharmacometrics and machine learning partner to advance clinical data analysis. Clin Pharmacol Ther. 2020;107:926–33.
7. Tang B-H, Guan Z, Allegaert K, Wu Y-E, Manolis E, Leroux S, et al. Drug clearance in neonates: a combination of population pharmacokinetic modelling and machine learning approaches to improve individual prediction. Clin Pharmacokinet. 2021;60:1435–48.
8. Hughes JH, Keizer RJ. A hybrid machine learning/pharmacokinetic approach outperforms maximum a posteriori Bayesian estimation by selectively flattening model priors. CPT Pharmacometrics Syst Pharmacol. 2021;10:1150–60.

Licence CC BY-NC-ND 3.0

9. Baklouti S, Gandia P, Concordet D. "De-shrinking" EBEs: the solution for Bayesian therapeutic drug monitoring. Clin Pharmacokinet. 2022;61:749–57.
10. Åsberg A, Bjerre A, Almaas R, Luis-Lima S, Robertsen I, Salvador CL, et al. Measured GFR by utilizing population pharmacokinetic methods to determine iohexol clearance. Kidney Int Rep. 2020;5:189–98.
11. Benz-de Bretagne I, Le Guellec C, Halimi JM, Gatault P, Barbet C, Alnajjar A, et al. New sampling strategy using a Bayesian approach to assess iohexol clearance in kidney transplant recipients. Ther Drug Monit. 2012;34:289–97.
12. Taubert M, Ebert N, Martus P, van der Giet M, Fuhr U, Schaeffner E. Using a three-compartment model improves the estimation of iohexol clearance to assess glomerular filtration rate. Sci Rep. 2018;8:17723.
13. Taubert M, Schaeffner E, Martus P, van der Giet M, Fuhr U, Lösment A, et al. Advancement of pharmacokinetic models of iohexol in patients aged 70 years or older with impaired kidney function. Sci Rep. 2021;11:22656.
14. Salmon Gandonnière C, Helms J, Le Tilly O, Benz-de Bretagne I, Bretagnol A, Bodet-Contentin L, et al. Glomerular hyper- and hypofiltration during acute circulatory failure: iohexol-based gold-standard descriptive study. Crit Care Med. 2019;47:e623–9.
15. Woillard J-B, Salmon Gandonnière C, Destere A, Ehrmann S, Merdji H, Mathonnet A, et al. A machine learning approach to estimate the glomerular filtration rate in intensive care unit patients based on plasma iohexol concentrations and covariates. Clin Pharmacokinet. 2021;60:223–33.
16. Destere A, Gandonnière CS, Åsberg A, Loustaud-Ratti V, Carrier P, Ehrmann S, et al. A single Bayesian estimator for iohexol clearance estimation in ICU, liver failure and renal transplant patients. Br J Clin Pharmacol. 2021;88:15197.
17. SimulX version 2020R1. Antony: Lixoft SAS; 2019. http://lixoft.com/products/monolix/. Accessed 18 May 2022.
18. Kuhn M, Wickham H. Tidymodels: a collection of packages for modeling and machine learning using tidyverse principles. 2020. https://www.tidymodels.org. Accessed 18 May 2022.
19. Chen T, Guestrin C. XGBoost: a scalable tree boosting system. In: Proceedings of the 22nd ACM SIGKDD International Conference on Knowledge Discovery and Data Mining. San Francisco (CA): ACM; 2016: 785–94. https://doi.org/10.1145/2939672.2939785. Accessed 24 Dec 2021.
20. Friedman J, Hastie T, Tibshirani R. Regularization paths for generalized linear models via coordinate descent. J Stat Softw. 2010;33:1–22.
21. Monolix version 2018R1. Antony: Lixoft SAS; 2018. http://lixoft.com/products/monolix/. Accessed 18 May 2022.
22. Woillard J, Labriffe M, Debord J, Marquet P. Mycophenolic acid exposure prediction using machine learning. Clin Pharmacol Ther. 2021;110:370–9.

Authors and Affiliations

Alexandre Destere[1,2,3] · Pierre Marquet[1,2] · Charlotte Salmon Gandonnière[4] · Anders Åsberg[5,6] · Véronique Loustaud-Ratti[1,7] · Paul Carrier[7] · Stephan Ehrmann[4,8] · Chantal Barin-Le Guellec[1] · Aurélie Premaud[1] · Jean-Baptiste Woillard[1,2]

1 Pharmacology and Transplantation, INSERM U1248, Université de Limoges, 2 rue du Pr Descottes, 87000 Limoges, France

2 Department of Pharmacology, Toxicology and Pharmacovigilance, CHU de Limoges, Limoges, France

3 Department of Pharmacology and Toxicology, University Hospital of Nice, Nice, France

4 Médecine Intensive Réanimation, INSERM CIC 1415, CRICS-TriggerSep Research Network, CHRU de Tours, Tours, France

5 Department of Transplantation Medicine, Oslo University Hospital Rikshospitalet, Oslo, Norway

6 Department of Pharmacy, University of Oslo, Oslo, Norway

7 Department of Hepato-Gastro-Enterology, University Hospital of Limoges, Limoges, France

8 Centre d'Etude des Pathologies Respiratoires INSERM U1100, Faculté de Médecine, Université de Tours, Tours, France

Licence CC BY-NC-ND 3.0

Supplemental data 1: Methodology for the development of a hybrid model.

Preparation of global dataset

I. Development and validation of population pharmacokinetic (POPPK) model and Maximum a posteriori Bayesian estimator (MAP-BE) based on limited sampling strategy (LSS)
II. Simulation of n profiles with x samples (x must be large enough to be used as a reference)
III. Importation of simulated profiles in R software
IV. Extract in each profile the samples times defined in the LSS and estimate the PK parameters with MAP-BE
V. Importation of results obtained to each profile with MAP-BE in R software
VI. Creation of global dataset with parameters PK reference of interest, MAP-BE LSS PK parameters, simulated covariates, simulated concentrations, predicted MAP-BE LSS concentrations.
VII. Setting up of features engineering in global dataset

Development of Machine Learning

R code

```
### Data splitting
set.seed(1234)
base_split_pro <- initial_split(base_sim, prop = 0.75)
base_ml_train_pro <- training(base_split_pro)
base_ml_test_pro <- testing(base_split_pro)

### Preprocessing
base_ml_rec_pro <- recipe(outcome~ .,  data = base_ml_train_pro) %>%
 step_dummy(ETUDE) %>% ##factorized the nominal variables
 step_normalize(all_numeric_predictors()) ## normalized the numerical variables

base_prep_recipe_pro <- prep(base_ml_rec_pro)
base_train_recipe_pro <- juice(base_prep_recipe_pro)
base_test_recipe_pro <- bake (base_prep_recipe_pro, new_data = base_ml_test_pro)

### definition of used model and hyperparameters to tune
xgb_spec <- boost_tree(mode = "regression",
                       mtry = tune(),
```


Licence CC BY-NC-ND 3.0

```
                min_n = tune(),
                tree_depth = tune(),
                learn_rate = tune()) %>% set_engine("xgboost")

## Creation of workflow, add of recipe and model
xgb_wf_pro <- workflow() %>%
 add_recipe(base_ml_rec_pro) %>%
 add_model(xgb_spec)

#Tuning of hyperparameters
set.seed(345)
tune_xgb_pro <- tune_grid(
 xgb_wf_pro,
 resamples = base_folds_pro,
 grid = 30,
 control= ctrl_grid
)

### Visualisation of results plot as function of rmse and rsq
autoplot(tune_xgb_pro, metric = c("rmse","rsq"),  scientific = FALSE) +
 ggtitle("tuning hyperparameter")

###Choice of best model
best_rmse_xgb_pro <- select_best(tune_xgb_pro, "rmse")
best_rsq_xgb_pro <- select_best(tune_xgb_pro, "rsq")

### Finalization of model with the best hyperparameters
final_xgb_pro<- finalize_model(
 xgb_spec,
 best_rmse_xgb_pro
)

### Creation of Variables Importance Plot

final_xgb_pro %>%
 set_engine("xgboost", importance = "permutation") %>%
 fit(outcome~ .,
    data = juice(base_prep_recipe_pro)
 )%>%
 vip::vip(geom = "col")
```


Licence CC BY-NC-ND 3.0

```
### Finalization of workflow
final_wf_xgb_pro <- workflow() %>%
 add_recipe(base_ml_rec_pro) %>%
 add_model(final_xgb_pro)

### Resamples
set.seed(456)
folds_pro <- vfold_cv(base_ml_train_pro)#par défaut 10 fois
set.seed(123)

### Fit with resampled training dataset
xgb_rs_pro <- fit_resamples(object = final_wf_xgb_pro, resamples = folds_pro, control =
control_resamples(verbose=T, save_pred = T))

### Obtain the predicted outcomes
pred_obs_xgb_pro <- xgb_rs_pro %>% collect_predictions()

###fit workflow
fit_workflow <- fit(final_wf_xgb_pro, base_ml_train_pro)
### Save fitworkflow
saveRDS(fit_workflow, file = "test_xgboost_sim_101220.rds")

### Prediction in testing dataset
predict(fit_workflow,base_ml_test_pro)
```


Licence CC BY-NC-ND 3.0

Supplemental data 2: Performance of the different models to predict refCL in comparison of MAP-BE based on different LSS in the training dataset.

	1 sample (9h)				6 samples			
	MAP-BE LSS	LOESS	Hybrid model Xgboost	Hybrid model GLMnet	MAP-BE LSS	LOESS	Hybrid model Xgboost	Hybrid model glmnet
MPE%	-5.7	-1.4	-1.8	-1.2	-0.9	-0.1	0	0.5
RMSE%	18.2	16.6	12.4	17.5	3.6	3.3	0.8	1.7
Profiles out of the 20% interval (%)	16.7	12.4	8.4	13.1	0.3	0.3	0	0

Licence CC BY-NC-ND 3.0

II.4. A hybrid algorithm combining population pharmacokinetic and machine learning for isavuconazole exposure prediction

Article en cours de reviewing dans *Clinical Pharmacokinetics*

Dans l'article précédemment présenté, une nouvelle approche hybride permettant d'associer un algorithme de machine learning corrigeant les prédictions réalisées par le modèle de POPPK a été proposée. Afin de confirmer et valider la méthodologie d'une telle approche, un autre cas d'étude avec le développement d'un modèle hybride pour estimer l'exposition à l'isavuconazole a été choisi.

Les objectifs de ce travail étaient (i) de créer un outil précis d'estimation de l'exposition à l'isavuconazole dans le but de maximiser les chances de succès thérapeutiques chez des patients transplantés rénaux, (ii) de confirmer la méthodologie proposée préalablement, (iii) de confirmer la source d'amélioration des prédictions.

Pour entrainer l'algorithme de machine learning à corriger les prédictions de la CL du MAP-BE à partir d'un seul prélèvement et a fortiori de l'AUC (AUC = Dose/CL), nous avons utilisé 12 variables. Comme dans la précédente étude [83], les paramètres PK estimés à partir du MAP-BE, la concentration résiduelle post-dose observées et prédites par le MAP-BE, les covariables démographiques simulées ainsi que des covariables informatives nouvellement crées ont été utilisées dans l'algorithme de machine learning.

Les résultats obtenus grâce à ce modèle hybride sont, comme précédemment, assez prometteurs avec aucun patient ayant un biais relatif de plus de 20% entre la clairance de référence et la clairance corrigée (*versus* MAP-BE = 5,6%) ainsi qu'un biais moyen et une imprécision diminués d'environ 90% et 70%, respectivement dans la base de validation.

Ne disposant pas d'une base de patients avec une cinétique complète pour établir une base de validation externe, des cinétiques complètes de patients ont été simulées à partir d'un autre modèle de la littérature basé sur les essais de phases 1 et 3 de l'isavuconazole [110]. L'utilisation de cette autre modèle permet de constituer une base de cinétiques complètes indépendante du modèle ayant servi à entrainer l'algorithme, nous affranchissant d'un potentiel surapprentissage.

Les résultats obtenus dans cette base externe permettent de confirmer les améliorations de prédictions de la CL. Cependant les améliorations sont moins importantes que celles observées dans la base de validation mais restent tout à fait acceptables avec une diminution de l'erreur moyenne et de l'imprécision de 30% et une diminution du nombre de patients ayant un biais relatif de plus de 20% entre la clairance de référence et la clairance corrigée d'environ 80%.

Licence CC BY-NC-ND 3.0

Lors de cette étude, la source de l'amélioration de nos prédictions a été confirmé. En effet, une diminution de 54% et de 58,5% du shrinkage dans la base d'entrainement et de validation (supplemental plot 1) a été observée.

Les résultats obtenus, avec ce modèle hybride pour la prédiction de l'exposition de l'isavuconazole, permettent de confirmer la précision d'estimation des modèles hybrides ouvrant la porte à une nouvelle génération de modèles permettant l'individualisation précise des posologies sur la base d'un nombre très limité de prélèvements et d'un modèle POPPK.

Licence CC BY-NC-ND 3.0

Manuscript

Click here to view linked References

Click here to access/download;Manuscript;Isavuconazole 020922 clinpk.do

A hybrid algorithm combining population pharmacokinetic and machine learning for isavuconazole exposure prediction

Alexandre Destere[1,2], Pierre Marquet[1,3], Marc Labriffe[1,3], Milou-Daniel Drici[2], Jean-Baptiste Woillard[1,3]

[1] Pharmacology and Transplantation, INSERM U1248, Université de Limoges, 2 rue du Pr Descottes, 87000 Limoges, France
[2] Department of Pharmacology and Pharmacovigilance Center, Côte d'Azur University Medical Center, Nice, France
[3] Department of Pharmacology, Toxicology and Pharmacovigilance, CHU de Limoges, Limoges, France

Corresponding author:
Jean-Baptiste Woillard
Title: PharmD, PhD
ORCID: 0000-0003-1695-0695
Address:
Univ. Limoges,
INSERM U1248 IPPRITT,
2 rue du Pr Descottes,
F-87000 Limoges, France.
Phone: +33 5 55 05 61 40
Fax: +33 5 55 05 61 62
Email: jean-baptiste.woillard@unilim.fr

Funding information:
No funding was received for this study

Conflicts of Interest/Competing Interests:
None of the author have any conflicts of interest to declare in relation to this work.

Consent for Publication:
All the authors read and approved the final manuscript.

Data availability:
Data generated for this study are available upon request to the corresponding author.

Authors contributions:
AD, JBW contributed to the conception and design of the study, analysis and interpretation of data, PM contributed to the conception and design of the study and interpretation of data, MLB and MD contributed to the interpretation of data. All the authors participated in drafting the article and approved the final version submitted.

Acknowledgments
We gratefully thank Miss Karen Poole for manuscript editing.

Keywords: isavuconazole; machine learning; population pharmacokinetics; fungal infections

Licence CC BY-NC-ND 3.0

Abstract

Objectives

Therapeutic drug monitoring of isavuconazole, a second-generation triazole antifungal agent is based on post-dose trough plasma or serum concentrations (C24h) by analogy with voriconazole, whereas it would be more appropriate to use its area under the curve (AUC). The aim of this study was to develop a hybrid algorithm combining population pharmacokinetics (POPPK), maximum a posteriori Bayesian estimation (MAP-BE) and machine learning (ML) to accurately predict isavuconazole clearance.

Methods

A total of 1727 isavuconazole rich PK profiles were simulated using a POPPK model from the literature, and MAP-BE was used to estimate the clearance based on: (i) the full PK profiles (refCL); and (ii) C24h only (C24h-CL). Xgboost was trained to correct the error between refCL and C24h-CL in the training dataset (75%). C24h-CL as well as ML-corrected C24h-CL were evaluated in a testing dataset (25%) and then in a set of PK profiles simulated using another published POPPK model.

Results

A strong decrease in mean predictive error (MPE%), imprecision (RMSE%) and the number of profiles outside ±20% MPE% (n-out20%) was observed with the hybrid algorithm (decreased in MPE% by 95.8% and 85.6%; RMSE% by 69.5% and 69.0%; n-out20% by 97.4% and 100% in the training and testing sets, respectively. In the external validation set, the hybrid algorithm decreased MPE% by 30%, RMSE% by 34% and n-out20% by 79.5%.

Conclusion

The hybrid model proposed significantly improved isavuconazole AUC estimation over MAP-BE based on the sole C24h and may improve dose adjustment.

Licence CC BY-NC-ND 3.0

Study Highlight

- **What question did this study address?**

This study evaluated the performances of a hybrid model combining population pharmacokinetics and machine learning to improve individual isavuconazole clearance estimation using a single plasmatic concentration.

- **What does this study add to our knowledge?**

A decreased by about 90% and 70% of the bias and imprecision was observed in comparison to the MAP-BE alone.

- **How might this change drug discovery, development, and/or therapeutics?**

The hybrid model developed may spearhead a new generation of tools for MIPD in routine practice.

Licence CC BY-NC-ND 3.0

1. Introduction

Isavuconazole (ISA) is a second-generation triazole antifungal agent approved by the regulatory authorities in several countries. It is indicated for the treatment of invasive fungal infections such as aspergillosis and mucormycosis [1]. In this indication, it is administered by intravenous infusion over at least one hour. However, the off-label use of ISA, which has a proven track record, has increased, e.g. for the treatment of other invasive mycoses (*Candida sp*.) [2,3] or as a prophylaxis in high-risk hematology patients [4]. ISA is a substrate and inhibitor of cytochrome 3A4/3A5 and is subject to numerous drug-drug interactions or drug-food interactions [5]. It is considered to exhibit stable pharmacokinetics [6,7] and to be equally effective as, but safer than, other triazole antifungal agents (less hepatotoxicity, neurotoxicity and cardiac toxicity). However, ISA toxicity was observed in 33% of patients [8]. For ISA therapeutic drug monitoring, the PK/PD index that has been proposed and studied is the AUC/minimum inhibitory concentration (MIC) ratio [9–11]. Based on Monte Carlo simulations, manufacturer dosing recommendations are likely to attain the AUC/MIC target for the treatment of infections caused by Aspergillus fumigatus (MIC ≤ 0.5 mg/L). However, it only led to attainment of the targets in less than 20% of cases in infections of *Candida albicans* and *Candida glabrata* with MIC of 0.25 mg/L and 1 mg/L, respectively [12]. In routine practice, AUC is sometimes difficult to obtain and is often replaced by trough concentrations (C24h)/MIC. However, since no C24h target has been defined for ISA, it is generally replaced by that of voriconazole (1-5 mg/L), rendering TDM imprecise. In contrast, there is scientific evidence to use AUC = 100 h.mg/L as a probabilistic target, in the absence of MIC and an individual AUC target [13]. ISA population pharmacokinetic (POPPK) models have even been developed to estimate the probability of target attainment using Monte Carlo simulations [12–14]. Recently, we developed an innovative strategy to increase the prediction accuracy of maximum a posteriori Bayesian estimation (MAP-BE) based on POPPK by means of Machine Learning (ML), and we successfully applied it to plasma iohexol to estimate the glomerular filtration rate (GFR) [15]. We also recently showed that machine learning algorithms can be trained on data simulated using a published POPPK model and accurately predict drug exposure [16]. The aim of this study was to apply the two strategies to ISA AUC estimation,

Licence CC BY-NC-ND 3.0

through the development of a hybrid model combining MAP-BE and a ML algorithm, using simulated data as the learning set.

2. Material & Methods

2.1. Population Pharmacokinetic

2.1.1. Data simulation and estimation of clearance using MAP-BE

The population parameters and relevant covariates of the POPPK model developed by Wu et al. [12] using 471 samples from 79 solid organ transplant patients were used to simulate 2000 rich PK profiles at steady-state for a typical dose of 200 mg once daily administered by intravenous infusion over one hour. Each profile was made up of 49 concentration-time points between 0 and 24h (one every 30 minutes) simulated using the 'mrgsolve' R package [17]. The sex ratio was 50/50 and the body mass index (BMI) was simulated based on a truncated normal distribution using the data of the original article (mean ± SD [min to max] = 25.4 ± 5.96 [14.6 to 45.2] (as no information was provided in the original article about the correlation between sex and BMI, the same BMI range was used for both men and women). Briefly, the model consisted of a 2-compartment model with inter-individual variability on the apparent clearance (CL) and peripheral volume of distribution (V2), 2 covariates (sex and BMI) and a proportional residual error. ISA clearance (CL) was almost twice higher in men than in women and the V2 increased with BMI. Simulations were performed using a shrunken residual error of 0.1% in order to obtain less noisy profiles [16,18,19]. As previously described, filters were applied to the simulated PK profiles by removing those with CL and V2 below the 1st and above the 99th percentiles, to eliminate extreme outliers.

The MAPBAYR package [20] was then used to estimate the individual PK parameters and individual concentrations using MAP-BE based on: (i) the simulated full PK profiles to derive the reference clearance values (refCL) and (ii) the simulated trough concentrations to derive C24h-CL (the degraded estimates to be corrected using the hybrid strategy). At this step, the original residual error (20.5%) was used [12]. To avoid aberrant refCL, the simulated full PK profiles that failed to be processed by MAPBAYR (individual CL = typical CL) were removed.

Licence CC BY-NC-ND 3.0

2.2. Machine Learning

2.2.1. Preparation of the Data and Feature Engineering

The raw estimation error between refCL and C24h-CL was calculated using the following formula:

$$Error = refCL - C24h\text{-}CL$$

This error was considered as the outcome to be predicted by ML (regression problem). The variables used as predictors were: (i) the PK parameters (CL and V2) obtained using the MAP-BE on C24h, (ii) the simulated C24h (SC_{24h}), (iii) the MAP-BE estimated C24h (EC_{24h}), (iv) the simulated sex and BMI and (v) the η of MAP-BE CL and V2 (corresponding to the estimated deviation (in %) relative to the typical population CL and V2). Additionally, as in previous papers [15] some features were engineered to add information: (i) the differences between SC_{24h} and EC_{24h}; (ii) the ratio between SC_{24h} and EC_{24h}; (iii) the relative ratio between SC_{24h} and EC_{24h}. Finally, a total of 12 features were available for training the ML algorithm.

2.2.2. Training the machine learning algorithm

Simulations were split into training (75%) and testing (25%) datasets, which were compared using the Wilcoxon test ($p < 0.05$). An Xgboost algorithm was trained to predict the errors of C24h-CL as compared to refCL, using the Tidymodels framework in R [21]. Briefly, a ten-fold cross-validation was applied to the training dataset to tune the hyperparameters and evaluate the model performances based on the r^2. A variable importance plot was drawn to evaluate the relative influence of the variables on the error. The predicted error was added to C24h-CL to obtain the corrected CL (corCL):

$$corCL = C24h\text{-}CL + Xgboost\ predicted\ error$$

2.2.3. Xgboost performance in the training and testing datasets

The performances of the Xgboost algorithm developed to correct ISA CL in another 10-fold cross-validation set from the training set (to check out overfitting) and in the testing dataset were evaluated using the MPE%, the relative RMSE% and the percentage of profiles with MPE% out of the ± 20% MPE interval between corCL and refCL. The unexplained error between the refCL and C24h-CL or corCL was plotted as a function of CL to check the dispersion over the CL range.

Licence CC BY-NC-ND 3.0

2.2.4. Evaluation of the shrinkage before and after correction

The shrinkage of C24h-CL and hybrid model was estimated in the training and testing datasets using the formula proposed by Monolix [22]:

$$Shrinkage = 1 - \frac{var(\eta CL_x)}{\omega_{CL}^2}$$

Where x is the method used, ηCL_x is the random effect of the parameter and ω_{CL}^2 is the variance of the parameter estimate.

2.2.5. External evaluation with simulated patients using another POPPK model

As no "real" data was available for external validation of our hybrid algorithm, another set of simulations was obtained using another ISA POPPK model developed from pooled data of phase 1 and phase 3 studies, corresponding to 421 individuals and 6363 drug concentrations [13]. The same methodology as above (including simulations, filtering out of outliers and MAP-BE using MAPBAYR) was applied to draw 200 simulated PK profiles receiving 200 mg/24h by intravenous infusion over one hour. The simulations were limited to non-healthy & non-Asian subjects (the covariate terms for healthy on V2 and Asian on CL were not used), only using BMI as a covariate on V2 (simulated following the publication data (median[min to max] = 23.6[13.9 to 41.1]). The unexplained errors of each method (MAP-BE and hybrid model) were graphically compared.

3. Results

3.1. Simulated Data

After excluding the 1% extreme percentiles in CL and V2 (n=233) and the thirty-five PK profiles failed to be estimated by MAPBAYR, 1727 (out of the 2000) simulated profiles remained. The description of the simulated data and features tested as predictors is presented in Table 1. No predictors were significantly different between the training and testing datasets.

3.2. Bayesian estimation of ISA clearance based on full PK profiles or post-dose trough plasma concentrations

The refCL and C24h-CL were (mean ± SD [min-max]) 4.9 ± 3.3[1.0-19.2] L/h and 4.4 ± 2.5[1.1-14.8], respectively. The density plot of the error between refCL and C24h-CL was skewed

Licence CC BY-NC-ND 3.0

towards high values (log-normal distribution) (Figure 1). Actually, C24h-CL showed a strong deviation toward an underestimation for high values (CL > 5 L/h) as shown in the Figure 2A.

The shrinkage represents the percentage regression to the mean of development distribution of PK parameter. The shrinkage of C24h-CL was 45.6% and 44.6% in the training and testing datasets, respectively.

3.3. Performance of ML to correct C24h-CL estimation errors in the training and testing datasets

The Xgboost algorithm predicted the error with $r^2 = 0.94$ in the training set and $r^2 = 0.98$ in the testing set (Figure 3). The 3 features engineered were the most important according to the variable importance plot (Figure 4), followed by the CL-related variables (ETA CL and CL predicted). The corCL was (mean ± SD [min-max]) 4.9 ± 3.3[0.9-19.5] L/h.

The MPE% represents the accuracy of the estimation, the RMSE% represents the imprecision of the estimation. Correction using Xgboost error estimates decreased drastically the MPE% (by 95.8% and 85.6%) and the RMSE% (by 69.5% and 69.0%) in the training and testing sets, respectively (Table 2, Figure 2B). Additionally, less than 1% of corCL were outside the ± 20% MPE interval in the training set and none in the testing set, corresponding to a decrease of 97.4% and 100% respectively in comparison to C24h-CL (Table 2).

The hybrid model decreased the shrinkage of ISA CL estimation by 54.0% and 58.5% respectively (training: 21.2% and testing: 18.5%) (supplemental figure 1).

3.4. Evaluation of the hybrid model on a dataset simulated using an independent POPPK model

After applying filters, 4/200 full PK profiles were removed. The refCL and C24h-CL were (mean ± SD [min-max]) 4.3 ± 2.8 [0.6-15.4] L/h and 3.6 ± 1.8 [0.7-8.8], respectively. The performances of the hybrid model (corCL) in comparison to the MAP-BE applied to C24H (C24h-CL) are presented in Table 2. The hybrid model decreased the MPE% by approximately 30% and the RMSE% by 34% as compared to MAP-BE alone. As for simulations from the first POPPK model, the unexplained error was underestimated (refCL-C24h-CL) for refCL larger for values > 5 L/h (Figure 5). The hybrid model corrected this underestimation accurately for most of the cases but slightly overcorrected for some of them.

Licence CC BY-NC-ND 3.0

4. Discussion

In this study, we developed and extensively validated a hybrid algorithm combining MAP-BE and ML, able to estimate very accurately ISA CL based on the steady-state C24h. The performance obtained with this hybrid algorithm was largely better than that of MAP-BE alone.

Another innovative characteristic of this study is that all data were obtained by simulation from two independent published POPPK models, one for the development [12]and the other for the validation [13] phases. The former was developed using data from solid organ transplant patients [12] and the latter using the data from the SECURE study [7], corresponding mainly to patients with hematologic malignancies, either active or at the stage of stem cell transplantation. This difference in patient populations may account for the slightly lower performance of our hybrid algorithm in the independent test set but it also suggests that it can be extrapolated to other types of patients on ISA.

MAP-BE fed only with C24h values strongly underestimated ISA CL for values >5 L/h, and the higher the C24h-CL, the stronger the correction made by the hybrid algorithm. Actually, with so little individual information (only 1 concentration), the estimated CL is largely shrunken toward the typical mean population value. Similarly, for values > 2.5 L/h, an overestimation is observed even if to a lower extent than the underpredicted values on Figures 4 and 5. Figure 5 also showed that in 10 cases with high CL values, the hybrid algorithm overcorrected the CL leading to an overestimation of refCL.

The PK/PD exposure marker initially used in the preclinical model for ISA was the AUC [9–11], but its use in routine practice is complicated since good Bayesian estimation would require more than one concentration-time point. In the present work, the algorithm developed yields very accurate estimation of ISA CL, hence of its AUC (CL = dose/AUC). Thereby, an individualized dose after intravenous administration of ISA can be proposed to reach an individual AUC target derived from the ECOFF or MIC [23]. Unfortunately, this hybrid algorithm cannot be used for oral ISA as it would require the development of a specific hybrid model and the pill dosages (multiple of 100 mg) do not allow precise dose individualization.

Licence CC BY-NC-ND 3.0

We previously developed a similar hybrid algorithm for the estimation of the glomerular filtration rate (GFR) after iohexol administration and found that it decreased the shrinkage and improved the individual predictions [15]. The present model confirms that this methodology can be applied to a larger domain, with even better performances and a larger decrease in individual prediction errors and shrinkage.

As previously reported [16,18,19], the use of a very low residual error for the initial simulations drastically improves ML, since it avoids learning imprecision. Similarly, the use of filters prevented Xgboost from learning from unrealistic profiles, even if this algorithm in particular makes nonlinear prediction and discretizes the continuous values into quantiles, which is less sensible to outliers data [24]. Supplemental Figure 2 shows a typical case illustrating that the patients filtered out were characterized by a typical value of CL assigned by MAPBAYR.

Interestingly, the most important variables for predicting the error between refCL and C24h-CL were those engineered and those related to CL. Indeed, these variables inform about the importance of deviation in respect to typical CL in the population.

Since this combined algorithm may be complicated to reproduce, we have developed a shiny interface to allow testing it, for research purposes only (https://hybrid-models.shinyapps.io/isavuconazole/).

This study has some limitations. First, the algorithm development and validation are only based on simulations, meaning that it still requires validation in “real” patients before it can be implemented in the clinics. Simulations were performed with a single dosage (200 mg) which corresponds to the recommended dose. The impact of ISA dose on pharmacokinetic parameters or as a predictor for the hybrid model was therefore not explored and PK linearity was assumed. However, the goal of such an algorithm is to propose different doses in the population so that each patient can reach a predefined target. The absence of clear AUC targets is another limitation and when the strain sensitivity is unknown, the mean AUC target of the SECURE study (100 h.mg/L) can be proposed [13]. Finally, the relevance of TDM has not been evaluated in this work which only proposes tools to perform it.

Licence CC BY-NC-ND 3.0

5. Conclusions

In conclusion, the hybrid model associating a POPPK model, MAP-BE with a limited sampling strategy and ML developed here may spearhead a new generation of tools for model-informed precision dosing in routine practice.

Licence CC BY-NC-ND 3.0

References

1. Rybak JM, Marx KR, Nishimoto AT, Rogers PD. Isavuconazole: Pharmacology, Pharmacodynamics, and Current Clinical Experience with a New Triazole Antifungal Agent. Pharmacotherapy. 2015;35:1037–51.

2. Kullberg BJ, Viscoli C, Pappas PG, Vazquez J, Ostrosky-Zeichner L, Rotstein C, et al. Isavuconazole Versus Caspofungin in the Treatment of Candidemia and Other Invasive Candida Infections: The ACTIVE Trial. Clinical Infectious Diseases. 2019;68:1981–9.

3. Jørgensen KM, Astvad KMT, Hare RK, Arendrup MC. EUCAST Susceptibility Testing of Isavuconazole: MIC Data for Contemporary Clinical Mold and Yeast Isolates. Antimicrob Agents Chemother. 2019;63:e00073-19.

4. Ping Y, Hongmei J, Bellmann C, Inês M, Macmillan T, Webb N, et al. Effectiveness and safety of isavuconazole prophylaxis for invasive fungal infections in the haematologic setting. Hematology. 2022;27:723–32.

5. Townsend R, Dietz A, Hale C, Akhtar S, Kowalski D, Lademacher C, et al. Pharmacokinetic Evaluation of CYP3A4-Mediated Drug-Drug Interactions of Isavuconazole With Rifampin, Ketoconazole, Midazolam, and Ethinyl Estradiol/Norethindrone in Healthy Adults. Clin Pharmacol Drug Dev. 2017;6:44–53.

6. Sivasubramanian G, Chandrasekar PH. Efficacy and safety of Isavuconazole for the treatment of invasive *Aspergillus* infection - an update of the literature. Expert Opinion on Pharmacotherapy. 2022;23:543–9.

7. Maertens JA, Raad II, Marr KA, Patterson TF, Kontoyiannis DP, Cornely OA, et al. Isavuconazole versus voriconazole for primary treatment of invasive mould disease caused by Aspergillus and other filamentous fungi (SECURE): a phase 3, randomised-controlled, non-inferiority trial. The Lancet. 2016;387:760–9.

8. Nwankwo L, Gilmartin D, Matharu S, Nuh A, Donovan J, Armstrong-James D, et al. Experience of Isavuconazole as a Salvage Therapy in Chronic Pulmonary Fungal Disease. JoF. 2022;8:362.

9. Warn PA, Sharp A, Parmar A, Majithiya J, Denning DW, Hope WW. Pharmacokinetics and Pharmacodynamics of a Novel Triazole, Isavuconazole: Mathematical Modeling, Importance of Tissue Concentrations, and Impact of Immune Status on Antifungal Effect. Antimicrob Agents Chemother. 2009;53:3453–61.

10. Seyedmousavi S, Brüggemann RJM, Meis JF, Melchers WJG, Verweij PE, Mouton JW. Pharmacodynamics of Isavuconazole in an Aspergillus fumigatus Mouse Infection Model. Antimicrob Agents Chemother. 2015;59:2855–66.

11. Lepak AJ, Marchillo K, VanHecker J, Diekema D, Andes DR. Isavuconazole Pharmacodynamic Target Determination for Candida Species in an *In Vivo* Murine Disseminated Candidiasis Model. Antimicrob Agents Chemother. 2013;57:5642–8.

Licence CC BY-NC-ND 3.0

12. Wu X, Venkataramanan R, Rivosecchi RM, Tang C, Marini RV, Shields RK, et al. Population Pharmacokinetics of Intravenous Isavuconazole in Solid-Organ Transplant Recipients. Antimicrob Agents Chemother. 2020;64:e01728-19.

13. Desai A, Kovanda L, Kowalski D, Lu Q, Townsend R, Bonate PL. Population Pharmacokinetics of Isavuconazole from Phase 1 and Phase 3 (SECURE) Trials in Adults and Target Attainment in Patients with Invasive Infections Due to Aspergillus and Other Filamentous Fungi. Antimicrob Agents Chemother. 2016;60:5483–91.

14. Kovanda LL, Desai AV, Lu Q, Townsend RW, Akhtar S, Bonate P, et al. Isavuconazole Population Pharmacokinetic Analysis Using Nonparametric Estimation in Patients with Invasive Fungal Disease (Results from the VITAL Study). Antimicrob Agents Chemother. 2016;60:4568–76.

15. Destere A, Marquet P, Gandonnière CS, Åsberg A, Loustaud-Ratti V, Carrier P, et al. A Hybrid Model Associating Population Pharmacokinetics with Machine Learning: A Case Study with Iohexol Clearance Estimation. Clin Pharmacokinet [Internet]. 2022 [cited 2022 Jun 9]; Available from: https://link.springer.com/10.1007/s40262-022-01138-x

16. Woillard J-B, Labriffe M, Prémaud A, Marquet P. Estimation of drug exposure by machine learning based on simulations from published pharmacokinetic models: The example of tacrolimus. Pharmacological Research. 2021;167:105578.

17. Baron KT. mrgsolve: Simulate from ODE-Based Models [Internet]. 2022. Available from: https://CRAN.R-project.org/package=mrgsolve

18. Ponthier L, Ensuque P, Destere A, Marquet P, Labriffe M, Jacqz-Aigrain E, et al. Optimization of Vancomycin Initial Dose in Term and Preterm Neonates by Machine Learning. Pharm Res [Internet]. 2022 [cited 2022 Aug 11]; Available from: https://link.springer.com/10.1007/s11095-022-03351-6

19. Labriffe M, Woillard J, Debord J, Marquet P. Machine learning algorithms to estimate everolimus exposure trained on simulated and patient pharmacokinetic profiles. CPT Pharmacom & Syst Pharma. 2022;psp4.12810.

20. Le Louedec F, Puisset F, Thomas F, Chatelut É, White-Koning M. Easy and reliable maximum *a posteriori* Bayesian estimation of pharmacokinetic parameters with the open-source R package mapbayr. CPT Pharmacometrics Syst Pharmacol. 2021;10:1208–20.

21. Kuhn M, Wickham H. Tidymodels: a collection of packages for modeling and machine learning using tidyverse principles. [Internet]. 2020. Available from: https://www.tidymodels.org

22. Monolix version 2018R1. Antony, France: Lixoft SAS, 2018. http://lixoft.com/products/monolix/.

23. Arendrup MC, Meletiadis J, Mouton JW, Guinea J, Cuenca-Estrella M, Lagrou K, et al. EUCAST technical note on isavuconazole breakpoints for Aspergillus, itraconazole breakpoints

Licence CC BY-NC-ND 3.0

for Candida and updates for the antifungal susceptibility testing method documents. Clinical Microbiology and Infection. 2016;22:571.e1-571.e4.

24. Chen T, Guestrin C. XGBoost: A Scalable Tree Boosting System. Proceedings of the 22nd ACM SIGKDD International Conference on Knowledge Discovery and Data Mining [Internet]. San Francisco California USA: ACM; 2016 [cited 2021 Dec 24]. p. 785–94. Available from: https://dl.acm.org/doi/10.1145/2939672.2939785

Licence CC BY-NC-ND 3.0

Table 1 Comparison of predictors in the training and testing datasets.

	Training set	Testing set	p-value
Simulated concentrations at 24h (SC_{24h}) (mg/L)	2.1 [0.3-10.1]	2.1 [0.3-9.5]	NS
Predicted concentrations at 24h (EC_{24h}) (mg/L)	1.9 [0.3-7.2]	1.8 [0.3-6.8]	NS
Difference between SC_{24h} and EC_{24h} (mg/L)	0.2 [-0.2-2.9]	0.2 [-0.2-2.7]	NS
Ratio between SC_{24h} and EC_{24h}	0.9 [0.7-1.6]	0.9 [0.7-1.5]	NS
Relative ratio between SC_{24h} and EC_{24h}	0.1 [-0.6-0.3]	0.1 [-0.5-0.3]	NS
Clearance (CL) (L/h)	3.8 [1.1-14.8]	3.9 [1.1-14.5]	NS
Peripheric volume (V2) (L)	501.0 [89.6-1022.2]	493.0 [95.0-1026.6]	NS
Eta of MAP-BE CL (ETA 1)	0.1 [-1.1-1.4]	0.1 [-1.0-1.3]	NS
Eta of MAP-BE V2 (ETA 2)	-2.6×10^{-4} [-0.1-0.2]	-2.0×10^{-5} [-0.1-0.2]	NS
Body Mass Index (BMI) (kg/m^2)	26.2 [14.9-39.7]	26.6 [15.2-39.7]	NS
Sex (%)	M: 50.8%	M: 46.8%	NS

ETA is the relative deviation of PK parameters from the typical value of that parameter. The quantitative data were presented in median [min-max]. The Wilcoxon test was performed to compare the 2 sets. EC24h is the predicted concentrations at 24h, SC24h is the simulated concentrations at 24h. NS: not significant (with a threshold of 0.05).

Licence CC BY-NC-ND 3.0

Table 2 Performances of different method (MAP-BE and hybrid model) in the training and testing datasets and in the external set obtained by simulation from Desai A. et al. POPPK model

	Training set		Testing set		External validation [13]	
	C24h-CL	Hybrid model	C24h-CL	Hybrid model	C24h-CL	Hybrid model
MPE (%)	3.4	- 0.15	3.6	- 0.5	7.8	5.4
RMSE (%)	11.2	3.4	11.4	3.5	16.3	10.8
Out of ± 20% error interval (%)	7.6	0.2	5.6	0	22.4	4.6

MPE is mean predictive error, RMSE is root mean square error and MAP-BE is maximum a posteriori Bayesian estimator

Licence CC BY-NC-ND 3.0

Figure Legends

Figure 1: Density plot of C24h-CL error in the overall simulations.

Figure 2: Unexplained error (true CL – MAP-BE LSS C24H CL or true CL – hybrid CL) before and after correction of clearances in the training (A) and testing (B) dataset.

Figure 3: Correlation between C24h-CL error and Xgboost estimation error in the training (A) and testing (B) dataset.

Figure 4: Variable Importance Plot for the prediction of the error (reference CL based on MAP-BE applied on one simulated sample every 30min between 0 and 24h – CL obtained using MAP-BE applied on C24H only) by the Xgboost algorithm.

Figure 5: Unexplained error in CL prediction (ref CL –C24h-CL (grey round) or ref CL – hybrid CL (black square)) as function of refCL in the external validation set.

Supplementary Materials

Supplemental Figure 1: Shrinkage before (A and B) and after (C and D) MAP-BE CL correction with the hybrid model in the training (A and C) and testing datasets (B and D).

Supplemental figure 2: Observed and individual predicted concentrations in a removed simulation. black point: "simulated concentrations"; black line: "individual predicted concentrations".

Licence CC BY-NC-ND 3.0

Figure 1 Figure 1

Click here to access/download;Figure;Figure 1.pdf

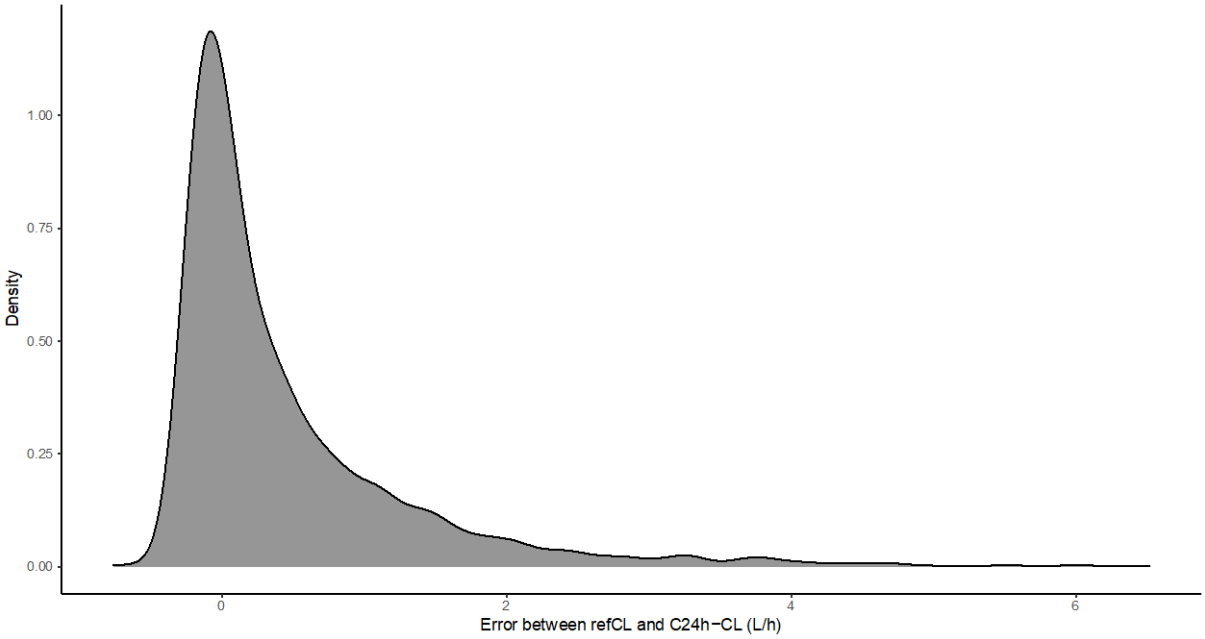

Figure 2 Figure 2

Click here to access/download;Figure;Figure 2.pdf

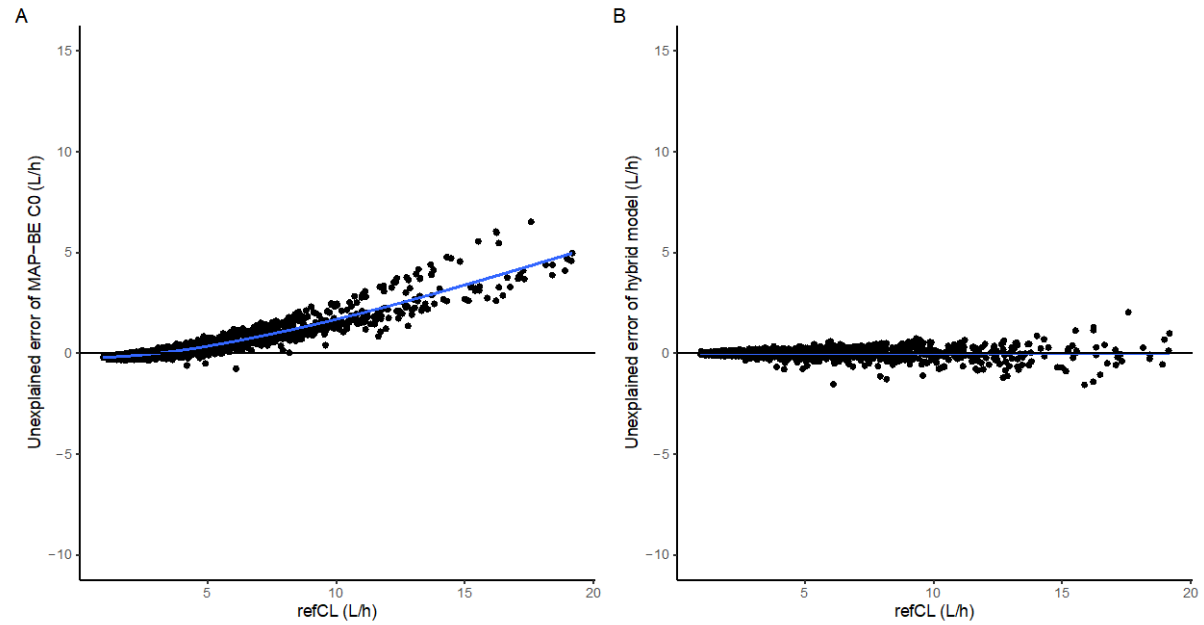

Licence CC BY-NC-ND 3.0

Figure 3

Click here to access/download;Figure;Figure 3.pdf

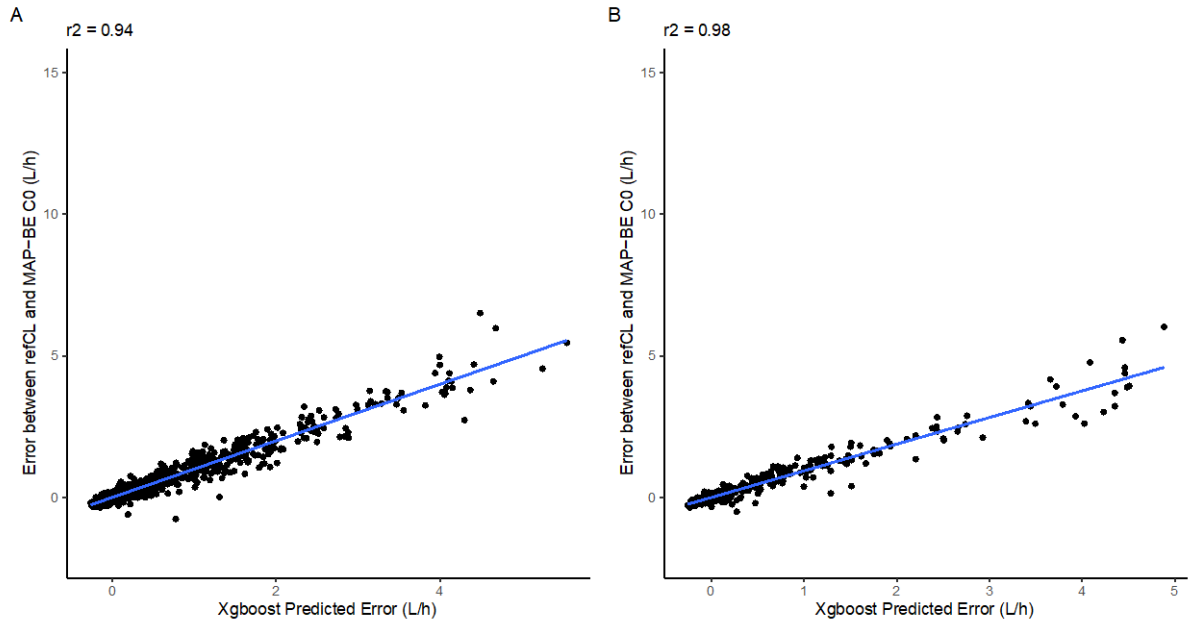

Figure 4

Figure 4

Click here to access/download;Figure;Figure 4.pdf

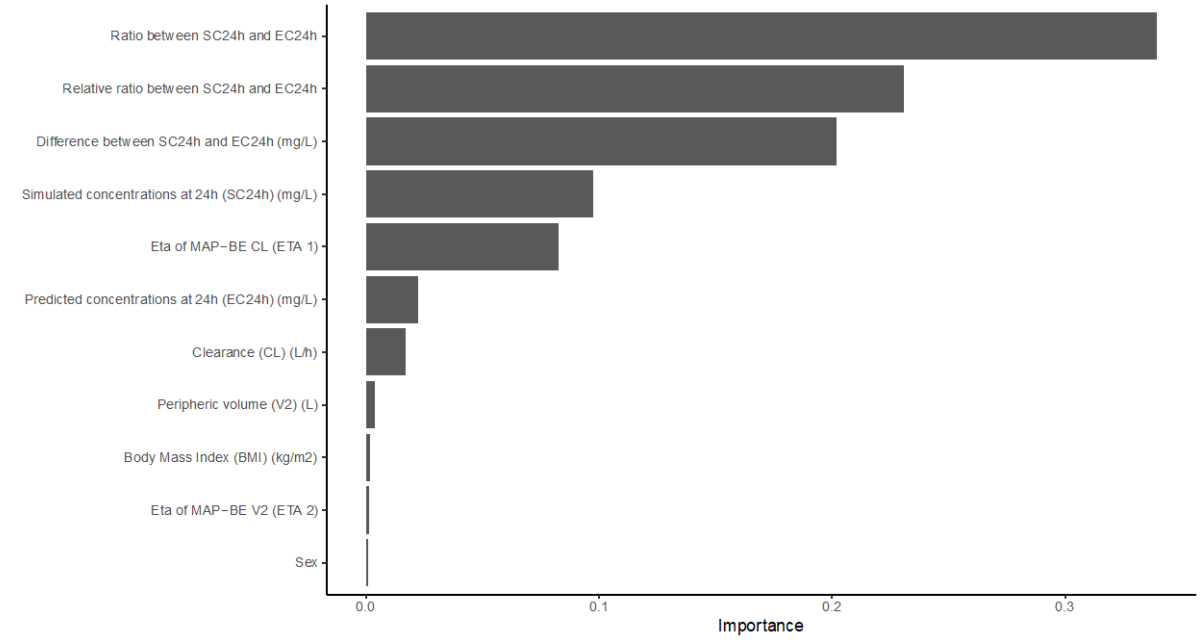

Licence CC BY-NC-ND 3.0

Figure 5 Figure 5

Click here to access/download;Figure;Figure 5.pdf

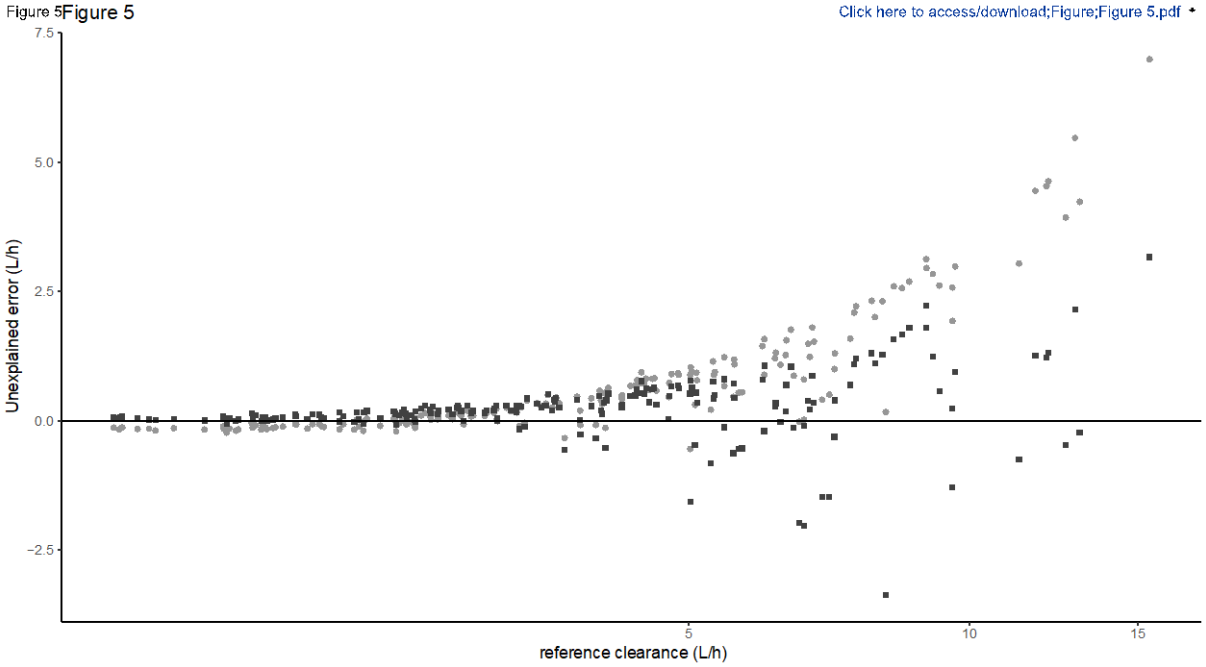

Supplemental figure 1 Supplemental figure 1

Click here to access/download;Figure;Supp figure 1.pdf

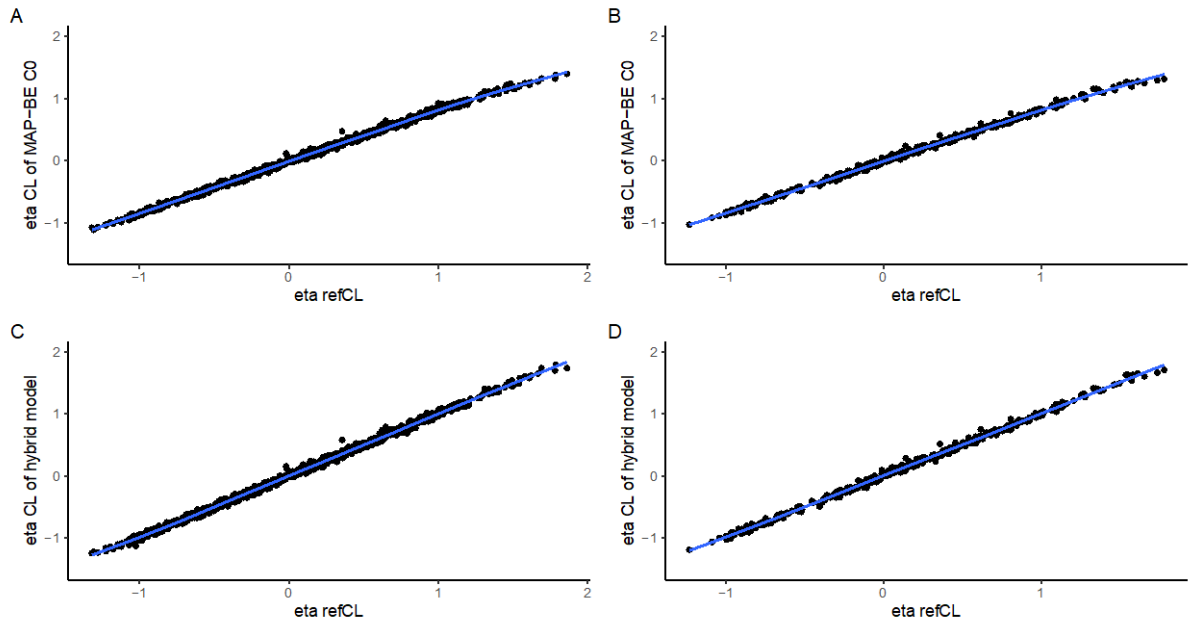

Licence CC BY-NC-ND 3.0

Supplemental figure 2

Click here to access/download;Figure;Supp figure 2.pdf

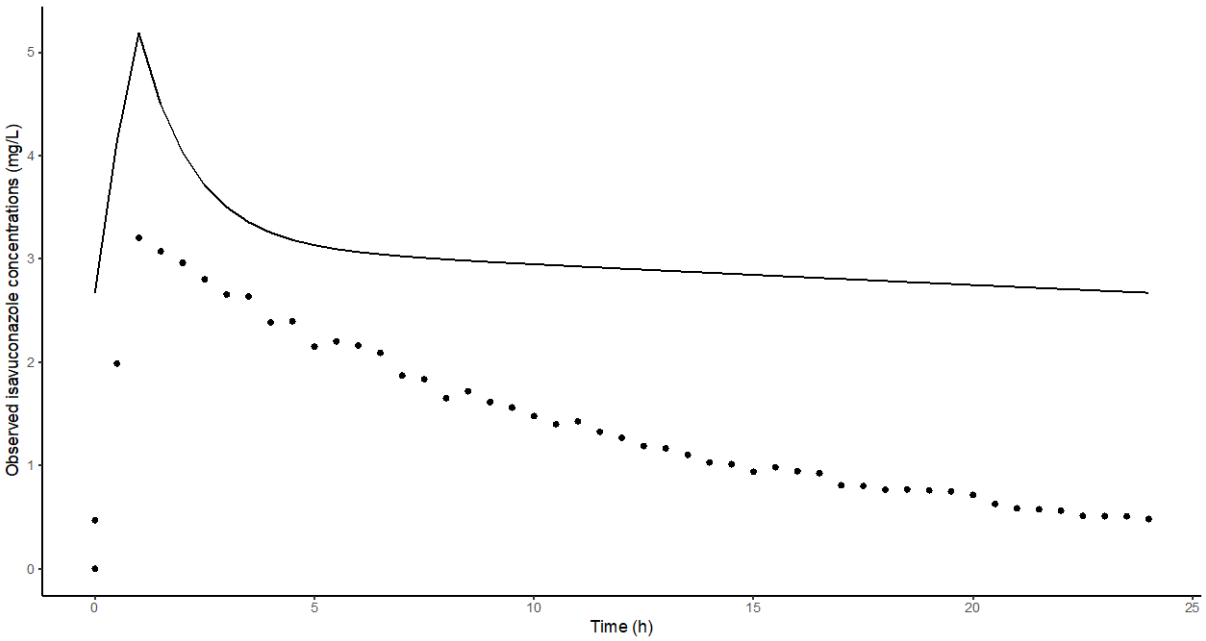

Licence CC BY-NC-ND 3.0

Alexandre Destere | Thèse de doctorat | Université de Limoges | 2022
Licence CC BY-NC-ND 3.0

Graphical abstract

Click here to access/download;Other;graphical abstract_260822.pdf

Simulation of full individual PK profiles of isavuconazole (ISA) from a literature model and extraction of C24h

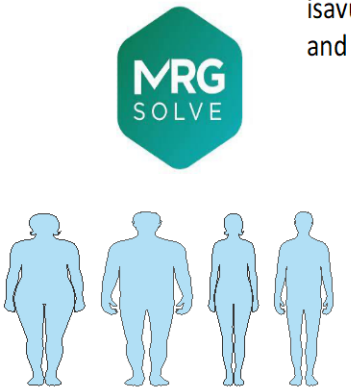

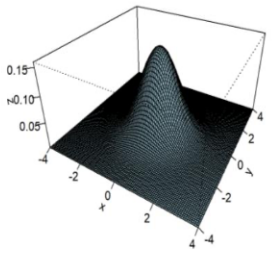

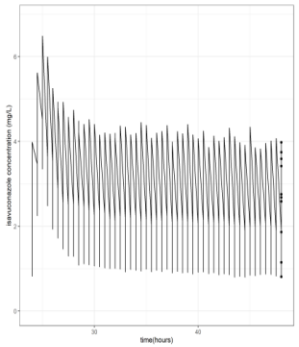

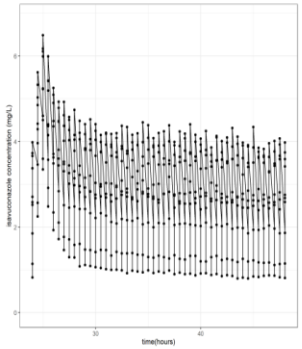

$Cl_{isavuconazole}$ C24h

$Cl_{isavuconazole}$ all points

ISA Clearance (CL) estimation using Maximum a posteriori Bayesian estimation from

- 1 sample at 24h
- All sample at 24h

Learning of the error between C24h-CL and ref-CL using Xgboost and correction of the individual CL

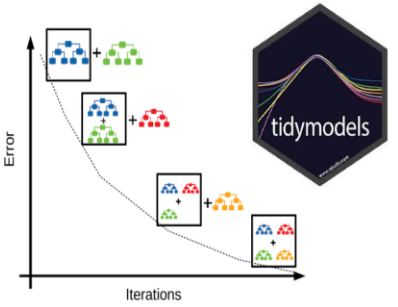

$$corCL = C24h - CL + Xgboost\ predicted\ error$$

Large improvement in individual CL estimation after correction by the hybrid algorithm combining population pharmacokinetic and machine Learning

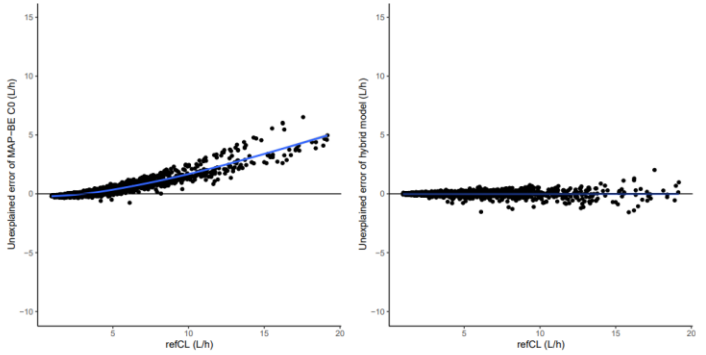

II.5. Longitudinal exposure to tacrolimus and new onset diabetes mellitus in renal transplant patients

Article accepté dans *Therapeutic Drug Monitoring*

Les connaissances actuelles permettent d'affirmer que l'exposition au tacrolimus augmente le risque de survenue de diabète [111]. Malheureusement peu d'études ont établi une relation direct entre les indices d'exposition usuellement utilisés (C0 et AUC) dans le STP du tacrolimus et l'apparition de diabètes [31,112,113]. En revanche, la surexposition cumulée au tacrolimus dans les premiers mois de greffe semble être un facteur de risque de survenue du diabète post-transplantation [33].

Les objectifs de ce travail étaient (i) d'identifier des marqueurs de surexposition au tacrolimus à partir des C0 de tacrolimus dans les 3 premiers mois post-transplantation et (ii) d'explorer la relation entre la surexposition et la survenue du diabète post-transplantation.

Trois marqueurs d'exposition ont été considérés pour quantifier la surexposition au tacrolimus : (i) la proportion de C0 supérieures à un valeur seuil, permettant de quantifier la fréquence de la surexposition au-dessus d'un seuil, (ii) la moyenne des valeurs de C0 supérieures à une valeur seuil permettant d'objectiver l'intensité de la surexposition, et (iii) le pourcentage d'AUC des C0 supérieures à une valeur seuil normalisé par le temps de suivi, reflet du temps passé en surexposition.

La valeur seuil de 15 µg/L correspond à la valeur haute de l'intervalle thérapeutique définie par la seconde conférence de consensus européenne [32].

Pour étudier l'association entre chacun de ces marqueurs et l'apparition de diabète post-transplantation, une analyse, univariée et multivarié, par modèle de Cox a été réalisée. Les données de 452 patients transplantés rénaux, issus des études EPIGREN/EPHEGREN, dont 27 avaient développé un diabète dans les 3 premiers post-transplantation ont été analysées dans cette étude. En plus de ces 3 marqueurs, l'impact des covariables démographiques du donneur et du receveur (sexe, âge, indice de masse corporelle…), des covariables concernant l'anamnèse du donneur (thérapie d'induction reçu, greffe antérieure…) et des covariables biologiques (infections à CMV et EBV, human leukocyte antigen (HLA) mismatch) a été étudié. L'analyse univariée du modèle de Cox a souligné la relation ($p<0,1$) de plusieurs variables avec notamment 2 des 3 nouveaux marqueurs d'exposition (pourcentage de C0 > 15 µg/L et pourcentage de C0 > 15 µg/L). Une relation entre la présence d'un surpoids chez le receveur et l'âge du receveur a également été mise en évidence avec des *hazard ratio* (HR) (intervalle de confiance à 95%) de 2,4 (1,1-5,3) et 1,0 (1,0-1,1), confirmant les résultats de la littérature [114].

Licence CC BY-NC-ND 3.0

En revanche, dans l'analyse multivariée, seul le pourcentage de C0 > 15 µg/L reste significativement associé à un risque de développement de diabète. On observe, par augmentation de 10% de la proportion de C0 > 15 µg/L, un HR (intervalle de confiance à 95%) de 1,73 (1,43-2,10). La validation par analyse boostrap a confirmé la pertinence sélection du pourcentage de C0 > 15 µg/L, facteur retenu dans 92,6% des cas. Ces résultats devront être validés dans une base externe.

Par la suite, un seuil discriminant le surrisque de développer un diabète à partir de cette dernière a été déterminé proche des 20%. Une analyse univariée pour déterminer un possible effet d'une variable catégorielle a été effectuée. Lorsqu'un patient possède 20% de ses C0 > 15 µg/L celui-ci a environ 5 fois plus de risque de développer un diabète post-transplantation.

La mise en évidence de l'association entre la surexposition au tacrolimus (déterminée au moyen d'un des marqueurs de surexposition), et l'apparition de diabète post-transplantation confirme la nécessité de la mise en place d'un STP régulier du tacrolimus et notamment dans les premiers mois de greffe afin d'éviter la surexposition. Même si les marqueurs de surexpression au tacrolimus identifiés dans cette étude semblent difficiles à utiliser en routine, ils pourraient contribuer à étudier l'association entre exposition au tacrolimus et ses effets indésirables tels que la néphrotoxicité ou la neurotoxicité.

Licence CC BY-NC-ND 3.0

Therapeutic Drug Monitoring Publish Ahead of Print
DOI: 10.1097/FTD.0000000000001035

Longitudinal exposure to tacrolimus and new-onset diabetes mellitus in renal transplant patients

Alexandre DESTERE PharmD[1,3], Aurélie PREMAUD PhD, PharmD[1], Caroline MONCHAUD PhD, PharmD[1,2], Pierre MARQUET PhD, MD[1,2], Jean-Baptiste WOILLARD PhD, PharmD [1,2]

[1]Pharmacology & Transplantation, INSERM U1248, Université de Limoges, Limoges, France

[2]Department of Pharmacology, Toxicology and Pharmacovigilance, University Hospital of Limoges, Limoges, France

[3]Department of Pharmacology and Toxicology, University Hospital of Nice, Nice, France

Conflict's interest: The authors declare no competing interests to declare in relation to this work

Corresponding author: Jean-Baptiste Woillard, Title: PharmD, PhD, ORCID: 0000-0003-1695-[illegible], Address: Univ. Limoges, INSERM U1248 IPPRITT, 2 rue du Pr Descottes, F-87000 Limoges, France. Phone: +33 5 55 05 61 40, Fax: +33 5 55 05 61 62, Email: jean-baptiste.woillard@unilim.fr

Acknowledgment

Funding information

Copyright © 2022 Wolters Kluwer Health, Inc. Unauthorized reproduction of this article is prohibited.

ACCEPTED

Licence CC BY-NC-ND 3.0

No funding was received for this study

Word counts: 2494

Numbers of tables and figures: 2 tables and 5 figures

ACCEPTED

Abstract

Purpose:

Tacrolimus is an immunosuppressant widely used in transplantations requiring mandatory concentration-controlled dosing to prevent acute rejection or adverse effects, including new-onset diabetes mellitus (NODM). However, no relationship between NODM and tacrolimus exposure has been established. This study aimed to evaluate the relationship between cumulative tacrolimus exposure and NODM occurrence.

Methods:

A total of 452 kidney transplant patients were included in this study. Sixteen patients developed NODM during the first three months post-transplant. We considered all tacrolimus concentrations (C0) values collected until the diagnosis of NODM in these patients and until three months post-transplant in the others. New tacrolimus cumulative exposure metrics were derived from the time profile of the tacrolimus morning pre-dose concentration, C0: the percentage of C0 values > cut-off, the average of C0 values above the cut-off, and the percentage of the area under C0 vs. time curve,

Copyright © 2022 Wolters Kluwer Health, Inc. Unauthorized reproduction of this article is prohibited.

Licence CC BY-NC-ND 3.0

AUC_{C0}, above the cut-off. The cut-off chosen was 15 ng/mL, corresponding to the higher end of the therapeutic range for the early post-transplant period. The influence of these metrics on NODM and other clinical and biological characteristics was investigated using the Cox models.

Results:

The percentage of C0 > 15 µg/L was statistically different between patients with and without NODM (p = 0.01). Only these tacrolimus C0-derived metrics were significantly associated with an increased risk of NODM (HR:1.73 (1.43–2.10, p < 0.001)).

Conclusion:

This study shows that tacrolimus concentrations >15 µg/L affect the incidence of NODM.

Keywords: tacrolimus; diabetes mellitus; renal transplant; exposure; Cox model

ACCEPTED

Introduction

Tacrolimus is an immunosuppressant characterized by a narrow therapeutic index and large interindividual pharmacokinetic variability. Consequently, tacrolimus's therapeutic drug monitoring (TDM) is mandatory.[1] Individual dose adjustment is routinely based on the trough value of whole blood tacrolimus concentrations (C0). A recent consensus report recommended monitoring the tacrolimus dose AUC.[1]

Individual dose adjustment minimizes the risk of acute rejection and adverse effects such as nephrotoxicity and neurotoxicity, and to a lesser extent, new-onset diabetes mellitus (NODM). The incidence of diabetes post-transplantation was reported to be 13.4%, higher with tacrolimus than cyclosporine (16.6% vs. 9.8%).[2] In some cases, tacrolimus-induced diabetes may resolve by switching to cyclosporin.[3] Patients taking tacrolimus should have blood glucose monitored, especially in the first weeks after transplantation, when NODM mostly occurs.[4] Relationships between tacrolimus C0

Copyright © 2022 Wolters Kluwer Health, Inc. Unauthorized reproduction of this article is prohibited.

Licence CC BY-NC-ND 3.0

or AUC and NODM have been explored in different studies, but no direct association was found.[5–7] Other tacrolimus exposure indices were explored: Maes et al. [8] showed that the incidence of NODM increased parallel to the tacrolimus concentrations >15 µg/L in the first month. Similarly, the first tacrolimus C0 value after transplantation was associated with an increased risk of diabetes in the first year.[9]

The objectives of the present study were: (i) to derive different exposure metrics from the longitudinal evolution of tacrolimus C0 in the first three months post-transplant and (ii) to explore the relationships between these tacrolimus exposure metrics and the occurrence of NODM.

Materials and Methods

PATIENTS AND DATA COLLECTED

Data were collected from adult kidney transplant recipients enrolled in two successive observational pharmacoeconomic multicenter cohort studies called "EPIGREN" and "EPHEGREN"[10] (NCT01989832). "EPIGREN "was a pilot cohort study conducted in 3 French kidney transplantation centers (Bordeaux, Limoges, and Toulouse), and "EPHEGREN" was a second, larger cohort study conducted in the same and four other centers (Amiens, Rouen, Poitiers, and Tours). EPIGREN and EPHEGREN were designed to study graft survival in kidney transplant patients as a function of various factors (exposure to immunosuppressive drugs, viral infections, socioeconomic status, and comorbidity). The National Committee for Informatics and Liberties approved the electronic collection and handling of patient data under the No. 907275 ACT. All enrolled patients provided written informed consent to participate in the study.

The patients selected for the present study received a first kidney transplant between 2007 and 2016, were prescribed tacrolimus as part of their immunosuppressive regimen, and had at least two pre-dose concentrations (C0) of tacrolimus available in the study database over the first 3 months

Copyright © 2022 Wolters Kluwer Health, Inc. Unauthorized reproduction of this article is prohibited.

ACCEPTED

Licence CC BY-NC-ND 3.0

post-transplant. In each center, tacrolimus C0 was measured using a validated HPLC method. Exposure and clinical and demographic data were collected from patients' medical records as part of EPIGREN or EPHEGREN. The clinical and demographic data included height, weight, date of transplantation, sex, age, presence of pre-transplant diabetes in the graft donor or recipient, previous organ transplantations, onset of diabetes post-transplant and corresponding date, and EBV and CMV viral infections. The available exposure indices were the tacrolimus C0 values on the day of sampling. Patients were deemed diagnosed with NODM when antidiabetic drugs (biguanide, sulfamide, or insulin) were initiated after transplantation and had not been used before.

TACROLIMUS EXPOSURE

Different tacrolimus exposure metrics were derived for each patient from their longitudinal profile of tacrolimus C0 over the first three months after transplantation: the proportion of C0 values > cut-off (%C0 > 15 µg/L), the average of C0 values above the cut-off (Av_{C0} > 15 µg/L), and the percentage of the area under the C0 > cut-off vs. time curve (%AUC_{C0} > 15 µg/L).

- $\%\text{AUC}_{\text{C0}} > \text{cut-off}\ (\%) = \frac{\text{AUC of C0} > \text{cut-off}}{\text{total AUC of C0} > 0} \times 100$
- $\text{cut-off}\ (\%) = \frac{\text{number of C0} > \text{cut-off}}{\text{number of C0 total}} \times 100$
- $\text{average C0} > \text{cut-off} = mean\left(C0 > cut\text{-}off\right)$

The cut-off chosen was the upper limit of the therapeutic window immediately after kidney transplantation (15 µg/L), following recent recommendations.[1]

Copyright © 2022 Wolters Kluwer Health, Inc. Unauthorized reproduction of this article is prohibited.

ACCEPTED

Licence CC BY-NC-ND 3.0

The %AUC_{C0} > cut-off assesses the percentage of time patients were overexposed to tacrolimus and the intensity of overexposure. The percentage and average of C0 > cut-off (%) quantify the frequency and degree of overexposure to tacrolimus, respectively.

The AUC of C0 higher than the cut-off value was calculated using the "riverbed" R package.[11] For patients with NODM, the %AUC_{C0} was calculated between the first post-transplant C0 and the last C0 before the diagnosis of NODM. For non NODM patients, %AUC_{C0} was calculated from the first C0 post-transplant to C0 at the three-month study visit. Boxplots were drawn to highlight the possible differences in tacrolimus C0-derived metrics between patients with and without NODM. A correlation analysis was performed to identify the relationships between these tacrolimus exposure metrics.

RELATIONSHIPS BETWEEN TACROLIMUS EXPOSURE METRICS AND NODM

Cox models were built to investigate the relationships between the C0-derived exposure indices and the occurrence of NODM after adjusting for clinical/demographic data (donor age, recipient age, body mass index (BMI), sex, and previous transplant). The genetic polymorphisms *CYP3A4*22* and *CYP3A5*3*, *POR*28* or *PPAR alpha* could not be investigated, as only 38% of the patients had these data available, and none of them had NODM. Statistical analyses were performed using R (version 3.6.3) package "survival."[12] Variables with a P value < 0.1 determined by univariate analysis were included in an intermediate multivariable Cox model. The final model was obtained through stepwise backward selection, retaining only variables with P < 0.05. The statistical interactions between the covariates in the final model were evaluated. The robustness of the results was assessed with 1,000

ACCEPTED

Copyright © 2022 Wolters Kluwer Health, Inc. Unauthorized reproduction of this article is prohibited.

Licence CC BY-NC-ND 3.0

bootstraps using the BootstepAIC R package.[13] For Cox models, the proportionality of risks was assessed in the final model using Schoenfeld residues.

Receiver operating characteristic (ROC) analysis was performed to determine the most discriminative threshold for the final metric (s) based on the Youden index. Cumulative incidence curves of NODM in patients below or above this threshold were plotted and compared using the log-rank.

Results

Four hundred fifty-two patients out of the 820 patients in the EPIKRE-EPIKEGREN cohort studies had relevant data available over the first three months after transplantation and were selected for this study (Figure 1) (other patients had data missing in this early period post-transplantation, sometimes because they were included later after transplantation). The median [IQR] time of the 1st C0 was 3 (2–6) days. The cumulative incidence of NODM in the first three months accounted for 75% of the cumulative NODM incidence in the entire dataset. The characteristics of 452 patients are shown in Table 1. The density plot number of pre-dose concentrations in each type of patient (NODM vs. non NODM) (Figure 2) showed a larger number of pre-dose concentrations in non NODM patients (median number of samples per patient = 7.5 and 15 for NODM and non NODM, respectively). The median time to NODM was 14 days.

The median [min–max] of %C0 > 15 µg/L, %AUC_{C0} > 15 µg/L, and Av_{C0} > 15 µg/L are presented in Table 1 and graphically represented in Figure 3.

A statistical comparison of each tacrolimus C0-derived metric of the patients with and without NODM was made. Only %C0 > 15 µg/L was significantly different between the 2 subgroups (p = 0.001).

Copyright Ó 2022 Wolters Kluwer Health, Inc. Unauthorized reproduction of this article is prohibited.

ACCEPTED

Licence CC BY-NC-ND 3.0

The three C0-derived tacrolimus exposure metrics examined by the univariate analysis were significantly associated with an increased risk of NODM (Table 2). They were also highly correlated (Supplemental Figure 1, http://links.lww.com/TDM/A611): r [%C0 > 15 µg/L vs. %AUC_{0} > 15 µg/L] = 0.64; r [%C0 > 15 µg/L vs. Av_{0} > 15 µg/L] = 0.63; and r [Av_{0} > 15 µg/L vs. %AUC_{0} > 15 µg/L] = 0.99.

Patient BMI dichotomized as "not overweight" *vs.* "overweight," age and donor age were associated with an increased risk of NODM (Table 2).

In multivariate analysis, only %C0 > 15 µg/L remained significant (Table 2). This result was confirmed by bootstrap analysis: %C0 >15 µg/L was selected in 92.5% of the 1,000 bootstrap models. No statistical interaction was found between the tacrolimus C0-derived exposure metrics and dichotomized BMI. There was no deviation in risk proportionality for the final model (p = 0.81).

For %C0 > 15 µg/L, the best threshold obtained using ROC analysis and the Youden index (Figure 4) was 17.9% (AUC ROC = 0.67; sensitivity = 0.37; specificity = 0.90). This threshold was used to dichotomize the %C0 > 15 µg/L and this new binary variable was investigated using univariate Cox model showing a highly significant association with DODM: hazard ratio [HR]: 5.3, 95% CI [2.4–11.6], p < 0.001. Its inclusion in multivariate analysis (instead of %C0 > 15 µg/L) confirmed that it was the only variable significantly associated with NODM and was selected in 96% of the 1,000 bootstraps. The cumulative incidence curve of this dichotomized variable is shown in Figure 5.

Discussion

ACCEPTED

Copyright © 2022 Wolters Kluwer Health, Inc. Unauthorized reproduction of this article is prohibited.

Licence CC BY-NC-ND 3.0

In this study, we investigated the relationship between new tacrolimus C0-derived exposure metrics and NODM and found that the proportion of C0 values > 15 µg/L over the first three months post-transplant was significant and positively associated with the occurrence of NODM.

The new metrics developed in this study provided different pieces of information: the percentage of AUC_{C0} corresponding to C0 > 15 µg/L assesses the percentage of time patients are overexposed to tacrolimus and the intensity of such overexposure, whereas the percentage and average C0 values > 15 µg/L quantify the frequency and (in a different way) the intensity of overexposure to tacrolimus, respectively.

Each C0-derived exposure metric was significantly associated with an increased risk of NODM in the univariate Cox model. However, only a%C0 > 15 µg/L was retained in the multivariate model. This can probably be explained by the high correlation observed between metrics, as each of these metrics describes tacrolimus overexposure from a different angle.

For every 10% increase in the %C0 > 15 µg/L, the risk of developing post-transplant diabetes increased 2-fold, and even 5-fold for a 20% increase. This result is similar to that reported by Maes et al., who found an increased risk of NODM with an increase in tacrolimus concentrations > 15 µg/L in the first month. These results reinforce the hypothesis of a relationship between cumulative tacrolimus exposure and NODM. The advantage of the percentage over the number of C0 values > 15 µg/L is that it can be generalized to all patients regardless of the number of C0 tacrolimus during the first three months. Indeed, patients with more C0 measurements have an increased probability of values > 15 µg/L. In contrast, Rodrigo et al.[9] reported that only the initial tacrolimus C0, > 20 µg/L, was associated with an increased risk of developing diabetes. This finding was not observed in our cohort. Different mechanisms may explain the occurrence of NODM: (i) decreased insulin secretion in beta cells exposed to tacrolimus, causing an increase in intracellular calcium. (ii) Tacrolimus potentiates glucolipotoxicity via the AKT pathway. Cumulative overexposure to tacrolimus

Copyright Ó 2022 Wolters Kluwer Health, Inc. Unauthorized reproduction of this article is prohibited.

ACCEPTED

Licence CC BY-NC-ND 3.0

accelerates the decrease in insulin secretion and sensitivity, potentiating glucolipotoxicity. Poitout et al.[14] proposed a hypothetical representation of the occurrence of glucolipotoxicity when insulin gene expression and sensitivity decreased. However, these are putative hypotheses, as we do not have data to support them.

Unsurprisingly, BMI was another significant risk factor [4,9,15] since overweight transplant patients (> 25 kg/m^2) had a risk of NODM that increased by approximately 2.5-fold, but it was not retained in the final model. This suggests that C0-derived metrics are more specific to NODM, that is, to the circumstances of diabetes occurrence than BMI. Notably, no statistical interaction between C0-derived metrics and dichotomized BMI was found, possibly explaining the latter's exclusion from the final model.

A %C0 > 15 µg15µg/L seems difficult in clinical practice because it is dynamically changing, and its calculation may become tedious. Connecting an app to the patient's electronic health record that would automatically collect C0 values over the first 3 months and calculate %C0 > 15µg/L would improve its use. These results highlight the importance of tacrolimus exposure monitoring and model-informed precision dosing (MIPD), especially in the first three months of transplantation, in accordance with international recommendations.[1]

Among the tools available to prevent overexposure in the first week after transplantation, the use of dosing algorithms to propose a first dose based on individual covariates or MIPD based on individual information [16–19] could limit overexposure and reduce the occurrence of NODM.

The frequency of NODM was 6%, close to the lower limit of 3–47% found in the literature[2], depending on the studies. We have no clear explanation for this, as it was an observational study, and the patient did not benefit from modified or reinforced follow-up. A possible explanation might

ACCEPTED

Copyright © 2022 Wolters Kluwer Health, Inc. Unauthorized reproduction of this article is prohibited.

Licence CC BY-NC-ND 3.0

be the definition of NODM used in the present study that differs from the literature. In addition, we only had access to an indirect diagnostic method based on NODM treatment.

The density plot for the number of samples per patient stratified by NODM showed that the number of samples was lower for patients with NODM and followed a bimodal distribution. This is a major limitation of the present study. Indeed, in the case of only two C0 values, having one [illegible] 15 µg/L would lead to 50% of C0 > 15 ng/mL. We show that the median number of [illegible]les per [illegible]DM patient was approximately seven (twice lower than the number of samples for non NO[illegible]patients), but the metric used normalizes for the number of C0. This may h[illegible]ve [illegible]duced ou[illegible] findings. We have no real explanation for the bimodal distribution. Neve[illegible]less, we co[illegible]ed the %C0 > 15 ng/mL between the two modes of the curve in patients with NODM ([illegible]20 C0 vs. > 20 C0) and found no significant difference (pMW = 0.5564).There a[illegible] othe[illegible]mitations in our study: its retrospective design, leading possibly to inconsistencies in the data[illegible] and the absence of covariates of potential interest such as the dose of corticoste[illegible]d (all p[illegible]ients rec[illegible]ved corticosteroids, but the dose was not accessible), viral infections (e.g., hepatitis [illegible]virus), or genetic polymorphisms (only 14% of the patients were genotyped, n[illegible] enough to inve[illegible]igate the gene effect shown to increase the risk of NODM.[20,21] Ethnicity [illegible]s not [illegible]ilable[illegible]s it was forbidden in France to collect such data, but we hypothesized th[illegible] most of the patients included were from Caucasian ancestors. Another limitation is the multicente[illegible]servati[illegible]nal design, leading to different manners of C0 monitoring and dose adapta[illegible]ion[illegible] there was no uniform protocol. Finally, a limitation is the absence of external validation of the relationship between C0-derived tacrolimus exposure metrics and NODM; we assessed its robustness by internal evaluation using 1,000 bootstraps.

Conclusion

In conclusion, we investigated different C0 metrics that could take into account the longitudinal exposure to tacrolimus at three months post-transplantation. We found that %C0

Copyright Ó 2022 Wolters Kluwer Health, Inc. Unauthorized reproduction of this article is prohibited.

ACCEPTED

Licence CC BY-NC-ND 3.0

> 15µg/L was associated with an increased risk of NODM even if routine care use seems difficult.

In future studies, the C0-derived tacrolimus exposure metrics developed here could be used to investigate the relationship between cumulative exposure (or overexposure) and efficacy or adverse effects.

ACCEPTED

Copyright Ó 2022 Wolters Kluwer Health, Inc. Unauthorized reproduction of this article is prohibited.

Licence CC BY-NC-ND 3.0

Table 1. Patients' characteristics

	New Onset of Diabetes Mellitus		
	No	Yes	Overall
n	425	27	
Age			
Median (IQR)	52.0 (20.0)	57.0 (16	53.0 (19)
Min, Max	19.0, 85.0	76.0	19.0, 85.0
Missing	1		1
Sex			
Female	16 38.6%)	6(22.2%)	170(37.6%)
Male	260(	21(77.8%)	281(62.2%)
Missing	1(0.2%)	0	1(0.02%)
Height (cm)			
Median (IQR)	170.0 (14.5)	173.0 (8)	170.0 (14.0)
Min, Max	57.0, 196.0	155.0, 185.0	57.0, 196.0
Missing	70	0	70
Weight (kg)			

ACCEPTED

Copyright Ó 2022 Wolters Kluwer Health, Inc. Unauthorized reproduction of this article is prohibited.

Licence CC BY-NC-ND 3.0

Median (IQR)	70.0 (22.0)	78.00 (10)	70.0 (21.0)
Min, Max	37.0, 159.0	55.0, 99.0	37.0, 159.0
Missing	11	0	11
BMI (kg/m^2)			
< 25: n(%)	194(45.6%)	9(33.3%)	203(.9%)
> 25: n(%)	156(36.7%)	18(66.7%)	174(8.5%)
Missing	75(17.6%)	0(0%)	75(16.6%)
Time of diabetes onset (post-transplant years)			
Median (IQR)	-	0.04 (0.02)	0.03 (0.1)
Min, Max	-	0.02, 0.24	0.02, 0.2
Missing		0	0
%AUC$_{C0}$ with >15 µg/L			
Median [min - max]	0.0 [0.0 – 18.0]	0.2 [0.0 – 22.8]	(p=0.4)
%C0 >15 µg/L			
Median [min - max]	0.0 [0.0 – 66.7]	4 [0.0 – 66.7]	(p=0.06)
Average of C0 >15 µg/L			

ACCEPTED

Copyright © 2022 Wolters Kluwer Health, Inc. Unauthorized reproduction of this article is prohibited.

Licence CC BY-NC-ND 3.0

Median [min - max]	15.0 [15.0 – 17.5]	15.2 [15.0.0 – 18.0]	(p=0.4)
Previous transplant n(%) Yes No Missing	 62(14.6%) 300(70.6%) 63(14.8%)	 3(11.1%) 24(88.9%) 0(0%)	 65(14.4%) 3[illegible]4(71.7 63([illegible]%)
known pathologies (3 most frequent) n(%)	Various nephropathies:102(24%) Polycystic kidney disease: 51(12%) Glomer[illegible]phritis: 39(9.2%) Other:71(16.7%) Missing: 162(38.1%)	Various [illegible]ephropath[illegible] 8(2[illegible]%) Po[illegible]ystic kidney disease: 5(18.5%) Glomerulonephritis: 2(7.4%) Amylose: 1(3.7%) Other: 11(40.1%)	-
HL[illegible]mismatch leve[illegible] n(%): 0 1 2 3	 2(0.4%) 5(1.1%) 15(3.5%) 35(8.2%)	 1(3.7%) 0(0%) 0(0%) 0(0%)	3(0.7%) 5(1.2%) 15(3.3%) 35(7.7%) 67(14.8%)

ACCEPTED

Copyright Ó 2022 Wolters Kluwer Health, Inc. Unauthorized reproduction of this article is prohibited.

Licence CC BY-NC-ND 3.0

4	62(14.6%)	5(18.5%)	73(16.2%)
5	67(15.7%)	6(22.2%)	70(15.5%)
6	62(14.6%)	8(29.6%)	51(11.2%)
7	48(11.3%)	3(11.1%)	15(3.3%)
8	13(3.1%)	2(7.4%)	118(26.1
missing	116(27.3%)	2(7.4)	
Acute rejection n(%):			
Yes	15(3.5%)	3(11.1%)	18(4.0%)
No	410(9 .5%)	24(89.9%)	434(96.0%)
CMV recipient n(%):			
Yes	118(27.8%)	16(59.3%)	134(29.6%)
No	146(34.4%)	11(40.7%)	157(34.7%)
mis	161(37.9%)	0(0%)	161(35.6%)
CMV d nor (n):			
Yes	141(33.2%)	14(51.9%)	155(34.3%)
No	123(28.9%)	13(48.1%)	136(30.1%)
missing	161(37.9%)	0(0%)	161(35.6%)

ACCEPTED

Copyright Ó 2022 Wolters Kluwer Health, Inc. Unauthorized reproduction of this article is prohibited.

Licence CC BY-NC-ND 3.0

EBV recipient n(%):			
Yes	253(59.5%)	27(100%)	280(61.9%)
No	11(2.6%)	0(100%)	11(2.4%)
missing	161(37.9%)	0(100%)	161(35.6%)
EBV donor n(%):			
Yes: n(%)	255(60.0%)	27(100%)	282(62.4%)
No: n(%)	9(2.1%)	0(0%)	9(2.0%)
missing	161(37.9%)	0(0%)	161(35.6%)
Use of glucocorticoid n(%)			
Yes	250(58.8%)	27(100%)	277(61.3%)
No	0(0%)	0(0%)	0(0%)
Missing	175(41.2%)	0(0%)	175(38.7%)
Induction n(			
No ind	164(38.6%)	9(33.3%)	173(38.3%)
Monoclonal	235(55.3%)	17(63.0%)	252(55.8%)
Polyclonal	26(6.1%)	1(3.7%)	27(59.7%)
CYP3A4*22 (rs35599367) n(%)	129(30.3%)	0(0%)	129(28.5%)

ACCEPTED

Copyright Ó 2022 Wolters Kluwer Health, Inc. Unauthorized reproduction of this article is prohibited.

Licence CC BY-NC-ND 3.0

CC CT missing	14(3.3%) 282(66.4%)	0(0%) 27(100%)	14(3.1%) 309(68.4%)
CYP3A5*3 (rs776746) n(%) AA GA GG missing	5(1.2%) 43(10.1%) 97(22.8%) 280(65.9%)	0(0%) 0(0%) 0%) 27(100%)	5(1.1%) 43(9.5%) 97(21.5%) 307(67.9%)
PPAR alpha (rs4253728) n(%) AA GA GG ing	17(4.0%) 57(13.4%) 69(16.2%) 282(66.4%)	0(0%) 0(0%) 0(0%) 27(100%)	17(1.1%) 57(9.5%) 69(21.5%) 309(68.4%)
POR*2 (rs1057868) n(%) CC CT TT	80(18.8%) 54(12.7%) 11(2.6%)	0(0%) 0(0%) 0(0%)	80(17.7%) 54(11.9%) 11(2.4%)

ACCEPTED

Copyright © 2022 Wolters Kluwer Health, Inc. Unauthorized reproduction of this article is prohibited.

Licence CC BY-NC-ND 3.0

missing	280(65.9%)	27(100%)	307(67.9%)

ACCEPTED

Copyright Ó 2022 Wolters Kluwer Health, Inc. Unauthorized reproduction of this article is prohibited.

Licence CC BY-NC-ND 3.0

Table 2. Univariate and multivariate analyses of the relationships between tacrolimus exposure indices and patient characteristics related to the new onset of diabetes mellitus (NODM)

NODM	HR (95% CI, p-value) (univariate)	HR (95% CI, p-value) (multivariate)	Covariates selected by bootstrap analysis (%)
%C0 >15 µg/L (*per 10% increase*)	1.73 (1.43-2.10, p<0.001)	1.73 (1.43-2.10, p<0.001)	92.6
%AUC_{C0} with C0 >15µg/L (*per 10% increase*)	1.08 (0.99-1.18, p=0.09)	Not retained	27.8
Average C0 >15µg/L (*per unit increase*)	1.75 (0.87-3.5, p=0.12)	-	-
Sex (Male vs Female)	1.13 (0.52-2.43, p=0.76)	-	-
BMI > 25 vs <25	2.38 (1.07-5.29, p=0.03)	Not retained	73.1

ACCEPTED

Copyright © 2022 Wolters Kluwer Health, Inc. Unauthorized reproduction of this article is prohibited.

Licence CC BY-NC-ND 3.0

NODM	HR (95% CI, p-value) (univariate)	HR (95% CI, p-value) (multivariate)	Covariates selected by bootstrap analysis (%)
Age *(per year)*	1.03 (1.0-1.07, p=0.03)	Not retained	6.9
Donor sex (Male vs Female)	1.13 (0.52-2.43, p=0.76)		-
Donor age *(per year)*	1.03 (1.0-1.07, p=0.03)	Not retained	63.7
Previous transplant *(per unit increase)*	1.53 (0.20-2.18, p=0.49)	-	-
HLA mismatch *(per unit increase)*	1.18 (0.92-1.51, p=0.20)	-	-
Induction therapy (vs none) Monoclonal polyclonal	1.2[illegible]7-2.86, p=0.56) 0.69 (0.09-5.43, p=0.72)	- -	- -

ACCEPTED

Copyright © 2022 Wolters Kluwer Health, Inc. Unauthorized reproduction of this article is prohibited.

Licence CC BY-NC-ND 3.0

NODM	HR (95% CI, p-value) (univariate)	HR (95% CI, p-value) (multivariate)	Covariates selected by bootstrap analysis (%)
CMV donor (positive vs negative)	1.06 (0.44-2.00, p=0.87)	-	-
CMV Recipient (positive vs negative)	0.56 (0.83-3.85, p=0.14)		-
EBV Donor (positive vs negative)	0.01 (0.0- infinity, p=0.99)	-	-
EBV recipient (positive vs negative)	0.01 (0.0- infinity, p=0.99)	-	-

HLA: Human Leukocyte Antigen; CMV: cytomegalovirus; EBV: Epstein-Barr virus

ACCEPTED

Copyright © 2022 Wolters Kluwer Health, Inc. Unauthorized reproduction of this article is prohibited.

Licence CC BY-NC-ND 3.0

References

1. Brunet M, van Gelder T, Åsberg A, et al. Therapeutic Drug Monitoring of Tacrolimus-Personalized Therapy: Second Consensus Report. *Therapeutic Drug Monitoring*. 2019;41(3):261-307. doi:10.1097/FTD.0000000000000640

2. Heisel O, Heisel R, Balshaw R, Keown P. New Onset Diabetes Mellitus in Patients Receiving Calcineurin Inhibitors: A Systematic Review and Meta-Analysis. *American Journal of Transplantation*. 2004;4(4):583-595. doi:10.1046/j.1600-6143.2004.00372.x

3. Ramos-Cebrián M, Torregrosa JV, Gutiérrez-Dalmau A, Oppenheimer F, Campistol JM. Conversion From Tacrolimus to Cyclosporine Could Improve Control of Posttransplant Diabetes Mellitus After Renal Transplantation. *Transplantation Proceedings*. 2007;39(7):2251-2253. doi:10.1016/j.transproceed.2007.06.035

4. Cho YM, Park KS, Jung HS, et al. High Incidence of Tacrolimus-Associated Posttransplantation Diabetes in the Korean Renal Allograft Recipients According to American Diabetes Association Criteria. *Diabetes Care*. 2003;26(4):1123-1128. doi:10.2337/diacare.26.4.1123

5. Gastaca M, Ruiz P, Bustamante J, et al. Early tacrolimus exposure does not impact long-term outcomes after liver transplantation. *WJH*. 2021;13(3):362-374. doi:10.4254/wjh.v13.i3.362

6. Shao L, Jin J, Ye B, et al. New-Onset Diabetes Mellitus in Patients with Idiopathic Membranous Nephropathy Undergoing Tacrolimus and Low-Dose Corticosteroid Therapy. *Kidney Blood Press Res*. 2019;44(6):1352-1362. doi:10.1159/000502693

Copyright © 2022 Wolters Kluwer Health, Inc. Unauthorized reproduction of this article is prohibited.

ACCEPTED

Licence CC BY-NC-ND 3.0

7. Gourishankar S, Jhangri GS, Tonelli M, Wales LH, Cockfield SM. Development of Diabetes Mellitus Following Kidney Transplantation: A Canadian Experience. *Am J Transplant*. 2004;4(11):1876-1882. doi:10.1111/j.1600-6143.2004.00591.x

8. Maes BD, Kuypers D, Messiaen T, et al. POSTTRANSPLANTATION DIABETES MELLITUS IN FK-506-TREATED RENAL TRANSPLANT RECIPIENTS: ANALYSIS OF INCIDENCE AND RISK FACTORS. *Transplantation KW* -. 2001;72(10):1655-1661.

9. Rodrigo E, Pinera C, Cos MA, et al. Evolution of tacrolimus blood levels and concentration-dose ratios in patients who develop new onset diabetes mellitus after kidney transplantation. *Transplant Int*. 2005;18(9):1152-1157. doi:10.1111/j.1432-2277.2005.00191.x

10. Villeneuve C, Laroche ML, Bayle M, et al. Evolution and Determinants of Health-Related Quality-of-Life in Kidney Transplant Patients Over the First 3 Years After Transplantation. *Transplantation*. 2016;100(3):640-647. doi:10.1097/TP.0000000000000846

11. Vaudor L. *Riverbed: Surfaces and Volumes Based on Profiles.*; 2020. https://github.com/lvaudor/riverbed.git.

12. Therneau TM. *A Package for Survival Analysis in R.*; 2021. https://CRAN.R-project.org/package=survival.

13. Rizopoulos D. *BootStepAIC: Bootstrap StepAIC.*; 2009. https://CRAN.R-project.org/package=bootStepAIC.

14. Poitout V, Amyot J, Semache M, Zarrouki B, Hagman D, Fontés G. Glucolipotoxicity of the pancreatic beta cell. *Biochimica et Biophysica Acta (BBA) - Molecular and Cell Biology of*

Copyright © 2022 Wolters Kluwer Health, Inc. Unauthorized reproduction of this article is prohibited.

ACCEPTED

Licence CC BY-NC-ND 3.0

Lipids. 2010;1801(3):289-298. doi:10.1016/j.bbalip.2009.08.006

15. Zielińska K, Kukulski L, Wróbel M, Przybyłowski P, Zakliczyński M, Strojek K. Prevalence and Risk Factors of New-Onset Diabetes After Transplantation (NODAT). *Ann Transplant*. 2020;25. doi:10.12659/AOT.926556

16. Størset E, Åsberg A, Skauby M, et al. Improved Tacrolimus Target Concentration Achievement Using Computerized Dosing in Renal Transplant Recipients—A Prospective, Randomized Study. *Transplantation*. 2019;103(10):2158-2166. doi:10.1097/TP.0000000000000708

17. Francke MI, Andrews LM, Le HL, et al. Avoiding Tacrolimus Underexposure and Overexposure with a Dosing Algorithm for Renal Transplant Recipients: A Single Arm Prospective Intervention Trial. *Clin Pharmacol Ther*. 2021;110(1):169-178. doi:10.1002/cpt.2163

18. Benkali K, Rostaing L, Premaud A, et al. Population Pharmacokinetics and Bayesian Estimation of Tacrolimus Exposure in Renal Transplant Recipients on a New Once-Daily Formulation. *Clinical Pharmacokinetics*. 2010;49(10):683-692. doi:10.2165/11535950-000000000-00000

19. Woillard J, Labriffe M, Debord J, Marquet P. Tacrolimus Exposure Prediction Using Machine Learning. *Clin Pharmacol Ther*. 2021;110(2):361-369. doi:10.1002/cpt.2123

20. Li DW. Risk factors for new onset diabetes mellitus after liver transplantation: A meta-analysis. *WJG*. 2015;21(20):6329. doi:10.3748/wjg.v21.i20.6329

21. Hjelmesaeth J, Sagedal S, Hartmann A, et al. Asymptomatic cytomegalovirus infection

Copyright © 2022 Wolters Kluwer Health, Inc. Unauthorized reproduction of this article is prohibited.

ACCEPTED

Licence CC BY-NC-ND 3.0

is associated with increased risk of new-onset diabetes mellitus and impaired insulin release after renal transplantation. *Diabetologia*. 2004;47(9):1550-1556. doi:10.1007/s00125-004-1499-z

Figure legends

Figure 1: Flow chart of patients selected for developing the model. NODM: New onset of diabetes mellitus; C0: pre-dose concentration.

Figure 2: Density plot of the number of pre-dose concentrations as a function of new onset of diabetes mellitus.

Figure 3: Boxplot representing differences C0-derived metrics according to the occurrence of NODM.

Figure 4: Receiver Operating Characteristic (ROC) curve analysis to determine the percentage of C0 values above 15 µg/L.

Figure 5: Plot of cumulative incidence vs. the threshold for %C0 > 15g/L.

Copyright © 2022 Wolters Kluwer Health, Inc. Unauthorized reproduction of this article is prohibited.

ACCEPTED

Licence CC BY-NC-ND 3.0

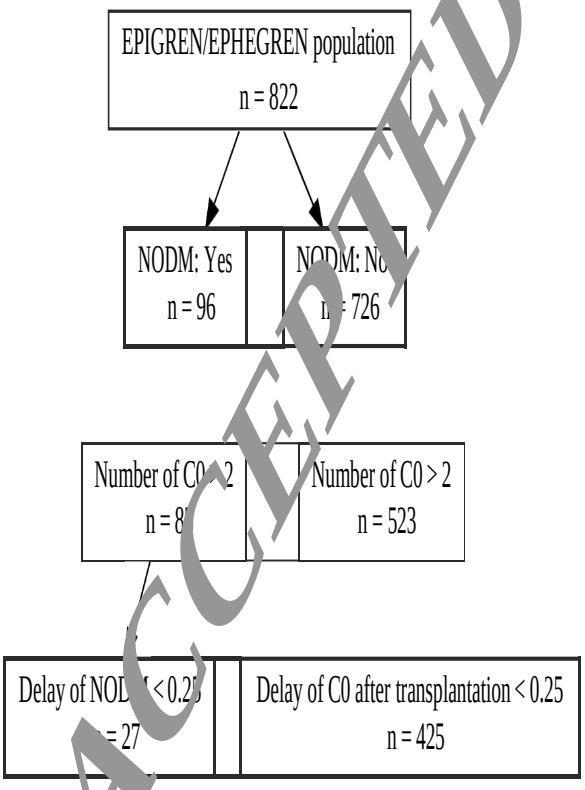

Figure 1: Flow chart of patients selected for developing the Cox model. NODM: New onset of diabetes mellitus; C0: pre-dose concentration.

ACCEPTED

Copyright © 2022 Wolters Kluwer Health, Inc. Unauthorized reproduction of this article is prohibited.

Licence CC BY-NC-ND 3.0

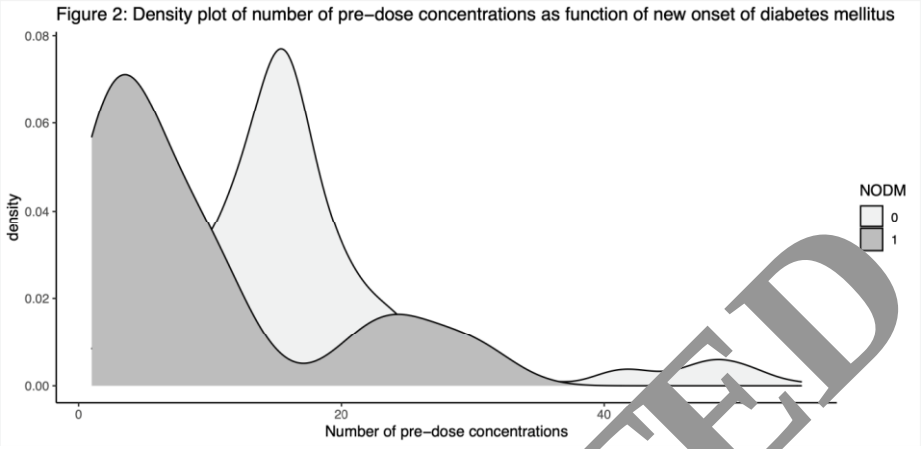

ACCEPTED

Copyright Ó 2022 Wolters Kluwer Health, Inc. Unauthorized reproduction of this article is prohibited.

Licence CC BY-NC-ND 3.0

Figure 3: Boxplot representing different Tac C0–derived metrics according to the occurrence of NODM

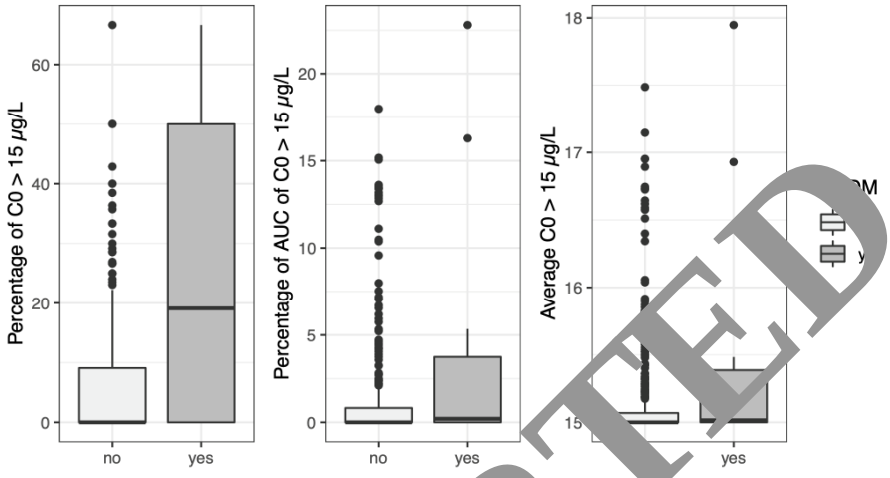

ACCEPTED

Copyright Ó 2022 Wolters Kluwer Health, Inc. Unauthorized reproduction of this article is prohibited.

Licence CC BY-NC-ND 3.0

Figure 4: Receiver Operating Characteristic (ROC) Curve analysis to determine the percentage of C0 values above 15µg/L

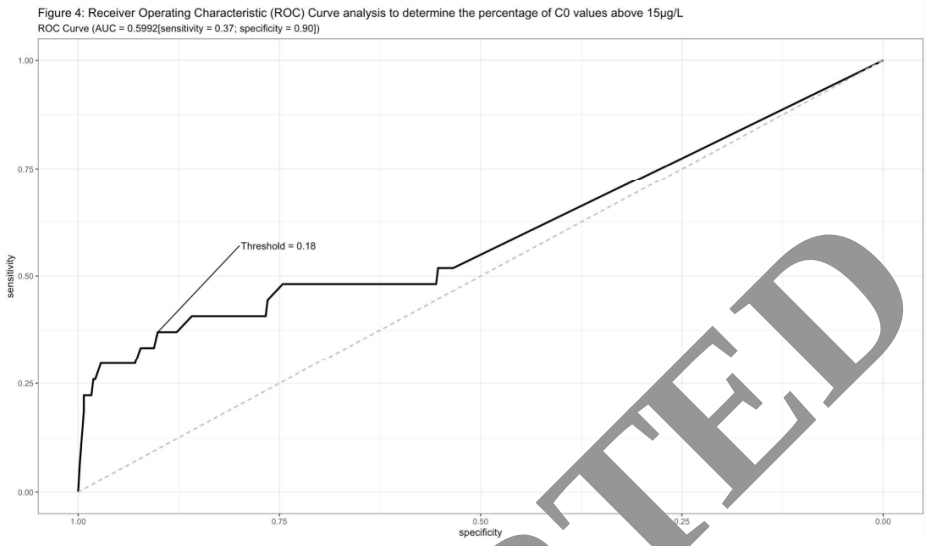

ACCEPTED

Copyright © 2022 Wolters Kluwer Health, Inc. Unauthorized reproduction of this article is prohibited.

Licence CC BY-NC-ND 3.0

Figure 5: Cumulative incidence plot vs. the threshold chosen for %C0 >15g/L

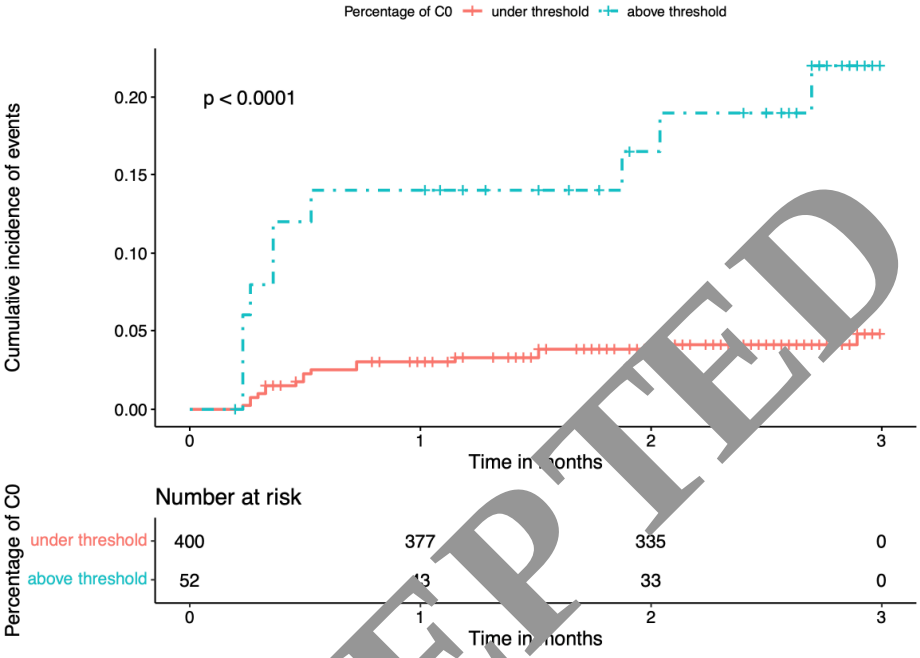

ACCEPTED

Copyright Ó 2022 Wolters Kluwer Health, Inc. Unauthorized reproduction of this article is prohibited.

Licence CC BY-NC-ND 3.0

Partie III. Discussion et Conclusion

L'objectif de ces travaux de thèse était le développement d'outils permettant un suivi individualisé de l'exposition au tacrolimus et de ses effets indésirables afin d'améliorer la prise en charge des patients transplantés rénaux.

Tout d'abord des outils visant à prédire de manière optimale l'exposition au tacrolimus dans le but d'individualiser les posologies proposées aux patients ont été développés. Puis des outils permettant de proposer un suivi précis de la fonction rénale des patients transplantés afin de détecter une néphrotoxicité possiblement liée au tacrolimus ou encore un rejet aigu du greffon ont été élaborés. Un outil permettant de prédire, chez des patients transplantés rénaux, l'exposition à l'isavuconazole utilisé en cas d'infections fongiques a été proposé. Enfin, l'influence d'une surexposition cumulée au tacrolimus dans l'apparition d'un diabète post-transplantation a été confirmée.

A ce jour, de nombreux modèles de POPPK visant à décrire la pharmacocinétique du tacrolimus et ses sources de variabilités ont déjà été publiés dans la littérature [115–118]. Mais à notre connaissance, aucun modèle n'a été développé pour une formulation générique du tacrolimus. Ce travail a donc permis de fournir un outil de plus au clinicien afin de personnaliser au mieux la thérapeutique immunosuppressive. Ce travail a également permis de montrer qu'un estimateur bayésien développé pour le princeps permettait des prédictions similaires à un estimateur bayésien développé pour le générique si les paramètres PK des 2 formulations sont similaires.

Dans cette étude, l'EBE développé n'incorporait pas de covariables. Toutefois, les performances de prédiction de l'exposition individuelle sont tout à fait acceptables avec un biais moyen et une imprécision inférieure à 5% et 10%, respectivement, et ceux quel que soit l'estimateur Bayésien (ancienne et nouvelle formulation). Notre conclusion est que les covariables n'apportent que peu d'information quand des concentrations individuelles sont disponibles ; elles sont nécessaires pour réaliser de simulations mais elles n'apportent que très peu d'information dans l'estimation *a posteriori* des paramètres. Nous ne pensons pas qu'il ne faut jamais inclure de covariables mais qu'il est important de se poser la question de « à quoi va servir le modèle » (« fit for purpose »). Comme l'avait déjà observé Sheiner et al., les informations apportées par les concentrations et les temps de prélèvements sont tout à fait suffisantes [70].

Licence CC BY-NC-ND 3.0

Ce travail a également permis la création d'outils permettant le suivi précis de la fonction rénale des patients transplantés (modèle POPPK et modèle hybride). Actuellement, la fonction rénale du patient transplanté est suivie en utilisant la concentration sérique de créatinine et des formules d'estimation du DFG (CKD-EPI, MDRD…). Cependant, la créatinine n'est pas un marqueur parfait pour mesurer la fonction rénale. La créatinine possède une sécrétion tubulaire et n'est donc pas exclusivement filtrée par le glomérule. La production de créatinine peut être également impactée par l'état physiopathologique des patients (fièvre, alitement prolongé, insuffisance hépatique…) [119] associée aux imperfections d'estimation des formules l'utilisant chez les transplantés rénaux [120]. C'est pour cela que l'utilisation de composés exogènes comme l'iohexol est un moyen d'estimer de manière plus précise le DFG d'un patient [54]. L'utilisation d'outils permettant d'estimer le DFG via l'estimation de la clairance de l'iohexol permet donc aux cliniciens de suivre la santé du greffon et d'objectiver la diminution de la fonction rénale (néphrotoxicité potentiellement due au tacrolimus ou possible rejet de greffe). Une des potentielles limites à son utilisation en routine est la possible néphrotoxicité induite par l'iohexol lors de son utilisation à la dose définie (30 g pour un adulte) dans le résumé des caractéristiques du produit [57]. Cependant, pour la détermination du DFG, le patient reçoit une dose 10 fois inférieure laissant présager une diminution de cette toxicité, confirmée par l'absence d'effets indésirables déclarés après 15 ans de pratique en routine [121].

Afin d'améliorer encore l'estimation du DFG, une approche innovante combinant à la fois un modèle de pharmacocinétique de population et un algorithme de machine Learning a été développé. Ce modèle hybride a montré d'excellentes performances pour la prédiction de la clairance de l'iohexol dans une base de validation externe. La principale source d'amélioration, amenée par le machine learning, était liée au « de-shrinkage » des estimations individuelles du MAP-BE basées sur une stratégie de prélèvements limités. Une des originalités de ce travail est que l'algorithme de machine learning a été entrainé à prédire l'erreur d'estimation de la CL, par le MAP-BE, grâce à des simulations issues du modèle de pharmacocinétique de population développés précédemment. En effet, un nombre conséquent de données patients est nécessaire pour développer ce type d'algorithme et l'utilisation de simulations nous permet donc de nous affranchir de cette limite [81].

La correction d'un seul des paramètres peut entrainer une modification de la corrélation entre les paramètres PK déterminés précédemment. La CL corrigée par le modèle hybride ne pourra, dans ce cas, qu'être utilisée à des fins de prédictions *a posteriori* et non pour effectuer des simulations (encore une fois la notion de « fit for purpose »). La correction de l'ensemble des

Licence CC BY-NC-ND 3.0

paramètres pourrait résoudre cette limite mais devrait faire appel à la correction d'un vecteur de paramètres et prendre en compte leur covariance, ce qui complexifie l'approche.

Les excellents résultats obtenus avec l'iohexol ont été confirmés lors du développement d'un modèle hybride afin de prédire l'exposition globale de l'isavuconazole, confirmant également la source de l'amélioration observée (« de-shrinkage »). Une des limites de ce travail portant sur la prédiction de l'exposition à l'isavuconazole est qu'il n'a pas fait l'objet d'une validation externe *stricto sensu*. Afin de confirmer les résultats, des patients ont été simulés en utilisant un autre modèle de POPPK de l'isavuconazole chez des patients ayant reçu une greffe de cellules souches [110]. L'amélioration de la prédiction du MAP-BE dans cette base externe de patients simulés confirmait ce que nous avions observé dans la base externe constituée de vrais patients lors du développement du modèle hybride de l'iohexol [83]. Enfin, nous pensons que ce nouveau type de modèle ouvre des perspectives vers une nouvelle génération de modèles, plus précis et facilement utilisable en routine (modèles basés sur une stratégie de prélèvements limités), afin d'individualiser plus finement la posologie.

Le dernier axe de cette thèse avait pour objectif l'amélioration de la compréhension de la relation entre l'exposition au tacrolimus et la survenue de diabète post-transplantation. Malheureusement à ce jour, peu d'études ont établi une relation direct entre les indices d'exposition usuellement utilisés (C0 et AUC) dans le STP du tacrolimus et l'apparition de diabètes [31,112,113]. Dans cette étude, la relation entre la surexposition cumulée au tacrolimus durant les 3 premiers mois post-transplantation et la survenue de diabète. Les résultats confirment les résultats précédemment publiés par Maes et al. [33]. Il est difficile de suivre l'exposition cumulée d'un médicament. Cependant il existe des moyens mathématiques simples permettant de réduire à un indice d'exposition fixe ce suivi. Dans ce travail, de nouveaux marqueurs de suivi comme la proportion de C0 supérieure à une valeur seuil, la C0 moyenne supérieure à une valeur seuil ou encore le pourcentage de temps où la C0 est supérieure à une valeur seuil dans le suivi de l'apparition du diabète ont été proposés. La mise en évidence de ce lien entre la surexposition cumulée via l'utilisation d'un de ces marqueurs (proportion de C0 > 15 µg/L durant les 3 premiers mois post-transplantation) et l'apparition de diabète post-transplantation offre la perspective de leur utilisation pour explorer l'existence d'autres relations « exposition cumulée au tacrolimus/effets indésirables » notamment la néphrotoxicité, la neurotoxicité ou la survenue d'infections.

Licence CC BY-NC-ND 3.0

Ces marqueurs restent malheureusement difficiles à utiliser en routine. Cette étude confirme la nécessité du STP du tacrolimus de manière fréquente et rigoureuse notamment dans les premiers mois de greffe.

Pour conclure, ces travaux de thèses ont donc permis de proposer de nouveaux outils permettant un suivi précis de l'exposition au tacrolimus, à l'isavuconazole ou de la fonction rénale ainsi que la mise en évidence d'un lien entre la surexposition cumulée et l'apparition de diabète post-transplantation. Outre l'apport clinique, cette thèse a également proposé de nouvelles méthodologies afin de résoudre des problèmes rencontrés lors du développement de modèles de POPPK et d'EBE (nombre de patients insuffisants pour le développement et la validation, présence de shrinkage…). De nouvelles approches de suivi de l'exposition longitudinale du tacrolimus, ont également été proposées avec notamment une relation avec la survenue d'effets indésirables (diabète post-transplantation).

Licence CC BY-NC-ND 3.0

Références bibliographiques

1. Tanaka H, Nakahara K, Hatanaka H, Inamura N, Kuroda A. Discovery and Development of a Novel Immunosuppressant, Tacrolimus Hydrate. YAKUGAKU ZASSHI. 1997;117:542–54.
2. Wallemacq PE, Reding R. FK506 (tacrolimus), a novel immunosuppressant in organ transplantation: clinical, biomedical, and analytical aspects. Clin Chem. 1993;39:2219–28.
3. Tsunashima D, Kawamura A, Murakami M, Sawamoto T, Undre N, Brown M, et al. Assessment of Tacrolimus Absorption From the Human Intestinal Tract: Open-Label, Randomized, 4-Way Crossover Study. Clin Ther. 2014;36:748–59.
4. Vanhove T, Annaert P, Kuypers DRJ. Clinical determinants of calcineurin inhibitor disposition: a mechanistic review. Drug Metab Rev. 2016;48:88–112.
5. Bekersky I, Dressler D, Mekki Q. Effect of Time of Meal Consumption on Bioavailability of a Single Oral 5 mg Tacrolimus Dose. J Clin Pharmacol. 2001;41:289–97.
6. Jacobson PA, Schladt D, Oetting WS, Leduc R, Guan W, Matas AJ, et al. Lower Calcineurin Inhibitor Doses in Older Compared to Younger Kidney Transplant Recipients Yield Similar Troughs: **Calcineurin Inhibitors in the Elderly**. Am J Transplant. 2012;12:3326–36.
7. Park S-I, Felipe CR, Pinheiro-Machado PG, Garcia R, Tedesco-Silva H, Medina-Pestana JO. Circadian and time-dependent variability in tacrolimus pharmacokinetics. Fundam Clin Pharmacol. 2007;21:191–7.
8. Fontova P, Colom H, Rigo-Bonnin R, van Merendonk LN, Vidal-Alabró A, Montero N, et al. Influence of the Circadian Timing System on Tacrolimus Pharmacokinetics and Pharmacodynamics After Kidney Transplantation. Front Pharmacol. 2021;12:636048.
9. Saint-Marcoux F, Woillard J-B, Jurado C, Marquet P. Ther Drug Monit. 2013;35:322–7.
10. Woillard J-B, Chouchana L, Picard N, Loriot M-A. Pharmacogenetics of immunosuppressants: State of the art and clinical implementation – recommendations from the French National Network of Pharmacogenetics (RNPGx). Therapies. 2017;72:285–99.
11. Reference SNP (refSNP) Cluster Report: rs776746. [cited 2022 Sep 24]; Available from: https://www.ncbi.nlm.nih.gov/snp/rs776746#frequency_tab
12. Tron C, Lemaitre F, Verstuyft C, Petitcollin A, Verdier M-C, Bellissant E. Pharmacogenetics of Membrane Transporters of Tacrolimus in Solid Organ Transplantation. Clin Pharmacokinet. 2019;58:593–613.
13. Faravelli I, Velardo D, Podestà MA, Ponticelli C. Immunosuppression-related neurological disorders in kidney transplantation. J Nephrol. 2021;34:539–55.
14. SAKAMOTO Y, Makuuchi M, HARIHARA Y, IMAMURA H, SATO H. Higher intracerebral concentration of tacrolimus after intermittent than continuous administration to rats. Liver Transplant KW -. 2001;7:1071–6.
15. SAKAMOTO Y, KAKUUCHI M, HARIHARA Y, IMAMURA H, SATO H. Correlation between Neurotoxic Events and Intracerebral Concentration of Tacrolimus in Rats. Biol Pharm Bull KW -. 2000;23:1008–10.
16. Langone A, Steinberg SM, Gedaly R, Chan LK, Shah T, Sethi KD, et al. Switching STudy of Kidney TRansplant PAtients with Tremor to LCP-TacrO (STRATO): an open-label, multicenter, prospective phase 3b study. Clin Transplant. 2015;29:796–805.
17. Sánchez Fructuoso A, Ruiz JC, Franco A, Diekmann F, Redondo D, Calviño J, et al. Effectiveness and safety of the conversion to MeltDose ® extended-release tacrolimus from other formulations of tacrolimus in stable kidney transplant patients: A retrospective study. Clin Transplant [Internet]. 2020 [cited 2022 Apr 20];34. Available from: https://onlinelibrary.wiley.com/doi/10.1111/ctr.13767
18. Braithwaite HE, Darley DR, Brett J, Day RO, Carland JE. Identifying the association

Licence CC BY-NC-ND 3.0

between tacrolimus exposure and toxicity in heart and lung transplant recipients: A systematic review. Transplant Rev. 2021;35:100610.
19. Jouve T, Fonrose X, Noble J, Janbon B, Fiard G, Malvezzi P, et al. The TOMATO Study (Tacrolimus Metabolization in Kidney Transplantation): Impact of the Concentration–Dose Ratio on Death-censored Graft Survival. Transplantation. 2020;104:1263–71.
20. Thölking G, Schütte-Nütgen K, Schmitz J, Rovas A, Dahmen M, Bautz J, et al. A Low Tacrolimus Concentration/Dose Ratio Increases the Risk for the Development of Acute Calcineurin Inhibitor-Induced Nephrotoxicity. J Clin Med KW -. 2019;8:1586.
21. Thölking G, Fortmann C, Koch R, Gerth HU, Pabst D, Pavenstädt H, et al. The Tacrolimus Metabolism Rate Influences Renal Function after Kidney Transplantation. Bueno V, editor. PLoS ONE. 2014;9:e111128.
22. Prusinskas B, Ohlsson S, Kathemann S, Pilic D, Kampmann K, Büscher R, et al. Role of Tacrolimus C/D Ratio in the First Year After Pediatric Liver Transplantation. Front Pediatr. 2021;9:659608.
23. Zegarska J, Hryniewiecka E, Zochowska D, Samborowska E, Jazwiec R, Borowiec A, et al. Tacrolimus Metabolite M-III May Have Nephrotoxic and Myelotoxic Effects and Increase the Incidence of Infections in Kidney Transplant Recipients. Transplant Proc. 2016;48:1539–42.
24. Tong L, Li W, Zhang Y, Zhou F, Zhao Y, Zhao L, et al. Tacrolimus inhibits insulin release and promotes apoptosis of Min6 cells through the inhibition of the PI3K/Akt/mTOR pathway. Mol Med Rep. 2021;24:658.
25. Rodriguez-Rodriguez AE, Porrini E, Torres A. Beta-Cell Dysfunction Induced by Tacrolimus: A Way to Explain Type 2 Diabetes? Int J Mol Sci. 2021;22:10311.
26. Han E, Kim MS, Kim YS, Kang ES. Risk assessment and management of post-transplant diabetes mellitus. Metabolism. 2016;65:1559–69.
27. Noble J, Terrec F, Malvezzi P, Rostaing L. Adverse effects of immunosuppression after liver transplantation. Best Pract Res Clin Gastroenterol. 2021;54–55:101762.
28. Bodziak KA, Hricik DE. New-onset diabetes mellitus after solid organ transplantation: New-onset diabetes after transplantation. Transpl Int. 2009;22:519–30.
29. Klangjareonchai T, Eguchi N, Tantisattamo E, Ferrey AJ, Reddy U, Dafoe DC, et al. Current Pharmacological Intervention and Medical Management for Diabetic Kidney Transplant Recipients. Pharmaceutics. 2021;13:413.
30. Rodrigo E, Pinera C, Cos MA, Sanchez B, Ruiz JC, Fernandez-Fresnedo G, et al. Evolution of tacrolimus blood levels and concentration-dose ratios in patients who develop new onset diabetes mellitus after kidney transplantation. Transpl Int. 2005;18:1152–7.
31. Gastaca M, Ruiz P, Bustamante J, Martinez-Indart L, Ventoso A, Fernandez JR, et al. Early tacrolimus exposure does not impact long-term outcomes after liver transplantation. World J Hepatol. 2021;13:362–74.
32. Brunet M, van Gelder T, Åsberg A, Haufroid V, Hesselink DA, Langman L, et al. Therapeutic Drug Monitoring of Tacrolimus-Personalized Therapy: Second Consensus Report. Ther Drug Monit. 2019;41:261–307.
33. Maes BD, Kuypers D, Messiaen T, Evenepoel P, Mathieu C, Coosemans W, et al. POSTTRANSPLANTATION DIABETES MELLITUS IN FK-506-TREATED RENAL TRANSPLANT RECIPIENTS: ANALYSIS OF INCIDENCE AND RISK FACTORS. Transplant KW -. 2001;72:1655–61.
34. Kizilbash SJ, Rheault MN, Bangdiwala A, Matas A, Chinnakotla S, Chavers BM. Infection rates in tacrolimus versus cyclosporine-treated pediatric kidney transplant recipients on a rapid discontinuation of prednisone protocol: 1-year analysis. Pediatr Transplant. 2017;21:e12919.
35. Mella A, Mariano F, Dolla C, Gallo E, Manzione AM, Di Vico MC, et al. Bacterial and

Licence CC BY-NC-ND 3.0

Viral Infection and Sepsis in Kidney Transplanted Patients. Biomedicines. 2022;10:701.
36. Papon N, Nevez G, Le Gal S, Vigneau C, Robert-Gangneux F, Bouchara J-P, et al. Fungal infections in transplant recipients: pros and cons of immunosuppressive and antimicrobial treatment. Lancet Microbe. 2021;2:e6–8.
37. Rubin RH, Ikonen T, Gummert JF, Morris RE. The therapeutic prescription for the organ transplant recipient: the linkage of immunosuppression and antimicrobial strategies: Linkage of immunosuppression and antimicrobial strategies. Transpl Infect Dis. 1999;1:29–39.
38. Yin S, Song T, Jiang Y, Li X, Fan Y, Lin T. Tacrolimus Trough Level at the First Month May Predict Renal Transplantation Outcomes Among Living Chinese Kidney Transplant Patients: A Propensity Score–Matched Analysis. Ther Drug Monit. 2019;41:308–16.
39. Hoyo I, Sanclemente G, Cervera C, Cofán F, Ricart MJ, Perez-Villa F, et al. Opportunistic Pulmonary Infections in Solid Organ Transplant Recipients. Transplant Proc. 2012;44:2673–5.
40. Haute Autorité de Santé. Guide du parcours de soins – Maladie rénale chronique de l'adulte (MRC). 2021;85.
41. Müller F, Weitz D, Mertsch K, König J, Fromm MF. Importance of OCT2 and MATE1 for the Cimetidine–Metformin Interaction: Insights from Investigations of Polarized Transport in Single- And Double-Transfected MDCK Cells with a Focus on Perpetrator Disposition. Mol Pharm. 2018;15:3425–33.
42. Haute Autorité de Santé - Evaluation du débit de filtration glomérulaire, et du dosage de la créatininémie dans le diagnostic de la maladie rénale chronique chez l'adulte - Rapport d'évaluation [Internet]. [cited 2019 May 7]. Available from: https://www.has-sante.fr/portail/jcms/c_1064297/fr/evaluation-du-debit-de-filtration-glomerulaire-et-du-dosage-de-la-creatininemie-dans-le-diagnostic-de-la-maladie-renale-chronique-chez-l-adulte-rapport-d-evaluation
43. Schwartz GJ, Haycock GB, Edelmann CM, Spitzer A. A simple estimate of glomerular filtration rate in children derived from body length and plasma creatinine. Pediatrics. 1976;58:259–63.
44. Levey AS, Bosch JP, Lewis JB, Greene T, Rogers N, Roth D. A more accurate method to estimate glomerular filtration rate from serum creatinine: a new prediction equation. Modification of Diet in Renal Disease Study Group. Ann Intern Med. 1999;130:461–70.
45. Levey AS, Stevens LA, Schmid CH, Zhang YL, Castro AF, Feldman HI, et al. A new equation to estimate glomerular filtration rate. Ann Intern Med. 2009;150:604–12.
46. Cockcroft DW, Gault H. Prediction of Creatinine Clearance from Serum Creatinine. Nephron. 1976;16:31–41.
47. Livio F, Biollaz J, Burnier M. [Renal function estimation by MDRD equation: interest and limitations for drug dosing]. Rev Med Suisse. 2008;4:2596–600.
48. Flamant M, Haymann J-P, Vidal-Petiot E, Letavernier E, Clerici C, Boffa J-J, et al. GFR Estimation Using the Cockcroft-Gault, MDRD Study, and CKD-EPI Equations in the Elderly. Am J Kidney Dis. 2012;60:847–9.
49. Randers E, Kornerup K, Erlandsen EJ, Hasling C, Danielsen H. Cystatin C levels in sera of patients with acute infectious diseases with high C-reactive protein levels. Scand J Clin Lab Invest. 2001;61:333–5.
50. Cimerman N, Brguljan PM, Krašovec M, Šuškovič S, Kos J. Twenty-four hour variations of cystatin C and total cysteine proteinase inhibitory activity in sera from healthy subjects. Clin Chim Acta. 2000;291:89–95.
51. Fricker M, Wiesli P, Brändle M, Schwegler B, Schmid C. Impact of thyroid dysfunction on serum cystatin C. Kidney Int. 2003;63:1944–7.
52. Knight EL, Verhave JC, Spiegelman D, Hillege HL, de Zeeuw D, Curhan GC, et al. Factors influencing serum cystatin C levels other than renal function and the impact on renal

Licence CC BY-NC-ND 3.0

function measurement. Kidney Int. 2004;65:1416–21.
53. Inker LA, Schmid CH, Tighiouart H, Eckfeldt JH, Feldman HI, Greene T, et al. Estimating Glomerular Filtration Rate from Serum Creatinine and Cystatin C. N Engl J Med. 2012;367:20–9.
54. Soveri I, Berg UB, Björk J, Elinder C-G, Grubb A, Mejare I, et al. Measuring GFR: a systematic review. Am J Kidney Dis Off J Natl Kidney Found. 2014;64:411–24.
55. Khelifa A, Chentli K, Habbeche M, Bouyoucef SE. Mesure isotopique du débit de filtration glomérulaire : étude corrélative DFG au 99mTc-DTPA versus 51Cr-EDTA. Médecine Nucl. 2015;39:254.
56. Durand E, Chaumet-Riffaud P, Archambaud F, Moati F, Prigent A. Mesure de la fonction rénale par les méthodes radio-isotopiques. EMC - Néphrologie. 2006;1:1–15.
57. Résumé des caractéristiques du produit - OMNIPAQUE 350 mg d'I/mL, solution injectable - Base de données publique des médicaments [Internet]. [cited 2019 Apr 28]. Available from: http://base-donnees-publique.medicaments.gouv.fr/affichageDoc.php?specid=67846776&typedoc=R
58. Lewis R, Kerr N, Buren CV, Lowry P, Sandler C, Frazier OH, et al. COMPARATIVE EVALUATION OF UROGRAPHIC CONTRAST MEDIA, INULIN, AND 99mTc-DTPA CLEARANCE METHODS FOR DETERMINATION OF GLOMERULAR FILTRATION RATE IN CLINICAL TRANSPLANTATION: Transplantation. 1989;48:790–5.
59. Haute Autorité de Santé. Suivi ambulatoire de l'adulte transplanté rénal au-delà de 3 mois après transplantation. 2009 Jun;
60. Warty V, Zuckerman S, Venkataramanan R, Lever W, Chao J, Mckaveney T, et al. Tacrolimus Analysis: A Comparison of Different Methods and Matrices. Ther Drug Monit. 1995;17:159–67.
61. Bouamar R, Shuker N, Hesselink DA, Weimar W, Ekberg H, Kaplan B, et al. Tacrolimus Predose Concentrations Do Not Predict the Risk of Acute Rejection After Renal Transplantation: A Pooled Analysis From Three Randomized-Controlled Clinical Trials †: Tacrolimus Concentrations and Acute Rejection. Am J Transplant. 2013;13:1253–61.
62. Peng H, Cheung B. A review on pharmacokinetic modeling and the effects of environmental stressors on pharmacokinetics for operational medicine. 2009;
63. Sheiner LB, Rosenberg B, Melmon KL. Modelling of individual pharmacokinetics for computer-aided drug dosage. Comput Biomed Res. 1972;5:441–59.
64. Sheiner LB, Rosenberg B, Marathe VV. Estimation of population characteristics of pharmacokinetic parameters from routine clinical data. J Pharmacokinet Biopharm. 1977;5:445–79.
65. Sheiner LB, Beal SL. Evaluation of methods for estimating population pharmacokinetic parameters. I. Michaelis-menten model: Routine clinical pharmacokinetic data. J Pharmacokinet Biopharm. 1980;8:553–71.
66. Sheiner LB, Beal SL. Evaluation of methods for estimating population pharmacokinetic parameters II. Biexponential model and experimental pharmacokinetic data. J Pharmacokinet Biopharm. 1981;9:635–51.
67. Sheiner LB, Beal SL. Evaluation of methods for estimating population pharmacokinetic parameters. III. Monoexponential model: Routine clinical pharmacokinetic data. J Pharmacokinet Biopharm. 1983;11:303–19.
68. Sheiner LB, Grasela TH. Experience with Nonmem: Analysis of Routine Phenytoin Clinical Pharmacokinetic Data. Drug Metab Rev. 1984;15:293–303.
69. Sheiner LB. The Population Approach to Pharmacokinetic Data Analysis: Rationale and Standard Data Analysis Methods. Drug Metab Rev. 1984;15:153–71.
70. Sheiner LB, Beal S, Rosenberg B, Marathe VV. Forecasting individual pharmacokinetics. Clin Pharmacol Ther. 1979;26:294–305.

Licence CC BY-NC-ND 3.0

71. Xu XS, Yuan M, Karlsson MO, Dunne A, Nandy P, Vermeulen A. Shrinkage in Nonlinear Mixed-Effects Population Models: Quantification, Influencing Factors, and Impact. AAPS J. 2012;14:927–36.
72. Karlsson MO, Savic RM. Diagnosing Model Diagnostics. Clin Pharmacol Ther. 2007;82:17–20.
73. Monolix version 2018R1. Antony, France: Lixoft SAS, 2018. http://lixoft.com/products/monolix/.
74. Beal S, Sheiner L, Boeckmann A, Bauer R. NONMEM 7.4 users guides. ICON Plc Gaithersburg MD. 1989;2018.
75. Savic RM, Karlsson MO. Importance of Shrinkage in Empirical Bayes Estimates for Diagnostics: Problems and Solutions. :12.
76. Grégoire M, Dumont R, Ronchi L, Woillard J-B, Atthar V, Letessier E, et al. Prophylactic cefazolin concentrations in morbidly obese patients undergoing sleeve gastrectomy: do we achieve targets? Int J Antimicrob Agents. 2018;52:28–34.
77. Praet A, Bourguignon L, Vetele F, Breant V, Genestet C, Dumitrescu O, et al. Population Pharmacokinetic Modeling and Dosing Simulations of Tobramycin in Pediatric Patients with Cystic Fibrosis. Antimicrob Agents Chemother. 2021;65:e00737-21.
78. Bach T, Deye GA, Codd EE, Horton J, Winokur P, An G. Population Pharmacokinetic-Pharmacodynamic Model of Oxfendazole in Healthy Adults in a Multiple Ascending Dose and Food Effect Study and Target Attainment Analysis. Antimicrob Agents Chemother. 2022;66:e01432-21.
79. Desborough L, Jaffe K, Hanna J, Ulloa J, Kaiserman K. Transforming Evidence Generation for Drug Label Changes: A Case Study. Ann Biomed Eng [Internet]. 2022 [cited 2022 Sep 24]; Available from: https://link.springer.com/10.1007/s10439-022-03062-4
80. Visentin R, Giegerich C, Jäger R, Dahmen R, Boss A, Grant M, et al. Improving Efficacy of Inhaled Technosphere Insulin (Afrezza) by Postmeal Dosing: In-silico Clinical Trial with the University of Virginia/Padova Type 1 Diabetes Simulator. Diabetes Technol Ther. 2016;18:574–85.
81. Labriffe M, Woillard J, Debord J, Marquet P. Machine learning algorithms to estimate everolimus exposure trained on simulated and patient pharmacokinetic profiles. CPT Pharmacomet Syst Pharmacol. 2022;psp4.12810.
82. Woillard J-B, Salmon Gandonnière C, Destere A, Ehrmann S, Merdji H, Mathonnet A, et al. A Machine Learning Approach to Estimate the Glomerular Filtration Rate in Intensive Care Unit Patients Based on Plasma Iohexol Concentrations and Covariates. Clin Pharmacokinet [Internet]. 2020 [cited 2020 Aug 14]; Available from: http://link.springer.com/10.1007/s40262-020-00927-6
83. Destere A, Marquet P, Gandonnière CS, Åsberg A, Loustaud-Ratti V, Carrier P, et al. A Hybrid Model Associating Population Pharmacokinetics with Machine Learning: A Case Study with Iohexol Clearance Estimation. Clin Pharmacokinet [Internet]. 2022 [cited 2022 Jun 9]; Available from: https://link.springer.com/10.1007/s40262-022-01138-x
84. Marchello G, Fresse A, Corneli M, Bouveyron C. Co-clustering of evolving count matrices in pharmacovigilance with the dynamic latent block model. :42.
85. Wright MN, Ziegler A. ranger: A Fast Implementation of Random Forests for High Dimensional Data in C++ and R. J Stat Softw. 2017;77:1–17.
86. Chen T, Guestrin C. XGBoost: A Scalable Tree Boosting System. Proc 22nd ACM SIGKDD Int Conf Knowl Discov Data Min [Internet]. San Francisco California USA: ACM; 2016 [cited 2021 Dec 24]. p. 785–94. Available from: https://dl.acm.org/doi/10.1145/2939672.2939785
87. Cortes C, Vapnik V. Support-vector networks. Mach Learn. Springer; 1995;20:273–97.
88. Hastie SMD from mda:mars by T, wrapper RTUAMF utilities with TL leaps. earth:

Licence CC BY-NC-ND 3.0

Multivariate Adaptive Regression Splines [Internet]. 2021. Available from: https://CRAN.R-project.org/package=earth
89. Garcia Leiva R, Fernandez Anta A, Mancuso V, Casari P. A Novel Hyperparameter-Free Approach to Decision Tree Construction That Avoids Overfitting by Design. IEEE Access. 2019;7:99978–87.
90. Rajkomar A, Dean J, Kohane I. Machine Learning in Medicine. N Engl J Med. 2019;380:1347–58.
91. Sibieude E, Khandelwal A, Girard P, Hesthaven JS, Terranova N. Population pharmacokinetic model selection assisted by machine learning. J Pharmacokinet Pharmacodyn [Internet]. 2021 [cited 2021 Dec 13]; Available from: https://link.springer.com/10.1007/s10928-021-09793-6
92. Ismail M, Sale M, Yu Y, Pillai N, Liu S, Pflug B, et al. Development of a genetic algorithm and NONMEM workbench for automating and improving population pharmacokinetic/pharmacodynamic model selection. J Pharmacokinet Pharmacodyn. 2022;49:243–56.
93. Karatza E, Papachristos A, Sivolapenko GB, Gonzalez D. Machine learning-guided covariate selection for time-to-event models developed from a small sample of real-world patients receiving bevacizumab treatment. CPT Pharmacomet Syst Pharmacol. 2022;psp4.12848.
94. Bunte K, Smith DJ, Chappell MJ, Hassan-Smith ZK, Tomlinson JW, Arlt W, et al. Learning pharmacokinetic models for in vivo glucocorticoid activation. J Theor Biol. 2018;455:222–31.
95. Ponthier L, Ensuque P, Destere A, Marquet P, Labriffe M, Jacqz-Aigrain E, et al. Optimization of Vancomycin Initial Dose in Term and Preterm Neonates by Machine Learning. Pharm Res [Internet]. 2022 [cited 2022 Aug 11]; Available from: https://link.springer.com/10.1007/s11095-022-03351-6
96. Asiimwe IG, Blockman M, Cohen K, Cupido C, Hutchinson C, Jacobson B, et al. Stable warfarin dose prediction in sub-Saharan African patients: A machine-learning approach and external validation of a clinical dose-initiation algorithm. CPT Pharmacomet Syst Pharmacol. 2022;11:20–9.
97. Bououda M, Uster DW, Sidorov E, Labriffe M, Marquet P, Wicha SG, et al. A Machine Learning Approach to Predict Interdose Vancomycin Exposure. Pharm Res. 2022;39:721–31.
98. Woillard J, Labriffe M, Debord J, Marquet P. Mycophenolic Acid Exposure Prediction Using Machine Learning. Clin Pharmacol Ther. 2021;110:370–9.
99. Woillard J, Labriffe M, Debord J, Marquet P. Tacrolimus Exposure Prediction Using Machine Learning. Clin Pharmacol Ther. 2021;110:361–9.
100. Tang B-H, Guan Z, Allegaert K, Wu Y-E, Manolis E, Leroux S, et al. Drug Clearance in Neonates: A Combination of Population Pharmacokinetic Modelling and Machine Learning Approaches to Improve Individual Prediction. Clin Pharmacokinet. 2021;60:1435–48.
101. Hughes JH, Keizer RJ. A hybrid machine learning/pharmacokinetic approach outperforms maximum a posteriori Bayesian estimation by selectively flattening model priors. CPT Pharmacomet Syst Pharmacol. 2021;10:1150–60.
102. Robertsen I, Åsberg A, Ingerø AO, Vethe NT, Bremer S, Bergan S, et al. Use of Generic Tacrolimus in Elderly Renal Transplant Recipients: Precaution Is Needed. Transplantation. 2015;99:528–32.
103. Benz-de Bretagne I, Le Guellec C, Halimi JM, Gatault P, Barbet C, Alnajjar A, et al. New sampling strategy using a Bayesian approach to assess iohexol clearance in kidney transplant recipients. Ther Drug Monit. 2012;34:289–97.
104. Riff C, Besombes J, Gatault P, Barbet C, Büchler M, Blasco H, et al. Assessment of the glomerular filtration rate (GFR) in kidney transplant recipients using Bayesian estimation of

Licence CC BY-NC-ND 3.0

the iohexol clearance. Clin Chem Lab Med CCLM. 2020;58:577–87.
105. Taubert M, Ebert N, Martus P, van der Giet M, Fuhr U, Schaeffner E. Using a three-compartment model improves the estimation of iohexol clearance to assess glomerular filtration rate. Sci Rep [Internet]. 2018 [cited 2019 May 9];8. Available from: http://www.nature.com/articles/s41598-018-35989-x
106. Taubert M, Schaeffner E, Martus P, van der Giet M, Fuhr U, Lösment A, et al. Advancement of pharmacokinetic models of iohexol in patients aged 70 years or older with impaired kidney function. Sci Rep. 2021;11:22656.
107. Åsberg A, Bjerre A, Almaas R, Luis-Lima S, Robertsen I, Salvador CL, et al. Measured GFR by Utilizing Population Pharmacokinetic Methods to Determine Iohexol Clearance. Kidney Int Rep. 2020;5:189–98.
108. Destere A, Gandonnière CS, Åsberg A, Loustaud-Ratti V, Carrier P, Ehrmann S, et al. A single Bayesian estimator for iohexol clearance estimation in ICU, liver failure and renal transplant patients. Br J Clin Pharmacol. 2021;bcp.15197.
109. Baklouti S, Gandia P, Concordet D. "De-Shrinking" EBEs: The Solution for Bayesian Therapeutic Drug Monitoring. Clin Pharmacokinet [Internet]. 2022 [cited 2022 Feb 25]; Available from: https://link.springer.com/10.1007/s40262-021-01105-y
110. Desai A, Kovanda L, Kowalski D, Lu Q, Townsend R, Bonate PL. Population Pharmacokinetics of Isavuconazole from Phase 1 and Phase 3 (SECURE) Trials in Adults and Target Attainment in Patients with Invasive Infections Due to Aspergillus and Other Filamentous Fungi. Antimicrob Agents Chemother. 2016;60:5483–91.
111. Heisel O, Heisel R, Balshaw R, Keown P. New Onset Diabetes Mellitus in Patients Receiving Calcineurin Inhibitors: A Systematic Review and Meta-Analysis. Am J Transplant. 2004;4:583–95.
112. Shao L, Jin J, Ye B, Xu B, Li Y, Gong J, et al. New-Onset Diabetes Mellitus in Patients with Idiopathic Membranous Nephropathy Undergoing Tacrolimus and Low-Dose Corticosteroid Therapy. Kidney Blood Press Res. 2019;44:1352–62.
113. Gourishankar S, Jhangri GS, Tonelli M, Wales LH, Cockfield SM. Development of Diabetes Mellitus Following Kidney Transplantation: A Canadian Experience. Am J Transplant. 2004;4:1876–82.
114. Zielińska K, Kukulski L, Wróbel M, Przybyłowski P, Zakliczyński M, Strojek K. Prevalence and Risk Factors of New-Onset Diabetes After Transplantation (NODAT). Ann Transplant [Internet]. 2020 [cited 2021 Sep 1];25. Available from: https://www.annalsoftransplantation.com/abstract/index/idArt/926556
115. Riff C, Debord J, Monchaud C, Marquet P, Woillard J. Population pharmacokinetic model and Bayesian estimator for 2 tacrolimus formulations in adult liver transplant patients. Br J Clin Pharmacol. 2019;85:1740–50.
116. Woillard J-B, Saint-Marcoux F, Debord J, Åsberg A. Pharmacokinetic models to assist the prescriber in choosing the best tacrolimus dose. Pharmacol Res. 2018;130:316–21.
117. Woillard J-B, de Winter BCM, Kamar N, Marquet P, Rostaing L, Rousseau A. Population pharmacokinetic model and Bayesian estimator for two tacrolimus formulations - twice daily Prograf® and once daily Advagraf®: Bayesian estimator for both Prograf® and Advagraf®. Br J Clin Pharmacol. 2011;71:391–402.
118. Woillard J-B, Debord J, Monchaud C, Saint-Marcoux F, Marquet P. Population Pharmacokinetics and Bayesian Estimators for Refined Dose Adjustment of a New Tacrolimus Formulation in Kidney and Liver Transplant Patients. Clin Pharmacokinet. 2017;56:1491–8.
119. Neuschwander A, Journois D. La créatinine en anesthésie réanimation : une fausse amie ! :10.
120. Luis Lima S, Marrero Miranda D, González Rinne A, Negrín Mena N, Pérez Tamajón L,

Licence CC BY-NC-ND 3.0

Rodríguez A, et al. Estimated GFR Slope in Kidney Transplant Patients: When the Error Is Random. Transplantation. 2022;106:391–400.
121. Nilsson-Ehle P. Iohexol Clearance for the Determination of Glomerular Filtration Rate: 15 Years' Experience in Clinical Practice. EJIFCC. 2001;13:48–52.

Licence CC BY-NC-ND 3.0

Annexe 1: Development of new tacrolimus C0-based metrics and their association with new onset diabetes mellitus in renal transplant patients

Poster commenté présenté lors du congrès de la Société Française de Pharmacologie et de Thérapeutique le 14 juin 2022 à Lille.

Congrès SFPT 2022 - Lille – Poster PM1-010

Development of new tacrolimus C0-based metrics and their association with new onset diabetes mellitus in renal transplant patients

A Destere[a], A Premaud[b], C Monchaud[c], P Marquet[c], JB Woillard[c]

a. Department Of Pharmacology, Toxicology, University Hospital Of Nice, Nice, France - Nice (France)

b. INSERM, UMR 1248, University of Limoges, Limoges, France

c. Department Of Pharmacology, Toxicology And Pharmacovigilance, University Hospital Of Limoges, Limoges, France - Limoges (France)

Contact: Destere.a@chu-nice.fr

INTRODUCTION

Tacrolimus (Tac) is an immunosuppressant widely used in transplantation and its **therapeutic drug monitoring** (TDM) is mandatory [1] to prevent acute rejection and reduce adverse effects such as the development of **new onset diabetes mellitus** (NODM). No relationship between NODM and Tac exposure indices (concentrations (C0) or area under the curve (AUC)) has been clearly found [2]. However, cumulative exposure to Tac in the first 3 months appears to be associated to the development of diabetes mellitus [3].

OBJECTIVE

We aimed to **develop** metrics derived from Tac C0 to assess **cumulative exposure to Tac** and evaluate its **influence on NODM**.

MATERIAL & METHODS

Patients and data collected:

Data were collected from adult kidney transplant recipients enrolled in two successive multicentre cohort studies called "EPIGREN" and "EPHEGREN".

The patients include in this analysis must have:

- At least 2 pre-dose concentrations (C0)
- < 3 months post-transplant

Development of Cox model:

Cox models were built to investigate the relationships between the C0-derived exposure indices and the occurrence of NODM, after adjustment on clinical/demographic data.

Variables with **p value < 0.1** at univariate analysis were included in an intermediate multivariable Cox model. The final model was obtained through stepwise backward selection, retaining only variables with **p <0.05**. The statistical interactions between covariates in the final model were evaluated. The robustness of the results was assessed by **1000 bootstraps**.

Tacrolimus longitudinal exposure:

Different Tac exposure metrics were derived for each patient from their longitudinal profile of Tac C0 over the first three months after transplantation:

Percentage of C0 values > cut-off (%C0 >15 µg/L):

$$\%\mathbf{C0} > \boldsymbol{cut} - \mathbf{off}\ (\%) = \frac{\mathbf{number\ of\ C0} > \boldsymbol{cut} - \boldsymbol{off}}{\mathbf{number\ of\ C0}\ \boldsymbol{total}} \times \mathbf{100}$$

Percentage of the area under the C0 > cut-off vs. time curve (%AUC_{C0} >15 µg/L):

$$\%\boldsymbol{AUC_{C0}} > \boldsymbol{cut} - \mathbf{off}\ (\%) = \frac{\mathbf{AUC\ of\ C0}\ > \boldsymbol{cut} - \boldsymbol{off}}{\mathbf{total\ AUC\ of\ C0}\ > \mathbf{0}} \times \mathbf{100}$$

Average of C0 values above cut-off (Av_{C0} >15 µg/L):

$$\mathbf{Av_{C0}} > \boldsymbol{cut} - \mathbf{off}\ = \boldsymbol{mean}\ (\boldsymbol{C0}\ > \boldsymbol{cut} - \boldsymbol{off})$$

Cut-off = 15 µg/L (*upper limit of the therapeutic window just after kidney transplantation*) [1].

RESULTS

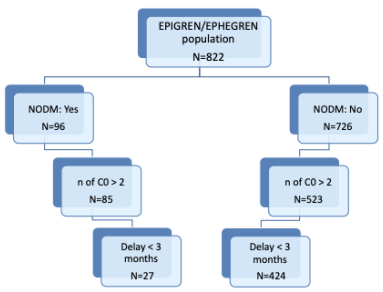

Figure 1: Flowchart of selected patients in the Cox model developments

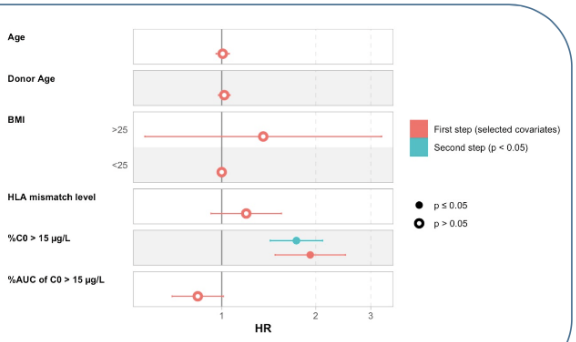

Figure 2: Cox models comparison after univariate analysis

- **%C0 > 15 µg/L** was significantly associated with NODM (per 10% increase: **HR[95% CI]= 1.73 [1.43-2.10, p<0.001]**) whereas no association was observed with %AUC of C0 > 15 µg/L **HR[95% CI]= 0.92 [0.81-1.05, p=0.23)** in multivariate analysis
- No deviation of proportional hazards was shown using the Schoenfeld residues
- A threshold for **%C0 > 15 µg/L** was investigated using ROC curve analysis and the value associated with the best sensitivity/specificity balance was **18%** (sensitivity = 37%, specificity = 90%).
- **%C0 > 15 µg/L** was recoded using this threshold and this binary exposure index was significantly associated with NOM (**under vs. above 15 µg/L: HR=5.3[2.4-11.6], p<0.001**). Figure 3 presents the corresponding Kaplan-Meier curves.

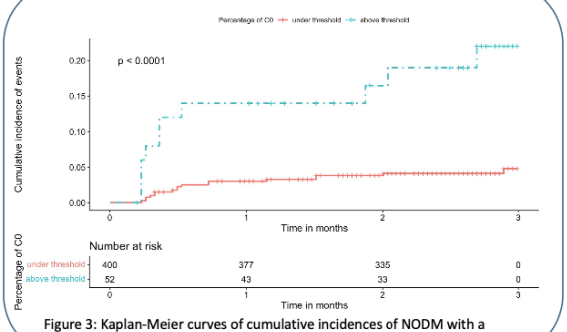

Figure 3: Kaplan-Meier curves of cumulative incidences of NODM with a percentage under or above threshold (18%)

REFERENCES

1-Brunet M. et al. Therapeutic Drug Monitoring. 2019;41:261–307.; 2-Heisel O. et al. Am J Transplant. 2004;4:583–95. ; 3- Maes B.D. et al. Transplantation KW - 2001, 72, 1655.

Licence CC BY-NC-ND 3.0

Suivi du patient transplanté rénal traité par tacrolimus par pharmacocinétique de population et machine learning

Le tacrolimus, pierre angulaire de la thérapie immunosuppressive dans la transplantation d'organe solide, possède un intervalle thérapeutique étroit ainsi qu'une variabilité interindividuelle importante exposant rapidement le patient à un risque de sous- ou surexposition. Quelle que soit la situation (sous- ou surexposition), le risque encouru par le patient n'est pas négligeable. La sous-exposition augmente les risques de survenue d'un rejet et la surexposition celui d'apparition d'effets indésirables (néphrotoxicité, neurotoxicité, diabète post-transplantation, infections…), motivant la mise en place du suivi thérapeutique pharmacologique pour cette molécule. A ce jour, la relation entre l'efficacité thérapeutique et les indices d'exposition est bien établie cependant celle concernant les effets indésirables restent encore à débat. Dans ces travaux de thèse, nous nous sommes focalisés sur le développement d'outils, utilisant la pharmacocinétique de population et le machine learning, pour prédire l'exposition au tacrolimus mais également estimer la fonction rénale et l'exposition à un anti-infectieux, utilisé chez le transplanté. Nous avons aussi développé des marqueurs de suivi de l'exposition longitudinale afin d'explorer l'influence de l'exposition cumulée et a fortiori celle de la surexposition cumulée au tacrolimus sur la survenue d'effets indésirables notamment la survenue de diabète post-transplantation.

Mots-clés : Tacrolimus, effets indésirables, pharmacocinétique de population, machine learning

Monitoring of renal transplant patients treated with tacrolimus using population pharmacokinetics and machine learning

Tacrolimus, the cornerstone of immunosuppressive therapy in solid organ transplantation, has a narrow therapeutic range and significant inter-individual variability that rapidly exposes the patient to the risk of under- or overexposure. In either situation (under or overexposure), the risk to the patient is not negligible. Under-exposure increases the risk of rejection and over-exposure increases the risk of adverse effects (nephrotoxicity, neurotoxicity, post-transplant diabetes, infections, etc.), hence the need for therapeutic pharmacological monitoring of this molecule. To date, the relationship between therapeutic efficacy and exposure indices is well established, but the relationship between adverse effects is still under debate. In this thesis, we focused on developing tools, using population pharmacokinetics and machine learning, to predict tacrolimus exposure but also to estimate renal function and exposure to an anti-infective drug used in transplant patients. We have also developed markers to follow longitudinal exposure in order to explore the influence of cumulative exposure and a fortiori that of cumulative overexposure to tacrolimus on the occurrence of adverse events, including the occurrence of post-transplant diabetes.

Keywords : Tacrolimus; adverse drug reactions; population pharmacokinetics; machine learning